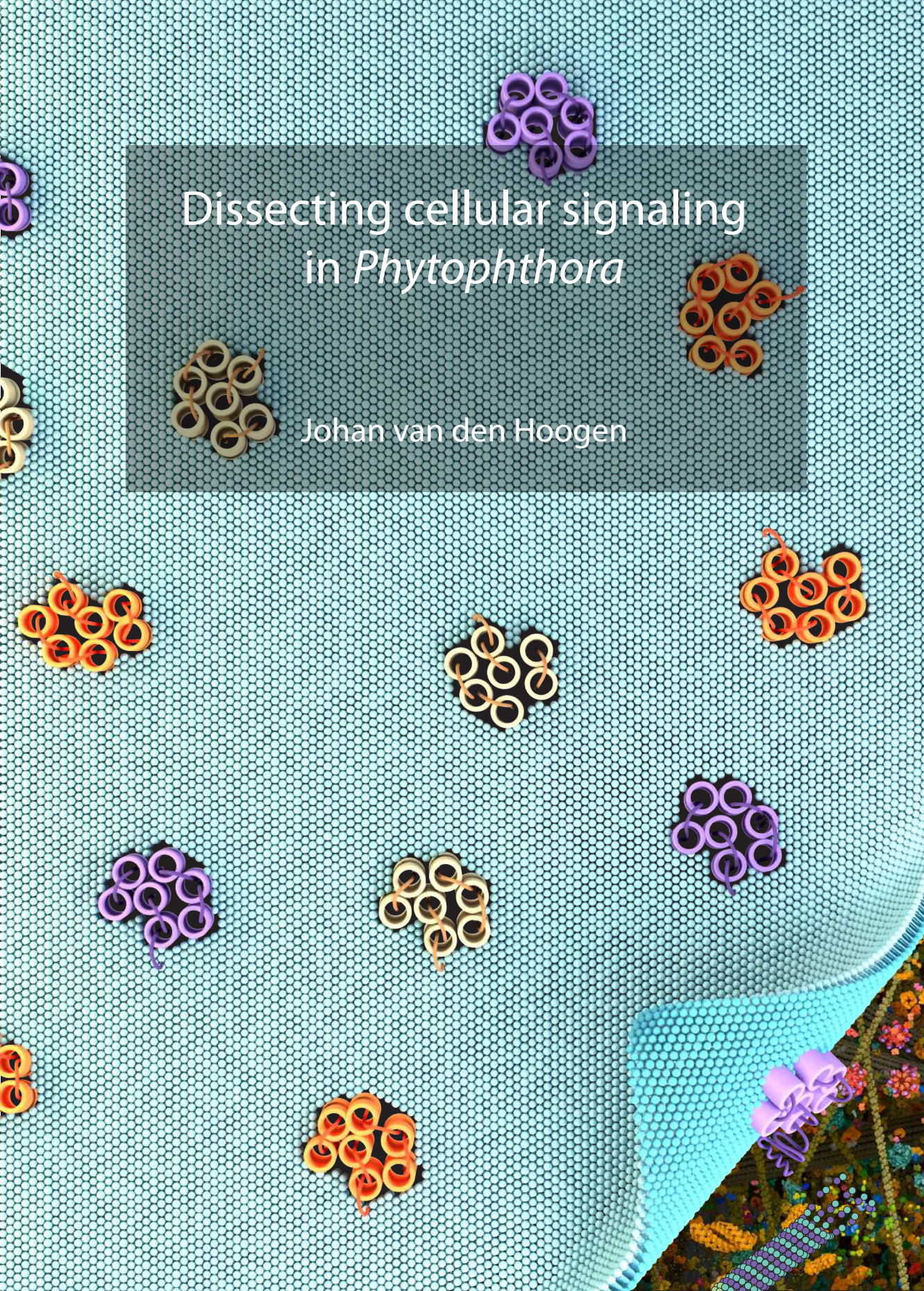
Dissecting cellular signaling
in *Phytophthora*
Johan van den Hoogen

Propositions

1. Oomycetes have unique cellular signaling components.
   (this thesis)

2. *Phytophthora infestans* is not a model organism.
   (this thesis)

3. A better understanding of the importance of quantum physics in biology will revolutionize current dogmas.

4. The seemingly universal assumption that one can just 'CRISPR' a gene is delusive.

5. Smartphone usage reduces the number of inspirational moments.

6. Satirical news sites, such as *De Speld*, are more accurate as news source than social media.

Propositions belonging to the thesis, entitled

'Dissecting cellular signaling in Phytophthora'

Johan van den Hoogen
Wageningen, 8 June 2018

Dissecting cellular signaling in *Phytophthora*

Johan van den Hoogen

Thesis committee

Promotor
Prof. Dr F.P.M. Govers
Personal chair at the Laboratory of Phytopathology
Wageningen University & Research

Other members
Prof. Dr D. de Ridder, Wageningen University & Research
Prof. Dr L.J. Grenville-Briggs, Swedish University of Agricultural Sciences, Alnarp, Sweden
Dr M.A. Jongsma, Wageningen University & Research
Dr R. Geurts, Wageningen University & Research

This research was conducted under the auspices of the Graduate School for Experimental Plant Sciences (EPS).

Dissecting cellular signaling in *Phytophthora*

Johan van den Hoogen

Thesis
submitted in fulfilment of the requirements for the degree of doctor
at Wageningen University
by the authority of the Rector Magnificus,
Prof. Dr A.P.J. Mol,
in the presence of the
Thesis Committee appointed by the Academic Board
to be defended in public
on Friday 8 June 2018
at 11 a.m. in the Aula.

Johan van den Hoogen
Dissecting cellular signaling in *Phytophthora*
144 pages.

PhD thesis, Wageningen University, Wageningen, the Netherlands (2018)
With references, with summary in English

ISBN: 978-94-6343-866-7
DOI: 10.18174/447045

Contents

What I cannot create,
I do not understand.

Richard Feynman

Chapter 1

Introduction

Arguably, the outbreak of the potato late blight epidemic leading to the Irish potato famine mid-19th century is one of the most important historic event due to a plant pathogenic organism. And yet to date, over 170 years later, the causal agent of the disease and later identified relatives are still causing enormous losses in economically important crops and have become threats to native species (Erwin & Ribeiro 1996).

The main subject of research in this thesis is the causal agent of potato and tomato late blight, *Phytophthora infestans*. *Phytophthora* spp. are eukaryotic filamentous organisms that belong to the class oomycetes. The aim of the research described in this thesis is to gain insight into cellular signaling and cytoskeleton dynamics in *Phytophthora*. Specific features of these essential cellular processes may hold potential as novel drug targets for control of oomycetes. In **this chapter**, I will introduce the impact of potato late blight from a historic perspective (**Box 1.1**) and the impact that oomycetes have nowadays. Further, I will give an overview of the current knowledge of signal transduction pathways in oomycetes. Finally, I will summarize recent technical advances in the oomycete research field and present the scope of this thesis.

1.1 Potato late blight

Generally, *P. infestans* is pathogenic on members of the plant family Solanaceae, (nightshades). Nearly 90 plant species can be infected by *P. infestans*, but under natural conditions, only a few get diseased (Erwin & Ribeiro 1996). The economically most important hosts susceptible to *P. infestans* are potato (*Solanum tuberosum*) and tomato (*Solanum lycopersicum*). The disease symptoms of potato late blight are usually first visible on leaves. Infected foliage initially becomes yellow, then water soaked and turns black (Erwin & Ribeiro 1996). Later in the season also tubers become affected. At first, brown or purple spots appear on the skin of the tubers whereafter the disease progresses rapidly in particular in damp soils. Subsequent infections by soil bacteria and fungi lead to further decay

Box 1.1 | The Irish Potato Famine

The first records of the occurrence of late blight on potato date back to 1843 in Eastern states of the USA, and in Belgium (Morren 1844; Bergsma 1845; Harting 1846). The following years, particularly in the wet and cold summer of 1845, the disease spread with frightening speed to cause widespread epidemics across Europe (Bourke 1964). In contrast to Northern America, where potatoes were a relatively small portion of the average diet, Northern Europe suffered from late blight epidemics (Dunn 2017). For an average farmer in Ireland, the daily diet consisted largely of potatoes. From 1845, for three consecutive years, potato harvests in Ireland and other Northern European countries almost completely failed. The disaster, recorded as the Irish potato famine, resulted in mass emigration and death of millions of people (Ristaino 2002).

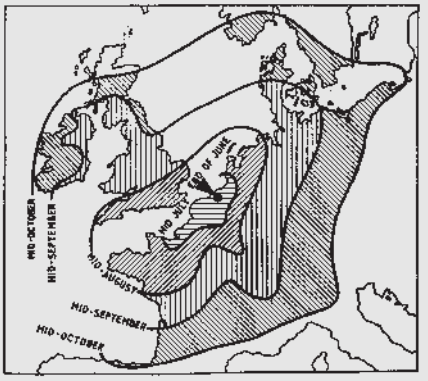

Occurences of potato late blight in Europe in 1845. Reproduced from Bourke (1964)

At the time, the moldy growth on the plants was regarded an effect of a disease rather than the cause. Instead, the potato failure was believed to be due to God's anger over the increased population, or pollution from steam locomotives. The female Belgian mycologist Marie-Anne Libert was the first to describe the infectious agent on diseased potato plants in detail and proposed the name *Botrytis vastatrix* (Libert 1845). Already in the same year, Camille Montagne renamed the species to *Botrytis infestans* (Montagne 1845). It was clergyman Miles Jones Berkeley who recognized *B. infestans* as the cause of blight in potato (Berkeley 1846; Ribeiro 2013). However, it was not until 1876 when Anton de Bary showed that the disease only developed on inoculated potato plants, and demonstrated that tubers could be infected by inoculation with sporangia. He subsequently renamed the genus *Phytophthora*, Greek for plant (phyton) and destruction (phthora) (de Bary 1876).

of the tubers, also known as 'wet rot' (Dowson & Jones 1951). Under cool, moist conditions, the lesions start sporulating, producing sporangia and zoospores. These spores are easily dislodged and can be transported by water or wind. After rainstorms sporangia or zoospores washed from infected leaves can infect tubers near the soil surface (Erwin & Ribeiro 1996; Ribeiro 2013). Within the course of a few weeks, entire potato fields can be destroyed. To control the disease, potato growers heavily rely on chemical control, and typically spray fungicides every 5-7 days, up to 16 times per growing season (Haverkort et al. 2008).

1.2 The class oomycetes

More than 170 years since the first appearance of late blight in Europe (Box 1) and the first description of the late blight pathogen by Marie-Anne Libert (Libert 1845), oomycetes are still often mistaken for fungi. Both show filamentous growth and produce mycelia in their vegetative stage, form spores for sexual and asexual reproduction, and have similar modes of nutrient uptake and ecological niches (Judelson & Blanco 2005; Richards et al. 2006). However, oomycetes and fungi are evolutionary unrelated. Their similarities in morphology and lifestyle are mainly a result of convergent evolution although some incidences of interkingdom horizontal gene transfer might have contributed as well (Richards et al. 2006; Richards et al. 2011; Savory et al. 2015). Key differences between fungi and oomycetes are ploidy levels in the vegetative life stages and the composition of the cell walls. Oomycetes lack a free haploid life stage, and their cell wall is composed of cellulose and β-glucans, whereas chitin is the main component of fungal cell walls (Bartnicki-Garcia 1968; Judelson & Blanco 2005).

Whereas fungi belong to the taxonomic lineage of unikonts, to which also metazoans (animals) and amoebozoans belong, oomycetes are heterokonts and are more closely related to brown algae and diatoms (**Figure 1.1**) (Koonin 2010). Together with these taxa, oomycetes constitute the lineage of stramenopiles. It is estimated that oomycetes and diatoms diverged 400 million years ago (mya), and that the two major oomycete lineages, Peronosporales and Saprolegniales (**Figure 1.1**), diverged 200 mya (McCarthy & Fitzpatrick 2017). Fossil records provide evidence for oomycete parasitism as early as 315 mya (Strullu-Derrien et al. 2011), and since the earliest branching oomycete *Eurychasma dicksonii* is a parasite of brown seaweeds (Kupper et al. 2006) it is likely that pathogenicity is an ancestral trait of oomycetes. Present-day oomycetes are either pathogenic on plants, insects, vertebrates, or microbes, or are saprophytic, in either aquatic or terrestrial ecosystems. While some genera such as *Phytophthora*, *Peronosporaceae*, and *Albuginaceae*, are entirely pathogenic others harbor both saprophytic and opportunistic pathogens. An example is the genus *Pythium* with the majority of species being plant pathogens, but some other species known to be pathogenic on mammals or other microorganisms. In aquatic ecosystems, Saprolegniales are among the most ubiquitous microbes, of which the majority are saprotrophs involved in nutrient cycling (Shearer et al. 2006). However,

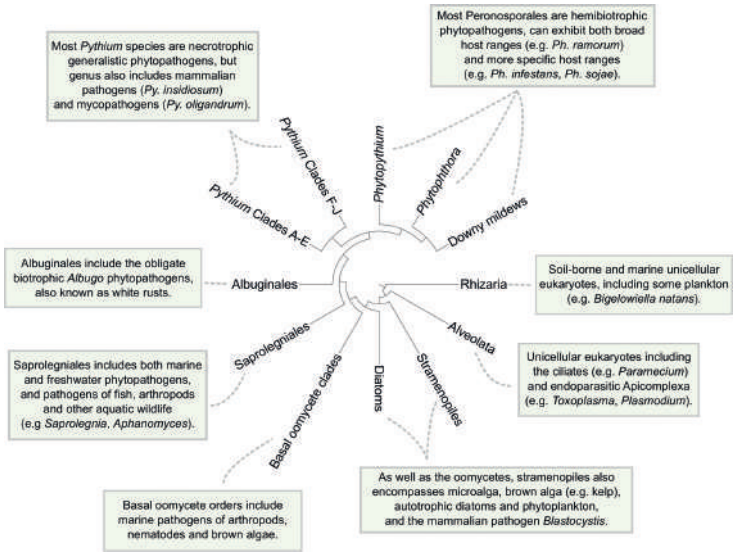

Figure 1.1 | Consensus cladogram of the class oomycetes. The cladogram also includes other lineages such as Diatoms, Alveolata, and Rhizaria. Reproduced from McCarthy and Fitzpatrick (2017).

some species from the genera *Saprolegnia* and *Aphanomyces* are pathogenic on economic important organisms such as salmon and crayfish (Dick 2001).

1.3 The harmful plant pathogens of the genus *Phytophthora*

The *Phytophthora* genus currently encompasses over 180 species, which are all plant pathogens (A. De Cock, personal communication). While some species have a narrow host range, others have a very wide host range. *Phytophthora palmivora* can infect over 170 species of host plants in the tropics and subtropics, including species such as cacao, citrus, rubber, coconut, and oil palm (Torres et al. 2016). *Phytophthora capisici* also has a broad host range with tomato, legumes and cucurbits as economically important crops (Kamoun et al. 2015). A more specialized species is *Phytophthora sojae* that only infects soybean (Kamoun et al. 2015). While most research focusses on *Phytophthora* diseases in agricultural settings, also native plants species are affected. For example, in Western Australia *Phytophthora cinnamomi*, known as the 'biological bulldozer', is pathogenic on over 3000 plant species (Hardham 2005; Ribeiro 2013). It caused the death of 75% of the flora in over hundreds of thousands of hectares of the jarrah forests (Weste & Marks 1987). *Phytophthora ramorum* is the causal agent of blight in a wide range of woody plants. In oak and tanoak, the disease is named sudden oak death and is responsible for a rapid decline in native tree species in states on the west coast of the U.S. (Rizzo & Garbelotto 2003; Grunwald et al. 2008).

Phytophthora spp. share a similar life cycle. During vegetative growth, a branching network of hyphae is formed, known as mycelium. As the life cycle progresses, asexual spores, or sporangia, are produced. Under the right environmental conditions, the sporangial cytoplasm cleaves, leading to a zoosporangium. The conditions under which a zoosporangium releases its zoospores differs between species; while for *P. infestans* cool, moist conditions are a stimulus for zoospore release, *P. palmivora* sporangia release zoospores upon exposure to light. Zoospores are the principal dispersal and infection propagules of oomycetes, and they are attracted towards a suitable infection site by chemotaxis. Also sporangia can serve as infection propagules, as they can directly germinate and penetrate host plant cells. Various compounds such as vitamins, organic acids, amino acids and phenolic compounds can serve as chemoattractants for *Phytophthora* spp. (Khew & Zentmyer 1973).

1.4 Eukaryotic cellular signal transduction pathways

Signaling through G-proteins

To respond to environmental cues, a molecular system capable of receiving and transducing extracellular signals is essential for any organism. In eukaryotes, a fundamental and universal signal transduction pathway is G-protein signaling. A simplified overview of this pathway is presented in **Figure 1.2**. G-protein signaling is shared by species from all eukaryotic supergroups and was already present in the last eukaryotic common ancestor (LECA) (de Mendoza et al. 2014). The central elements of G-protein signaling are guanine nucleotide binding (G) proteins and G-protein coupled receptors (GPCRs). Characteristic for the topology of GPCRs are the seven transmembrane (TM) spanning α-helices that are linked by three intracellular and three extracellular loops. A GPCR is oriented in such a way that the N-terminal tail is located extracellularly and the C-terminal tail intracellularly. The extracellular loops and the N-terminal tail make up the ligand binding pocket, while the intracellular domains are involved in downstream propagation of the signal.

In mammalians, G-protein signaling is involved in a wide variety of processes, such as sensory perception (e.g. taste, smell, and light), and sensing various compounds such as neurotransmitters, immunogenic compounds, hormones, or pheromones. Humans have over 1000 genes encoding GPCRs (Insel et al. 2012). However, many of these GPCRs are so-called orphans; receptors for which neither the ligand nor its function is known. In some animals the number of genes encoding GPCRs is even higher: in mice (*Mus musculus*) for example, over 2400 GPCRs are predicted and in elephants (*Loxodonta africana*) some 3400 (Insel et al. 2012). Due to their pivotal role in the regulation of several processes, such as cell proliferation, homeostasis, and metabolism, GPCRs are the primary targets of modern drugs in human medicine. More than 30% of human drugs target GPCRs (Santos et al. 2017). Lower eukaryotes typically have fewer GPCR genes. The slime mold *Dictyostelium discoideum*, for example, has 55 genes encoding GPCRs among which the well-studied

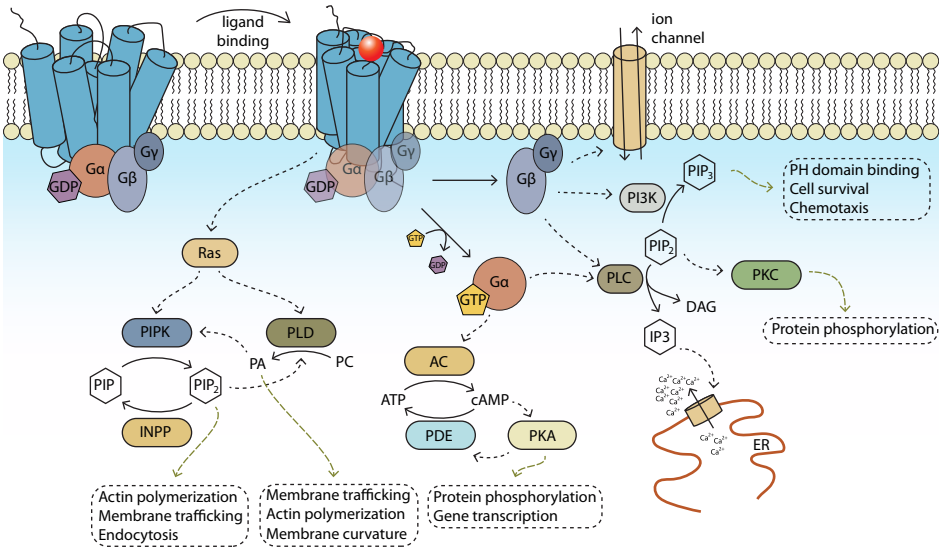

Figure 1.2 | Overview of the classical G-protein signaling pathway in a typical eukaryote. A GPCR is constituted by seven transmembrane domains (blue cylinders), and is associated with a heterotrimeric G-protein complex in its inactive state, in which Gα is bound to GDP. Upon ligand binding, the GPCR changes conformation, and Gα and Gβγ dissociate from each other and from the receptor. The activated Gα and Gβγ subunits lead to activation of downstream effector proteins. Alternatively, small G-proteins, such as Ras, can induce effector proteins. AC: adenylate cyclase; PDE: phosphodiesterase; PKA protein kinase A; PKC: protein kinase C; PLC: phospholipase C; PI3K phosphatidylinositol kinase; PIPK: phosphatidylinositolphosphate kinase; INPP: inositol polyphosphate phosphatase; PIP: phosphatidylinositolphosphate; PLD: phospholipase D; PA: phosphatidic acid; PC: phosphatidylcholine; ER: endoplasmatic reticulum; IP3: inositoltrisphosphate; DAG: diacylglycerol. Examples of cellular responses are depicted in dashed boxes.

cAMP receptors that coordinate aggregation of single cells into a multicellular organism (Prabhu et al. 2007). The yeast *Saccharomyces cerevisiae* has only three GPCR genes which are involved in the recognition of mating pheromones and sugars (Overton et al. 2005).

In its inactive, basal state, a typical GPCR is linked to a heterotrimeric G-protein complex, which consists of G-protein subunits α (Gα), β (Gβ), and γ (Gγ) (Rosenbaum et al. 2009), with Gα bound to GDP. Upon ligand binding, a conformational change is induced in the GPCR, after which the G-protein complex dissociates from the receptor, and GDP is exchanged for GTP on the Gα subunit (**Figure 1.2**). As a result, the 'switch' regions of Gα that are involved in nucleotide binding undergo a conformational change which leads to dissociation of Gα and Gβγ (Clapham & Neer 1997). In turn, the activated Gα and Gβγ subunits regulate downstream enzymes such as adenylate cyclase (AC), phospholipase C (PLC), or phosphoinositide 3-kinase (PI3K) (**Figure 1.2**). These effectors are involved in the production of secondary messengers, such as cAMP, Ca2+, and IP3 (Neves et al. 2002).

Other players in G-protein signaling are small G-proteins (or small GTPases). In contrast to

heterotrimeric G-proteins, small G-proteins act individually and are not directly activated by GPCRs (Sah et al. 2000). Instead, guanine nucleotide exchange factors (GEFs) and GTPase-activating proteins (GAPs) regulate small G-protein activity (Bos et al. 2007), by accelerating the exchange of GDP for GTP and subsequent hydrolysis, respectively. Small G-proteins can be subdivided in five main families: Ras, Rab, Rho/Rac/Cdc42, Sar/Arf1, and Ran (Takai et al. 2001). Rho-dependent pathways have been shown to regulate the phospholipid kinases PI3K and PI(4)P 5-kinase (PIP5K) (Sah et al. 2000). Cdc42 is an important cell cycle regulator.

Signaling through phospholipids

Phospholipids are amphiphilic molecules, composed of a phosphate-bound hydrophilic head group and two fatty acid tails, and are the main constituents of eukaryotic plasma membranes. Additionally, they play an important role as signaling molecules. An important class of phospholipids is that of phosphoinositides, which have inositol as a head group. The most basic form, phosphatidylinositol (PI) is synthesized from CDP-diacylglycerol and *myo*-inositol by PI-synthase (PIS) and can be phosphorylated on three positions on the inositol ring, to form PI-phosphate (PIP), PI-bisphosphate (PIP2), or PI-trisphosphate (PIP3). The enzymes responsible for the phosphorylation are named according to their substrate specificity and activity. For example, the enzyme PI(4)P 5-kinase phosphorylates the 5' position on the inositol ring of PI(4)P, yielding PI(4,5)P2. For simplicity, all different catalytic types of PIP kinases will be referred to as PIPKs. Dephosphorylation of PIPs is carried out by phosphatases from the class of inositol polyphosphate phosphatases (INPPs).

Based on the constitution of the polar head group, different protein targets can be activated to initiate downstream responses. Phospholipid-binding proteins often have specific affinity for a particular phosphorylation stage of the inositol head group. For example, the pleckstrin homology (PH) domain of mouse Sos1, a Ras GTPase, has been shown to have specific affinity for PI(4,5)P2, but not for PI(4)P (Kubiseski et al. 1997). Consequently, the phosphorylation stage of membrane phospholipids may contribute to its localization (Kubiseski et al. 1997). Phosphatidic acid (PA) is the simplest membrane phospholipid but is also a central signaling component acting as a second messenger (Wang et al. 2006). Two main pathways for synthesis of PA are via hydrolysis of phospholipids by phospholipase D (PLD), and phosphorylation of diacylglycerol (DAG) by DAG kinase (DGK) (Wang et al. 2006). Increased levels of cellular PA have been reported to influence a multitude of effector proteins, thereby regulating processes such as actin polymerization, vesicular trafficking, or polarized cell growth (Wang et al. 2006).

What signal transduction pathways are in play in oomycetes?

So far, research on G-protein signaling in oomycetes is primarily limited to studies in two *Phytophthora* species, *P. infestans* and *P. sojae*. In *P. infestans*, genes encoding Gα (*Pigpa1*) (Latijnhouwers et al. 2004) and Gβ (*Pigpb1*) (Latijnhouwers & Govers 2003) have been studied, and in *P. sojae* the genes encoding Gα (*Psgpa1*) (Hua et al. 2008) and a GPCR (*Psgpr11*) (Wang et al. 2010). Both *Pigpa1* and *Pigpb1* are differentially expressed in life stages of *P. infestans*, with the highest expression in sporangia (Laxalt et al. 2002). Gα mutants obtained by transcriptional silencing show impaired zoospore movement, and reduced auto-aggregation and chemotaxis (Latijnhouwers et al. 2004). This indicates a role for PiGPA1 in orienting, and/or moving towards a suitable site of infection. Silenced lines show reduced virulence when inoculated on potato (Latijnhouwers et al. 2004). Likewise, in *P. sojae*, *Psgpa1* silencing affected zoospore chemotaxis towards the soybean isoflavone daidzein, zoospore encystment and cyst germination, and *Psgpa1*-silenced transformants were unable to infect soybean (Hua et al. 2008). Similar to the phenotype observed in *Psgpa1*-silenced transformants, zoospore release was severely impaired in *PsGPR11*-silenced transformants (Wang et al. 2010). In contrast, no effects were observed in chemotaxis towards the soybean isoflavone daidzein. Silencing of the gene encoding Gβ in *P. infestans* resulted in a significant reduction of the number of sporangia when cultured on rye sucrose agar (RSA) (Latijnhouwers & Govers 2003). In addition, a few G-protein interacting proteins and potential downstream proteins have been identified (Dong et al. 2004; Zhang et al. 2016).

Oomycete phospholipid signaling holds unique features

A hallmark of oomycete phospholipid signaling is their expanded repertoire of phospholipid modifying and signaling enzymes (PMSEs), only a few of which resemble domain architectures as known from other eukaryotes (Meijer & Govers 2006; Jiang et al. 2013; Sharma et al. 2015). For example, several phospholipase Ds (PLDs) with N-terminal TM domains or a signal peptide, and distinct types of PI-kinases (PIKs) and PIPKs were identified. Of the 18 PLD genes in *P. infestans*, 17 represent novel subfamilies (Meijer et al. 2011), and similar compositions were found in *P. sojae* and *P. ramorum* (Meijer & Govers 2006). One subfamily contains potentially secreted PLDs, and indeed extracellular PLD activity was observed in several *P. infestans* strains (Meijer et al. 2011). Functional analysis of oomycete PMSEs is limited to a few studies (Hua et al. 2013; Lu et al. 2013; Yang et al. 2013).

1.5 CRISPR/Cas9

A molecular toolbox is elementary for functional gene analysis. By creating specific mutations in target genes, generating knockouts or altering gene expression levels, valuable information can be obtained providing insight into the role or function of a specific gene.

Perhaps one of the single most important advances in molecular biology in recent years was the development of a targeted genome editing system based on CRISPR/Cas9 (short for clustered regularly interspaced short palindromic repeats, and CRISPR associated protein 9, respectively). Genome editing using CRISPR/Cas9 offers an efficient approach for targeted mutagenesis and has been applied in a wide variety of prokaryotes and eukaryotes (Sander & Joung 2014).

For the past two decades or so, since the first reliable DNA transformation method for *Phytophthora* was developed (Judelson et al. 1991), gene silencing and localization of fluorescent fusion proteins have been the prime approaches for functional gene analysis in oomycetes. However, due to the random integration of transgenes and varying levels of silencing efficiency, results with transformed lines often vary not only between experiments and labs but also between biological replicates (Fang & Tyler 2016). Moreover, knockouts are not feasible due to random integration of transgenes and low rates of homologous recombination. After overcoming many technical difficulties, Fang and Tyler developed a CRISPR/Cas9 system (**Box 1.2**) for *P. sojae* and demonstrated the induction of targeted indels in the target gene, as well as gene replacement of the target gene (Fang & Tyler 2016). The system proved to be efficient in obtaining gene knockouts and gene deletions, and has since been used successfully for genome editing and knockout mutagenesis in *P. sojae* (Ma et al. 2017), *P. palmivora* (Gumtow et al. 2017), and *P. capsici* (Tyler, personal communication). With this addition, the molecular toolbox of oomycetes is up to par with that of other eukaryotes. However, to date, it has not yet been employed in *P. infestans*.

1.6 Scope of this thesis

The research presented in this thesis comprehends an integrated molecular and bioinformatic approach, aimed at gaining insight into cellular signaling and cytoskeletal dynamics of the late blight pathogen *P. infestans*. These are elementary cellular processes, and, although being highly conserved in the eukaryotic kingdom, hold many unique features. With the ultimate goal in mind of identifying novel targets for specific control of *P. infestans*, functional characterization of cellular signaling and cytoskeletal dynamics will provide invaluable insights in this respect.

The first two experimental chapters deal with components of G-protein signaling in oomycetes. In **Chapter 2** of this thesis, a molecular phylogeny of a unique family of GPCRs with a phospholipid kinase (PIPK) domain is presented and the sporadic distribution of this so-called GPCR-bigram over various supergroups in the tree-of-life is analysed. Further, we inventoried the proteome of *P. infestans* for GPCRs, with specific emphasis on identifying additional GPCR-bigrams. In **Chapter 3** of this thesis *Pigpg1*, a gene encoding a putative G-protein γ subunit of *P. infestans*, is analyzed in detail. Gα and Gβ have been described and characterized before, and here we present *in silico* and *in vivo* data on the smallest subunit of the heterotrimeric G-protein complex in *P. infestans*.

Chapter 4 covers a study on the microtubule cytoskeleton of *Phytophthora*. An inventory of tubulin- and microtubule-associated protein (MAP) encoding genes in *P. infestans* is provided and we present the first live cell imaging of the tubulin cytoskeleton in *Phytophthora*.

A recent advance in targeted genome editing using CRISPR/Cas9 in *P. sojae* (Fang & Tyler 2016) enabled for the first time to obtain gene knockouts in an oomycete and to perform targeted mutagenesis. The CRISPR/Cas9 system would be asset for the molecular toolbox of *P. infestans*. In **Chapter 5**, a case study on the establishment of this system in *P. infestans* is presented.

In **Chapter 6**, the main results of this thesis are integrated and discussed in a broader context. Remarkable features of oomycetes and their cellular signaling systems are outlined, and future directions are proposed on how to exploit this knowledge for disease control.

Box 1.2 | CRISPR/Cas9 for genome editing

Little techniques have revolutionized the molecular biology field as much as genome editing using CRISPR/Cas9. First discovered as a bacterial and archaeal adaptive immune system against viral invaders (reviewed in (Bhaya et al. 2011, Lander 2016)), the real breakthrough came when the system was shown to be programmable to induce site-specific DNA cleavage *in vitro* (Jinek et al. 2012). Soon thereafter, CRISPR/Cas9-mediated introduction of targeted double-strand breaks (DSBs) in human cells (Cho et al. 2013), and in many other eukaryotic organisms (Sander & Joung 2014) was demonstrated.

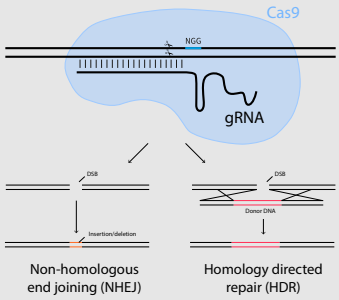

In CRISPR/Cas systems for genome editing, a nuclease, e.g. Cas9, is targeted to the desired DNA sequence by a so-called synthetic guide RNA (gRNA). The protospacer, twenty nucleotides at the 5' end of the gRNA, directs Cas9 to a specific target DNA site, which must be immediately 5' of a PAM (protospacer adjacent motif) sequence (Ran et al. 2013). The nature of the PAM sequence depends on the nuclease; for Cas9 the canonical form is NGG. When Cas9 is directed to the target site, it induces a DSB. Two major DNA damage repair pathways are available for repair of the DSB: the error-prone non-homologous end joining (NHEJ) and the high-fidelity homology-directed repair (HDR) pathway (Ran et al. 2013). When no repair template is present DSBs are repaired via NHEJ, which often leads to insertions/deletions (indels) around the position of the DSB. When in a coding region, these indels can cause frameshift mutations or premature stop codons. When a repair template is supplied, specific mutations can be introduced via repair using HDR, though this repair mechanism occurs at a lower frequency than NHEJ (Ran et al. 2013). Templates for HDR can be delivered as plasmid DNA or single-stranded oligodeoxynucleotides (ssODNs), and consist of the actual repair template containing the desired mutation(s) or the sequence to be integrated, flanked by sequences of sufficient length (50-150 nt for ssODNs, up to 1 kb for plasmid DNA) that are homologous to the sequences at the preferred integration site.

Chapter 2

The presence of GPCR-bigrams in the eukaryotic kingdom

Johan van den Hoogen, Harold J. G. Meijer, Michael F. Seidl, Francine Govers

This chapter is published as: The ancient link between G-protein coupled receptors and C-terminal phospholipid kinase domains (2018), *mBio* **9**. doi: 10.1128/mBio.02119-17

2.1 Abstract

Sensing external signals and transducing these into intracellular responses requires a molecular signaling system that is crucial for every living organism. Two important eukaryotic signal transduction pathways that are often interlinked are G-protein signaling and phospholipid signaling. Heterotrimeric G-protein subunits activated by G-protein-coupled receptors (GPCRs) are typical stimulators of phospholipid signaling enzymes such as phosphatidylinositol phosphate kinases (PIPKs) or phospholipase C (PLC). However, a direct connection between the two pathways likely exists in oomycetes and slime molds, as they possess a unique class of GPCRs that have a PIPK as an accessory domain. In principle, these so-called GPCR-PIPKs have the capacity of perceiving an external signal (via the GPCR domain) that, via PIPK, directly activates downstream phospholipid signaling. Here we reveal the sporadic occurrence of GPCR-PIPKs in all eukaryotic supergroups, except for plants. Notably, all species having GPCR-PIPKs are unicellular microorganisms that favor aquatic environments. Phylogenetic analysis revealed that GPCR-PIPKs are likely ancestral to eukaryotes and significantly expanded in the last common ancestor of oomycetes. In addition to GPCR-PIPKs, we identified five hitherto-unknown classes of GPCRs with accessory domains, four of which are universal players in signal transduction. Similar to GPCR-PIPKs, this enables a direct coupling between extracellular sensing and downstream signaling. Overall, our findings point to an ancestral signaling system in eukaryotes where GPCR mediated sensing is directly linked to downstream responses.

2.2 Importance

G-protein-coupled receptors (GPCRs) are central sensors that activate eukaryotic signaling and are the primary targets of human drugs. In this report, we provide evidence for the widespread though limited presence of a novel class of GPCRs in a variety of unicellular eukaryotes. These include free-living organisms and organisms that are pathogenic for plants, animals, and humans. The novel GPCRs have a C-terminal phospholipid kinase domain, pointing to a direct link between sensing external signals via GPCRs and downstream intracellular phospholipid signaling. Genes encoding these receptors were likely present in the last common eukaryotic ancestor and were lost during the evolution of higher eukaryotes. We further describe five other types of GPCRs with a catalytic accessory domain, the so-called GPCR-bigrams, four of which may potentially have a role in signaling. These findings shed new light onto signal transduction in microorganisms and provide evidence for alternative eukaryotic signaling pathways.

2.3 Introduction

To respond to environmental cues and changes, a molecular system that can receive external signals and transduce them to intracellular responses is fundamental for every living organism (de Mendoza et al. 2014). In eukaryotes, G-protein-coupled receptors (GPCRs) and their associated heterotrimeric G-protein complex are important and universal signal transduction components that transduce extracellular to intracellular signals. A characteristic feature of GPCRs is their topology with seven transmembrane (TM)-spanning helices flanked by an extracellular N-terminus and an intracellular C-terminus. Upon binding of a ligand to a GPCR, conformational changes lead to activation and dissociation of the heterotrimeric G-protein complex. G-protein subunits α, β, and γ regulate key effector enzymes such as adenylate cyclase (AC), phospholipase C (PLC), and phosphoinositide 3-kinase resulting in the production of secondary messengers, such as cAMP, Ca2+, and inositol trisphosphate (Dupre et al. 2009). GPCRs are encoded by an evolutionarily ancient gene family that was already present in the last eukaryotic common ancestor (LECA) (de Mendoza et al. 2014). In mammalians, this is the largest superfamily with genes encoding a very diverse group of transmembrane (TM) proteins. Humans, for example, have over 800 GPCRs (Fredriksson & Schioth 2005). They function in a wide variety of processes not only as sensory receptors for taste, smell, or light (rhodopsin) but also as receptors of neurotransmitters, hormones, and nucleotides (Fredriksson & Schioth 2005; Rosenbaum et al. 2009). Consequently, several GPCRs are important targets of modern drugs in human medicine, with over a third of all drugs targeting GPCRs (Rask-Andersen et al. 2011). Lower eukaryotes typically have fewer GPCRs than mammalians. For example, the slime mold *Dictyostelium discoideum* has 55 GPCR genes (Prabhu et al. 2007) while the yeast *Saccharomyces cerevisiae* has only 3 GPCR genes (Kraakman et al. 1999; Overton et al. 2005).

Our research focuses on plant-pathogenic microbes, organisms for which cellular sig-

naling is of utmost importance for responding to environmental cues but especially for recognizing suitable hosts for infection. Arguably, among the most important group of plant pathogens are oomycetes (also known as water molds). Oomycetes occupy environmental niches similar to fungi but do not belong to the fungal kingdom (Kamoun et al. 2015). Instead, oomycetes belong to the stramenopiles, a lineage that also includes, among others, brown algae and diatoms (Lévesque 2011). One of the most notorious oomycetes is the late blight pathogen *Phytophthora infestans*, the culprit responsible for the Irish potato famine in the mid-19th century (Fry 2008).

Genome comparisons between oomycetes and other eukaryotes revealed distinct features of their gene and protein repertoires (Govers & Gijzen 2006; Tyler et al. 2006). The number of distinct protein domain combinations, or bigrams, is significantly higher in oomycetes than in organisms with similar numbers of domain types, and many proteins involved in cellular signaling are composed of unique bigrams (Seidl et al. 2011). For example, there are many oomycete-specific classes of protein kinases with accessory domain combinations not observed in other lineages (Judelson & Ah-Fong 2010). Another unique protein domain combination was found in the family of GPCR-PIPKs, phosphatidylinositol phosphate kinases (PIPKs) with an N-terminal GPCR (Meijer & Govers 2006). The combination of a GPCR and a PIPK domain in one protein suggests that these proteins can function as a link between two important signaling networks, i.e. G-protein signaling and phospholipid signaling. The products of PIPKs, such as PI(4,5)P2, are both important membrane components and universal signaling components. For some time GPCR-PIPKs were thought to have limited phyletic distribution, as only one homolog was identified outside the oomycetes, namely RpkA (Bakthavatsalam et al. 2006), a receptor in the slime mold *Dictyostelium discoideum* that is involved in phagocytosis (Riyahi et al. 2011). More recently, GPCR-PIPK genes were identified in ciliates and in lower unikonts (Leondaritis et al. 2013), suggesting that GPCR-PIPKs are more widespread than previously thought.

The aim of this study was to provide a comprehensive overview of the distribution of GPCR-PIPKs among eukaryotes and to gain insight into their origin and evolution. We identified GPCR-PIPKs throughout eukaryotes and reconstructed their molecular phylogeny. With the aim to identify additional GPCR-bigrams, i.e. proteins with a GPCR domain and an accessory domain, we mined the *P. infestans* genome for GPCRs and identified five hitherto-unknown GPCR-bigram types, some of which are shared in other eukaryotes. Of these, four link GPCRs to accessory domains with roles in signaling. Taken together, our results suggest the presence of alternative signaling pathways in eukaryotes with GPCR-bigrams as central elements.

2.4 Results

GPCR-PIPKs are conserved in oomycetes

Previously, GPCR-PIPKs were identified in *Phytophthora* species but also in a few closely related downy mildews such as *Hyaloperonospora arabidopsidis* and *Plasmopara halstedii* (Meijer & Govers 2006; Haas et al. 2009; Baxter et al. 2010; Sharma et al. 2015). Here, we analyzed the genomes of 20 oomycetes (**S2.1**) for the presence of GPCR-PIPKs. These 20 include species from different genera and are pathogenic for both plants and animals. We found that the GPCR-PIPK family is conserved in all 20 oomycetes with 9 to 13 GPCR-PIPK genes in each species (**Table S2.1**). The genes were named D1 through D12, in line with the nomenclature of and similarity to *P. infestans* GPCR-PIPKs (**Table S2.2**) (Haas et al. 2009). Despite the high conservation of the GPCR-PIPK family throughout oomycetes, we observed some differences between species. For example, duplications of several GPCR-PIPKs are found in *Albugo*, *Aphanomyces*, and *Saprolgenia* species, while GPCR-PIPK D9 is found only in *Hyaloperonospora*, *Phytophthora*, and *Pythium* species (**Table S2.2**).

GPCR-PIPKs are present in various eukaryotic genera

The finding that GPCR-PIPKs are not limited to oomycetes and amoebozoans but also occur in ciliates and Choanoflagellates (Riyahi et al. 2011; Leondaritis et al. 2013) raised the issue of how widespread GPCR-PIPKs are in eukaryotes. We performed a combination of iterative BLAST, hidden Markov model, and text-based searches (**Figure S2.1a**) against proteomic data from a wide range of species, including archaea, bacteria, and all eukaryotic supergroups. We identified 60 proteins that contain a 7TM domain preceding a PIPK domain and that are thus *bona fide* GPCR-PIPKs (**Table S2.3**). They are distributed over distantly related taxa in eukaryotic supergroups (**Figure 2.1**), with the exception of the plant kingdom. Within Stramenopiles, the lineage that comprises the oomycetes, we could detect GPCR-PIPKs in only one non-oomycete species, the alga *Aureococcus anophagefferens* (**S2.1**). GPCR-PIPKs occur in several Chromalveolates, the supergroup that includes the Stramenopiles and ciliates. In several ciliates, for example, in *Stylonychia lemnae*, we found numerous GPCR-PIPKs (**Table S2.1**). The haptophytes *Emiliania huxleyi* and *Chrysochromulina tobin* possess three and four GPCR-PIPKs, respectively. Haptophytes are a group of marine protists whose origin dates back to approximately 1,000 to 600 million years ago (mya) (Liu et al. 2010). In unikonts, the supergroup that includes the metazoans, homologs of *D. discoideum* RpkA could be identified in numerous amoebozoans (**Table S2.1**). GPCR-PIPKs were also identified in early branching unikonts such as the choanoflagellate *Salpingoeca rosetta* and the Apusozoa *Thecamonas trahens* (**Table S2.1**). Additionally, we identified GPCR-PIPKs in other premetazoans such as *Capsaspora owcarzaki* and the sponge *Amphimedon queenslandica*. However, GPCR-PIPKs seem to be absent from multicellular metazoans and fungi. Furthermore, homologs could be found

in two *Naegleria* species in the supergroup Excavates and as detailed below, in two species in the supergroup Rhizaria (**Table S2.1**). *Naegleria* spp. are free-living protists belonging to the Heterolobosea, a lineage that diverged from other eukaryotes over a billion years ago (Fritz-Laylin et al. 2010). In summary, GPCR-PIPKs seem to occur in multiple diverse genera throughout the eukaryotic tree of life and yet they are restricted to unicellular and, in most cases, to species that diverged early (**Figure 2.1**).

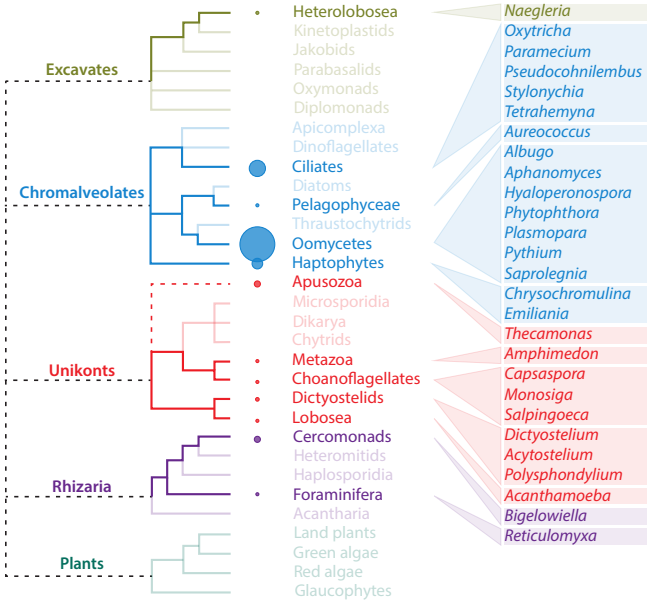

Figure 2.1 | Consensus cladogram of selected eukaryotes, highlighting in bold lineages and genera with species having one or more GPCR-PIPKs. The size of the circles is proportional to the average number of GPCR-PIPKs per taxon. The tree is based on phylogenies described by Keeling et al. (2005) and Koonin (2010), the placement of the Apusozoa is based on Paps et al. (2013). Dashed polytomies indicate unresolved relationships.

Most GPCR-PIPKs share a novel central conserved motif LRxGI

To identify conserved amino acid motifs in GPCR-PIPKs, we made a multiple sequence alignment of all identified GPCR-PIPKs. In most GPCR-PIPKs, conserved motifs, such as the catalytic DLGKS and MDYSL motifs (Anderson et al. 1999) and the (di)lysine motif in the activation loop (Bakthavatsalam et al. 2006), which is involved in substrate specificity (Kunz et al. 2000), can be identified in the PIPK domain (**Figure 2.2**). In between the GPCR and PIPK domain, we observed a short region that is highly conserved (**Figure 2.2**). The highest identity is traced across 13 amino acids and the consensus starts with a highly conserved leucine-arginine (LR) dimer followed by nine less extensively conserved amino acids and a glycine-isoleucine (GI) dimer at the end (**Figure 2.2**) - further referred to as the LRxGI motif. It consists of both hydrophobic and hydrophilic amino acids, and according to a preliminary secondary structure prediction using Phyre2 (Kelley et al. 2015) it most

likely adopts an α-helical structure (data not shown). The LRxGI motif is present in all 223 oomycete GPCR-PIPKs included in this study. Among the 60 non-oomycete GPCR-PIPKs the motif is absent in 9 gene models, mostly in ciliate GPCR-PIPKs (**Table S2.3**).

We next examined whether the LRxGI motif is unique for GPCR-PIPKs or also occurs in other protein sequences. Using the motif sequence as a query, BLAST and HMM searches resulted exclusively in hits in GPCR-PIPKs. Notably, two new GPCR-PIPKs were identified that were not detected in the search strategy mentioned above. Hits in *Reticulomyxa filosa*, a species in the supergroup Rhizaria, targeted two truncated gene models, one containing a GPCR region N-terminal of the LRxGI motif and the other with a PIPK domain at the C-terminus. The genome assembly of *R. filosa* is highly fragmented (Glockner et al. 2014), so the two gene models possibly represent only one GPCR-PIPK gene. Although the sequence overlap of the two gene models is too small, the presence of an LRxGI motif as hallmark of a GPCR-PIPK, led us to conclude that *R. filosa* has one or possibly more GPCR-PIPKs. By using the sequence of reconstituted *R. filosa* GPCR-PIPK as the search query, two more homologs in the Rhizaria supergroup were identified, namely, in the species *Bigelowiella natans*.

GPCR-PIPKs have distinct kinase domains

We next examined the evolutionary relationship of the GPCR-PIPKs. To this end we retrieved sequences of all PIPKs that are present in organisms in which we found one or more GPCR-PIPKs (**Table S2c, S2d**). A typical eukaryote contains three types of PIPKs, referred to as type I, II, and III, which are grouped based on their catalytic activity and differ in domain composition (**Figure 2.3a**). Since the *Phytophthora* GPCR-PIPKs and *Dictyostelium* RpkA form a separate branch in the phylogenetic tree, they were classified as type IV PIPKs (Riyahi et al. 2011). To reconstruct the overall PIPK phylogeny we included sequences of all four types and used only the regions covering the PIPK domain. Our phylogenetic analyses confirmed earlier studies (Bakthavatsalam et al. 2006; Meijer & Govers 2006), showing that the catalytic PIPK domains of GPCR-PIPKs (type IV) are distinct from the three other PIPK types. Moreover, type IV PIPKs seem to be more closely related to type I and II than to type III PIPKs (**Figure 2.3b**). Of the 445 PIPKs present in the tree, 9 are derived from gene models which either are truncated or have equivocal protein domain predictions (**Table S2.5**), and hence the classification based on domain composition is ambiguous. Although classified as type I, II, or III PIPKs they are most likely type IV PIPKs, i.e. GPCR-PIPKs (**Figure 2.3b**). The relationships between the PIPK domains of oomycete GPCR-PIPKs (**Figure S2.2**) reflect the oomycete species phylogeny (**Figure S2.3**), and as such, it is likely that GPCR-PIPKs and the subsequent expansion of the family are ancestral to oomycetes. Group D11 and D12 GPCR-PIPKs form a clade separate from other GPCR-PIPKs (**Figure 2.3b**), which might indicate a separate origin.

Some GPCR-PIPKs in phytoplanktonic species are present within the clades comprising

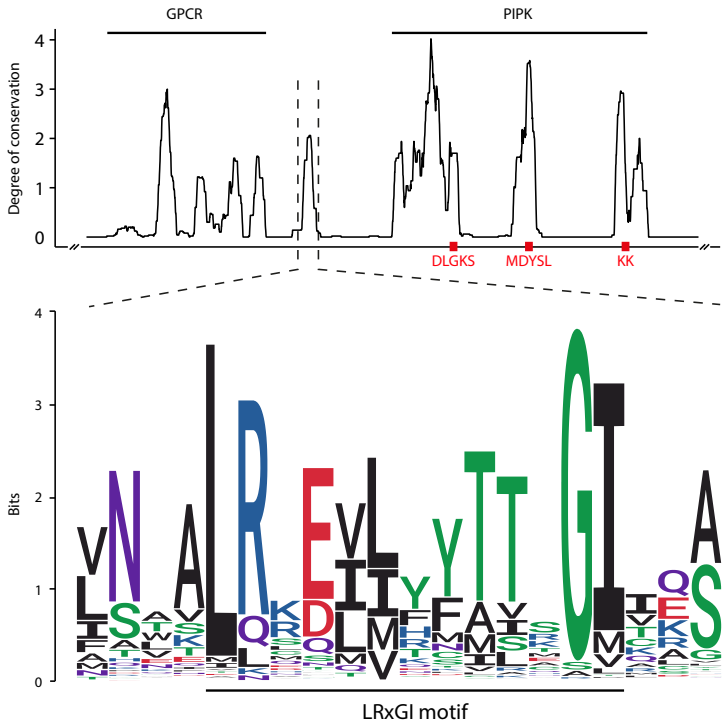

Figure 2.2 | Degree of conservation of all GPCR-PIPKs included in this study (**top**) and sequence logo of the newly identified LRxGI motif (**bottom**). The degree of conservation was determined by the use of a sliding moving average over 50 positions. The approximate positions of three conserved PIPK motifs (DLGKS, MDYSL, and KK) are indicated. Color coding of amino acid residues in the sequence logo is shown according to chemical properties as follows: red, acidic; blue, basic; black, hydrophobic; purple, neutral; green, polar.

primarily oomycete GPCR-PIPKs. For example, an *A. anophagefferens* GPCR-PIPK forms a clade together with the oomycete GPCR-PIPKs D9 (**Figure 2.3b**). The placement of two *E. huxleyi* and two *C. tobin* GPCR-PIPKs in the clade containing oomycete GPCR-PIPKs D11 and D12 is strongly supported by bootstrap analysis (**Figure 2.3b**). This indicates that an ancestral GPCR-PIPK was present in the ancestor of oomycetes, haptophytes, and *Pelagophyceae, which are* three lineages within the Chromalveolates. Notably, all ciliate GPCR-PIPKs cluster in one clade. Even though their phylogenetic position might suggest that these GPCR-PIPKs arose independently of the other GPCR-PIPKs, the phylogenetic support is insufficient to firmly establish this hypothesis. The recent whole-genome duplication events in *P. tetraurelia* (Aury et al. 2006) are clearly reflected in duplications of GPCR-PIPKs. A similar pattern is observed in the other ciliates included in this study.

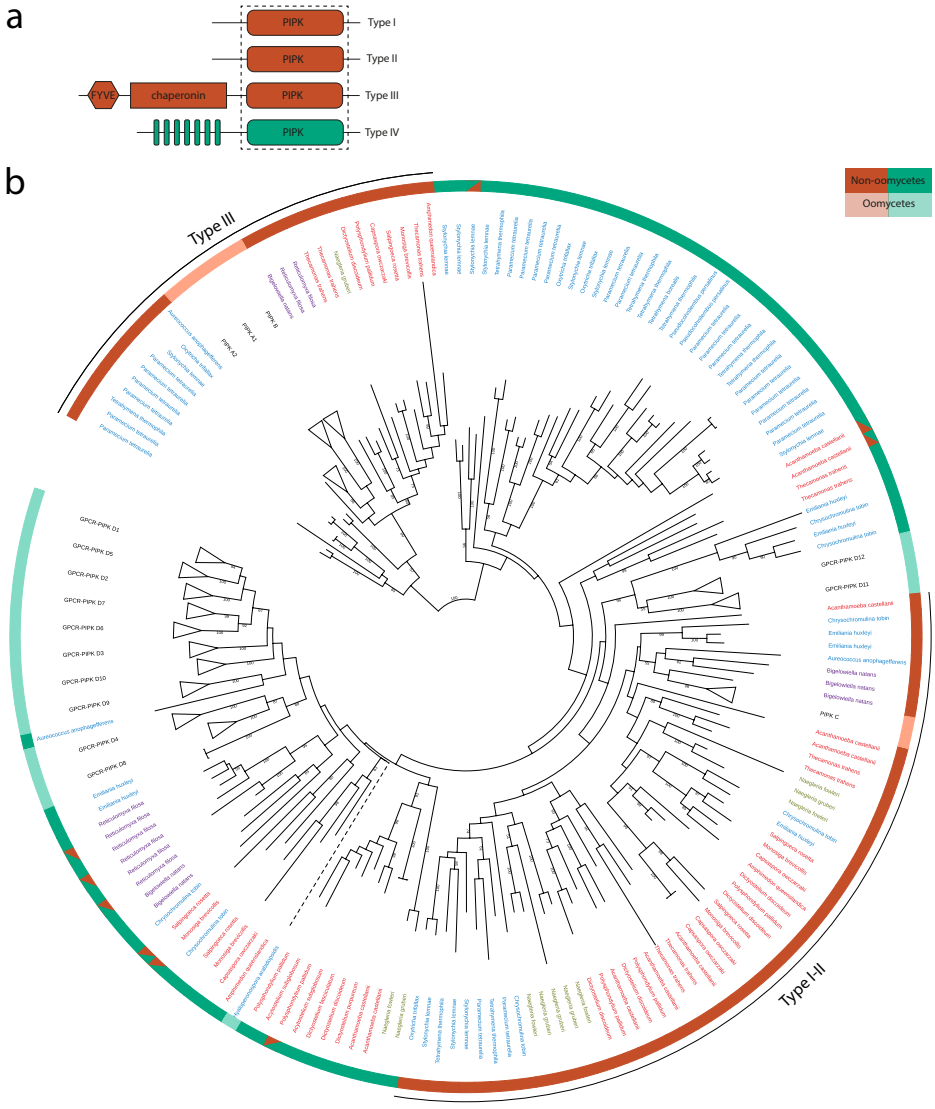

Figure 2.3 | (**a**) Typical domain organization in the four PIPK types. The regions contained in the dashed box are used for constructing the tree. Protein and domain lengths are not on scale. **b**) Phylogenetic tree of type I, II, III and IV PIPKs. The outer circle shows the classification of PIPKs based on domain composition with orange representing type I, II, and III PIPKs and lime type IV PIPKs (i.e. GPCR-PIPKs). Split-color bars indicate truncated gene models. The color coding of the species names corresponds to the supergroup colors in **Figure 2.1**. The numbers at the nodes are bootstrap support percentages from RaxML (500 replicates), bootstrap values <50 are omitted. Clades encompassing oomycete proteins are collapsed and classified based on homology with P. infestans PIPK classes (Meijer & Govers 2006). Dashed lines are truncated for simplification and indicate arbitrary branch lengths. A tree with non-collapsed clades and including codes of the gene models is provided in **Figure S2.2**

P. infestans and other oomycetes have multiple GPCR-bigrams

Oomycetes have an expanded repertoire of bigrams (Seidl et al. 2011) and many of these unique bigrams are predicted to have a role in cellular signaling. GPCR-PIPKs are one example, but is possible that there are other GPCR-bigrams that have the ability to link GPCR-mediated sensing directly to specific downstream signaling pathways. To identify other GPCR-bigrams, we first set out to identify all GPCRs present in *P. infestans* and then selected the subset in which the GPCR domain is flanked by an accessory domain. These were then used as a query to search for homologs in other oomycetes and more widely, in other eukaryotes.

Identification of GPCRs based on protein sequence can be troublesome due to the limited sequence conservation across phylogenetic lineages. Hence, we exploited the most characteristic attribute of GPCRs, their membrane topology with seven TM-spanning domains. To identify putative GPCRs in *P. infestans*, we scanned the proteome for TM domains (**Figure S2.1b**). Approximately 18% of the gene models were predicted to encode TM-containing proteins, which is comparable to other eukaryotes (data not shown). From a total of approximately 3200 gene models we selected 687 with 5 to 9 predicted TM regions. We then used different tools to predict accessory domains and discarded those encoding known non-GPCR TM proteins, such as transporters and ion channels. This resulted in 132 candidates with a putative GPCR signature (**Table S2.6**). Of these, 44 were GPCRs with an N- or C-terminal catalytic accessory domain, or GPCR-bigrams. These included the GPCR-PIPKs, but in addition, five novel types of GPCR-bigrams were identified (**Figure 2.4**) and are described below. Homologs for each of these GPCR-bigrams were found in other oomycetes, and the copy numbers in each species were in the same range as in *P. infestans*. However, the distribution of the other GPCR-bigrams outside the oomycetes was more restricted than the distribution of GPCR-PIPKs.

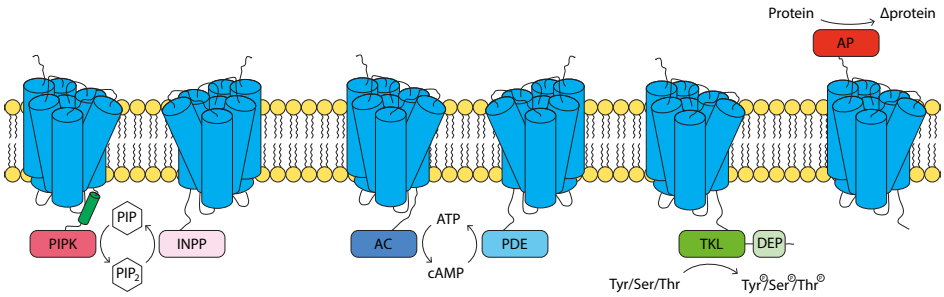

Figure 2.4 | Schematic representation of the domain organization of GPCR-bigrams in oomycetes and their predicted catalytic activities. Blue cylinders represent transmembrane helices. PIPK: phosphatidylinositol-4-phosphate 5-kinase; INPP: inositol polyphosphate phosphatase; PIP: phosphatidylinositol; AC: adenylyl cyclase; PDE: phosphodiesterase; DEP: Dishevelled, Egl-10 and Pleckstrin; AP: aspartic protease.

Of the 44 GPCR-bigrams found to be encoded on the *P. infestans* genome, 17 have a C-terminal tyrosine kinase-like (TKL) domain, making the GPCR-TKLs the largest group of GPCR-bigrams in *P. infestans*. The occurrence of bigrams consisting of a TKL domain and TM domains was already reported in a kinome inventory of *P. infestans* (Judelson & Ah-Fong 2010), but the notion that these proteins have a GPCR signature was not mentioned. Of the 17 *P. infestans* GPCR-TKLs, 8 have a single DEP domain located C-terminally of the kinase domain (**Table S2.7**). The DEP domain is found in several proteins involved in G-protein signaling and is important for interaction of those proteins with various partners at the membrane, including phospholipids and membrane receptors (Consonni et al. 2014).

The number of GPCR-TKL genes in most oomycetes is similar to that in *P. infestans* (**Tables S2.1, S2.7**). *H. arabidopsidis*, however, has only four homologs (**Table S2.1**), which is in line with previous reports that the kinome of *H. arabidopsidis* is smaller than that of *P. infestans* (Judelson & Ah-Fong 2010). The low number of GPCR-TKL genes predicted in *P. capsici* is likely due to poor coverage and/or annotation of the genome sequence. The slime mold *D. discoideum* has two proteins resembling oomycete GPCR-TKLs but lacking the DEP domain (Goldberg et al. 2006), with homologs in other amoebozoans (**Table S2.1**). We have no evidence for the presence of GPCR-TKLs in organisms from taxa other than oomycetes or amoebozoans.

The third largest group after the GPCR-TKLs and GPCR-PIPKs comprises GPCR-bigrams that have an inositol polyphosphate phosphatase (INPP) domain as accessory domain. *P. infestans* has seven GPCR-INPP genes and between one and nine homologs are present in other oomycetes (**Tables S2.1, S2.8**). INPPs are phosphatases that can dephosphorylate PIP2. Since PIP2 is a product of PIPK activity we speculate that the GPCR-PIPKs and GPCR-INPPs in oomycetes operate as a couple in a cycle of phospholipid phosphorylation-dephosporylation. In other eukaryotic taxa, the presence of GPCR-INPPs is limited to the microalga *Nannochloropsis gaditana*, a species that is in the Stramenopile lineage and thus is relatively closely related to oomycetes. Like *P. infestans*, *N. gaditana* has seven GPCR-INPP genes but in contrast it lacks GPCR-PIPKs (**Table S2.1**).

Two novel types of GPCR-bigrams identified in this study are likely involved in cAMP signaling. One type, encoded by four *P. infestans* gene models, has adenylyl cyclase (AC) as a C-terminal accessory domain while the other type, encoded by three gene models, has phosphodiesterase (PDE) as a C-terminal accessory domain. Adenylyl cyclases catalyze the conversion of ATP into cyclic AMP while PDE can hydrolyze cAMP or other cyclic nucleotides to ATP or NTP, respectively. Other oomycetes have comparable numbers of genes encoding GPCR-ACs and GPCR-PDEs, although genes encoding GPCR-PDEs could not be identified in some species (**Tables S2.1, S2.9, S2.10**). Outside oomycetes, no homologs of GPCR-ACs or GPCR-PDEs were found. These findings imply that, like phospholipid signaling, cAMP signaling in oomycetes is to some extent regulated by proteins with a N-terminal GPCR domain.

The last of the six types of GPCR-bigrams is an outlier. This GPCR-bigram has a C-terminal GPCR domain instead of an N-terminal GPCR domain, while the N-terminus harbors aspartic protease (AP) as an accessory domain. *P. infestans* has one AP-GPCR gene, *PiAP5*, which is one of the 12 *P. infestans* genes encoding an AP (Kay et al. 2011). On the basis of the predicted membrane topology of AP5, we assume that the catalytic domain is located extracellularly. This is supported by the presence of a signal peptide, which is likely required for proper translocation of the AP domain across the endoplasmic reticulum during posttranslational processing of the protein. All other oomycetes have a single homolog of *PiAP5* (**Tables S2.1, S2.11**). Outside the oomycetes however, no proteins with similarity to AP-GPCR could be identified.

2.5 Discussion

Domain rearrangements are perhaps among the most important factors in the evolution of multidomain proteins (Bjorklund et al. 2005). Such mechanisms, by recombining existing domains, can lead to novel multidomain proteins, possibly including proteins with different or new functions. Many multidomain proteins, often with domain combinations not found elsewhere, have been observed previously in oomycetes (Seidl et al. 2011). Several of these proteins have a GPCR domain, indicating a direct link between environmental sensing and intracellular signaling (Meijer & Govers 2006). Here we provide evidence for a more widespread presence of one such bigram type, the GPCR-PIPK. Also, we show that, in addition to GPCR-PIPKs, oomycetes have five other distinct types of GPCR-bigrams, four of which have potential roles in signal transduction.

GPCR-PIPKs were first identified in the genus *Phytophthora* (Meijer & Govers 2006). In this report, we show that all oomycetes species that have been sequenced to date have a family of at least nine GPCR-PIPKs and that several species in taxa other than oomycetes also have GPCR-PIPKs, albeit typically in smaller numbers. We identified GPCR-PIPKs in species belonging to four of the five eukaryotic supergroups, with the exception being plants; however, their presence is limited to a relatively small number of organisms. These organisms are evolutionary very distantly related. For example, the evolutionary distance between the genera *Phytophthora* and *Naegleria* is extremely large and likely similar to the distance to LECA, i.e. over a billion years (Koonin 2010; Koumandou et al. 2013). Taken that horizontal gene transfer (HGT) events are rare (Keeling & Palmer 2008), and that the general species phylogeny is reflected in the phylogenetic reconstruction of GPCR-PIPKs, HGT is unlikely to have had a major role in the evolution of GPCR-PIPKs. Moreover, features shared by *Naegleria* spp. and other eukaryotic groups are likely to have existed in their common ancestor (Fritz-Laylin et al. 2010). Consequently, the widespread presence of GPCR-PIPKs in taxonomically unrelated groups is best explained by a shared ancestry in the LECA, fitting earlier hypotheses (de Mendoza et al. 2014).

Despite their evolutionary distance, organisms with GPCR-PIPKs share some features. The

first, and most obvious, is that all can be regarded as unicellular microorganisms. Second, most organisms occupy similar environmental niches, residing in a watery environment, and have an important swimming life stage. While some are harmless microorganisms, many species, such as the human pathogens *Naegleria foweri* and *Acanthamoeba castellani* and the many plant and animal pathogenic oomycetes are important pathogens. Others, such as *Aureococcus anophagefferens* and *Emiliania huxleyi*, have an important environmental impact and can cause harmful algal blooms.

Although GPCRs and G-proteins are ubiquitously present in metazoans, GPCR-bigrams are rare or even nonexistent. Some metazoan GPCRs contain N- or C-terminal extensions, but these do not contain catalytic domains. Since GPCR-PIPK genes can be identified in the common ancestors of metazoans, such as sponges and choanoflagellates, it is likely that these genes were lost during the expansive evolution of the G-protein signaling network in higher metazoans. Notably, GPCR-PIPKs are absent in plants, including lower plants such as red algae and glaucophytes. However, GPCRs are rare in plants and plant G-proteins are self-activating and might act independently of GPCRs (Urano et al. 2013). Only one putative GPCR has been described in *Arabidopsis thaliana* (Pandey & Assmann 2004), but its precise role remains to be determined. It is possible that the ancestral GPCR-PIPK was lost together with other GPCRs during the early evolution of plants.

Our searches covered a wide variety of species, including archaea, bacteria and organisms from all eukaryotic supergroups. With the vast number of high-quality genome sequences of higher metazoans and plants available nowadays, it is unlikely that we have failed to detect GPCR-PIPKs in these highly developed multicellular organisms, so we are confident in stating that these organisms do not have GPCR-PIPKs. In contrast, this is less certain for other lineages, such as diatoms, brown algae, Rhizaria and Excavates, from which only a limited number of genomes have been sequenced. Consequently, it is not unlikely that with the release of new or higher-quality genome sequences more species with GPCR-PIPKs can and likely will be identified.

We have not observed a correlation between the presence of GPCR-PIPKs and the overall number of GPCRs, heterotrimeric G-proteins, or GPCR-regulatory proteins. For example, whereas some organisms identified to have GPCR-PIPKs have no or a very limited number of Gα subunits, *N. gruberi* and *B. natans* have over 30 Gα subunits (de Mendoza et al. 2014). Similarly, 229 regulators of G-protein signaling (RGS) are present in the *N. gruberi* genome, while a very limited number is present in other organisms with GPCR-PIPKs (de Mendoza et al. 2014).

The LRxGI motif is strictly limited to GPCR-PIPKs and is present in nearly all GPCR-PIPKs included in this study. The presence of such a specific and unique motif further strengthens the hypothesis of a shared ancestry of GPCR-PIPKs. The LRxGI motif is located relatively close to the GPCR region, leading to the inference that it is not likely to be an integral part of the PIPK domain. Its amphilicity, predicted secondary structure, and proximity to

the 7TM region are reminiscent of a structural motif that is often found in mammalian rhodopsin-like GPCRs as well as in angiotensin type 1 receptor (AT1R) (Hirst et al. 2015). This amphipathic 'helix 8' (H8) is present just following the last TM domain and lies parallel to the cytoplasmic membrane surface. H8 has been shown to be involved in G-protein activation, conformational stabilization of the GPCR and phospholipid interaction (Huynh et al. 2009; Feierler et al. 2011; Hirst et al. 2015). For example, H8 of AT1R specifically interacts with PI(4)P (Hirst et al. 2015). By disrupting the structural organization of the membrane, this interaction might trigger a conformational change of the GPCR (Hirst et al. 2015). Hypothetically, the LRxGI motif could operate by a similar mechanism. By forcing itself into the plasma membrane, potentially directed by PI(4)P, it could aid in phosphorylation by bringing the PIPK domain into closer proximity to the membrane. Alternatively, the LRxGI motif could serve as a linker to connect the GPCR and PIPK domain and modulate conformational shift(s). This is not very likely however, as this would not explain the particularly high sequence conservation in a relatively small region of the sequence linking the GPCR and PIPK domain.

While GPCR-PIPKs are present throughout the eukaryotic kingdom, the distribution of other GPCR-bigrams is more limited. Apart from oomycetes, GPCR-TKLs are found only in *Amoebozoa* and GPCR-INPPs only in the stramenopile alga *Nannochloropsis*, while GPCR-ACs, GPCR-PDEs, and AP-GPCR are restricted to oomycetes. The large number of genes encoding GPCR-bigrams in oomycetes (around 44 in each species) strongly suggests that these organisms evolved toward G-protein signaling pathways. The catalytic domains found in GPCR-bigrams are also found in proteins with a canonical domain organization. For example, *P. infestans* has four GPCR-ACs in addition to eight ACs with a universal domain composition (data not shown).

The processes in which GPCR-bigrams are predicted to be involved are typically regulated by G-proteins. For example, many ACs are activated by stimulatory Gα subunits (Gsα) or G$\beta\gamma$ subunits and deactivated by inhibitory Gα subunits (Giα). Higher metazoans have multiple Gα, Gβ, and Gγ subunits. Combinations of different subunits give rise to a large variety of heterotrimeric G-protein complexes, each with specific functions. In contrast, oomycetes have only one Gα, Gβ, and Gγ subunit and thus only one uniform heterotrimeric G-protein complex. Silencing of the Gα subunit gene or Gβ subunit gene in *P. infestans* results in aberrant swimming behavior of zoospores or deficiencies in sporulation, respectively, but does not affect viability (Latijnhouwers & Govers 2003; Latijnhouwers et al. 2004). This shows that the heterotrimeric G-protein complex is not by definition the preferred partner of GPCRs in all life stages of *P. infestans*. With respect to regulating AC activity, GPCR-ACs and GPCR-PDEs might provide a direct link between GPCR sensing and the cAMP signal transduction pathway, thereby bypassing G-protein intermediates.

Similarly, the large group of GPCR-TKLs might harness oomycetes with an alternative GPCR desensitization pathway. Desensitization of ligand-activated GPCRs is typically initiated by recruitment of β-arrestins upon phosphorylation of residues within the intra-

cellular loop and C-terminal tail of the GPCRs. The kinases involved are G-protein-coupled receptor kinases (GRKs), cAMP-dependent protein kinase (PKA), or protein kinase C (PKC) (Ferguson 2001). However, only one GRK was detected in *P. infestans* and no PKC was detected (Judelson & Ah-Fong 2010). PKC is also absent from other Chromalveolates, such as *Plasmodium*, and from *Arabidopsis* (plants), *Giardia* (Excavates) and *Dictyostelium* (unikonts) (Goldberg et al. 2006; Manning et al. 2011). It is present in yeast and higher unikonts, though, and it has hence been suggested that it arose late in evolution (Goldberg et al. 2006). Possibly GPCR-TKLs function as substitutes for PKC. Nearly half of the oomycete GPCR-TKLs contain a C-terminal DEP domain, a domain also found in RGS proteins that interact with internal loop regions and the intracellular C-terminal tails of GPCRs via the DEP domain (Croft et al. 2013). In *S. cerevisiae*, for example, the DEP domain has been shown to be involved in desensitization of GPCR signaling responses (Ballon et al. 2006). The presence of a DEP domain in GPCR-TKLs further suggests a function in regulation of G-protein signaling.

With respect to phospholipid signaling, the presence of GPCR-PIPKs and GPCR-INPPs is indicative of alternative pathways in oomycetes. Among the typical activators of PIPKs are Rho GTPases (Ren & Schwartz 1998), PKA (Park et al. 2001), and phosphatidic acid (Park et al. 2001). In *P. infestans*, only two proteins have similarity to Rho GTPases. Whether GPCR-PIPKs and GPCR-INPPs indeed bypass G-protein or other signaling intermediates by directly activating the catalytic domain upon ligand binding remains to be tested experimentally.

Thus far, experimental data on GPCR-bigrams are very limited and hence their function and catalytic activity remain elusive. Functions have been elucidated for some GPCR-PIPKs, though. Expression profiling showed that all 12 GPCR-PIPKs present in *P. infestans* and *P. sojae* are differentially expressed during development (Hua et al. 2013) and functional gene analyses based on gene silencing of three GPCR-PIPKs revealed roles in sexual reproduction and virulence (Hua et al. 2013; Yang et al. 2013). In *D. discoideum*, *RpkA* knockout mutants showed defects in bacterial defense and had reduced levels of phosphoinositides (Riyahi et al. 2011). However, nothing is known with respect to their catalytic activity and the same holds for the other GPCR-bigrams. For example, we cannot exclude that one or several of the predicted AC or PDE domains might actually function as a guanylyl cyclase or cGMP phosphodiesterase, respectively. Similarly, even though the kinase domains of GPCR-TKLs have sequence similarity to tyrosine kinases, they might well act biochemically as serine/threonine kinases (Goldberg et al. 2006; Judelson & Ah-Fong 2010). Elucidating the function and catalytic activity of these peculiar GPCR-bigrams and their roles in sensing and signaling might be instrumental for identifying novel classes of drug targets to combat pathogenic microorganisms.

2.6 Conclusion

The presence of six distinct types of GPCR-bigrams in oomycetes strongly suggests the presence of alternative G-protein signaling pathways. While a wide distribution of GPCR-PIPKs is observed throughout the eukaryotic kingdom, other GPCR-bigrams are more restricted in their presence. On the basis of our findings, it is most likely that GPCR-PIPKs are evolutionarily ancient and were likely already present in LECA, a hypothesis that is further strengthened by the ubiquitous presence of the unique, highly conserved LRxGI motif adjacent to the GPCR domain. Whether and how GPCR-bigrams regulate catalytic activity of the accesory domains remain to be elucidated experimentally. Taking the data together, the discovery of GPCR-bigrams and of the widespread presence of GPCR-PIPKs reveals an additional layer of the already intricate G-protein signaling pathway in eukaryotes and points to novel signaling pathways in microorganisms.

2.7 Materials and Methods

Search strategy for identification of GPCR-PIPKs

To identify GPCR-PIPKs, we applied an iterative search strategy, depicted in **Table S2.1a**. Protein sequences of previously annotated GPCR-PIPKs (Meijer & Govers 2006; Riyahi et al. 2011; Leondaritis et al. 2013; Sharma et al. 2015) were used as queries for BLAST searches (*E* value cutoff score of 1 e-1) against the NCBI, UniProt, FungiDB (Stajich et al. 2012), and EuPathDB database (Aurrecoechea et al. 2017) (last accessed 5 May 2017). These databases cover proteomes of a wide range of species, including archaea, bacteria, and organisms from all eukaryotic supergroups. In parallel, HMM searches (Finn et al. 2015) (default settings) were performed on the HMMER webserver, using individual protein sequences (phmmer) or multiple sequence alignments of full-length sequences, the PIPK domain, and the LRxGI motif of GPCR-PIPKs as a query (hmmsearch, jackhmmer). These methods were supplemented by text-based searches in the Uniprot database using keywords and protein domain identifiers. All potential candidates were analyzed for protein domain composition using SMART database (Schultz et al. 1998), and Pfam, Prints, and TIGRFAMs under InterProScan (Jones et al. 2014). TM domains were predicted using Phobius (Kall et al. 2004), TMHMM (Krogh et al. 2001), HMMTOP (Tusnady & Simon 2001), GPCRHMM (Wistrand et al. 2006), and SOSUI (Hirokawa et al. 1998). Proteins containing domains other than PIPK at the C-terminus and those without TM domains were discarded. Newly identified GPCR-PIPKs were then used in queries for iterative searches using the methods described above. All identified GPCR-PIPK sequences are available online under http://mbio.asm.org/content/9/1/e02119-17.

The degree of conservation of GPCR-PIPKs was calculated in Jalview using the AMAS method (Livingstone & Barton 1993), and presented as a sliding moving average calculated

over 50 positions. The WebLogo for the LRxGI motif was plotted using the ggseqlogo package (Wagih 2017) in R v3.3.2.

Retrieval of PIPK genes

All genomes in which GPCR-PIPK genes were identified (**Table S2.1**), were screened for type I, II, and III PIPK genes by BLAST, HMM searches, and text-based searches. All resulting hits were validated by analyzing the predicted protein domain composition using SMART (Schultz et al. 1998), and Pfam, Prints, and TIGRFAMs under InterProScan (Jones et al. 2014). All identified PIPK genes are listed in **Tables S2.4 and S2.5** (available online).

Phylogenetic reconstruction of PIPKs

PIPK domain regions were extracted from type I, II, III, and IV (GPCR-PIPKs) PIPKs, using the positions of SMART and InterProScan protein domain predictions as a guide (see positions of PIPK domain regions listed in **Tables S2.2, S2.3, S2.4, S2.5**). Extracted protein domains were aligned using MAFFT v7 (algorithm: G-INS-i) (Katoh & Standley 2013) under Geneious version r9.1.4 (Kearse et al. 2012). After alignment positions that contain more than 25% gaps were trimmed, a phylogenetic tree was reconstructed using the WAG amino acid substitution model with gamma model of rate heterogeneity, and bootstrapping (500 replicates) was performed with rapid bootstrap analyses on RAxML v8.2.4 (Stamatakis 2014). The phylogeny was annotated as a phylogram using the Interactive Tree of Life (iTOL) website (Letunic & Bork 2016).

P. infestans GPCR inventory

For making an inventory of *P. infestans* proteins with a GPCR signature the proteome was screened for proteins with 5 to 9 TM regions using methods described above. Next, the protein domain composition was predicted using methods desribed above. Protein models with sequence similarity to non-GPCR membrane proteins, such as ion channels, transporters, or non-GPCR receptor proteins. All identified GPCRs and GPCR-bigrams are listed in **Table S2.6**.

2.8 Acknowledgements

This work was supported by Division for Earth and Live Sciences (ALW) with financial aid from the Netherlands Organization for Scientific Research (NWO) in the framework of the ALW-JSTP program (project number 833.13.002; J.V.D.H.; F.G) and by an NWO-VIDI grant (project number 10281; H.J.G.M.) and a NWO-VENI grant (project number 863.15.005; M.F.S.). We thank Kelly Heckman and Chenlei Hua for support in the initial phase of this

study.

2.9 Supplementary files

Data availability

All supplementary files and data are available online on http://mbio.asm.org/content/9/1/e02119-17

Supplementary figures

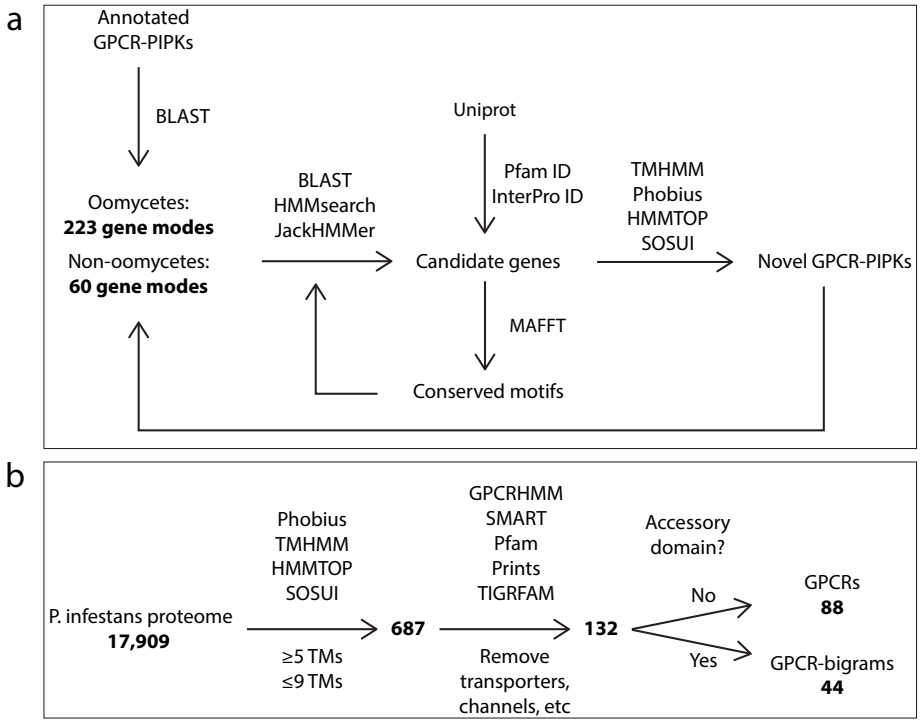

Figure S2.1 | a) Search strategy used to identify GPCR-PIPKs. The total numbers of identified GPCR-PIPKs are highlighted in bold. **b**) Search strategy used to inventory GPCRs and GPCR-bigrams in P. infestans. The numbers in bold represent the number of protein models present after each successive step.

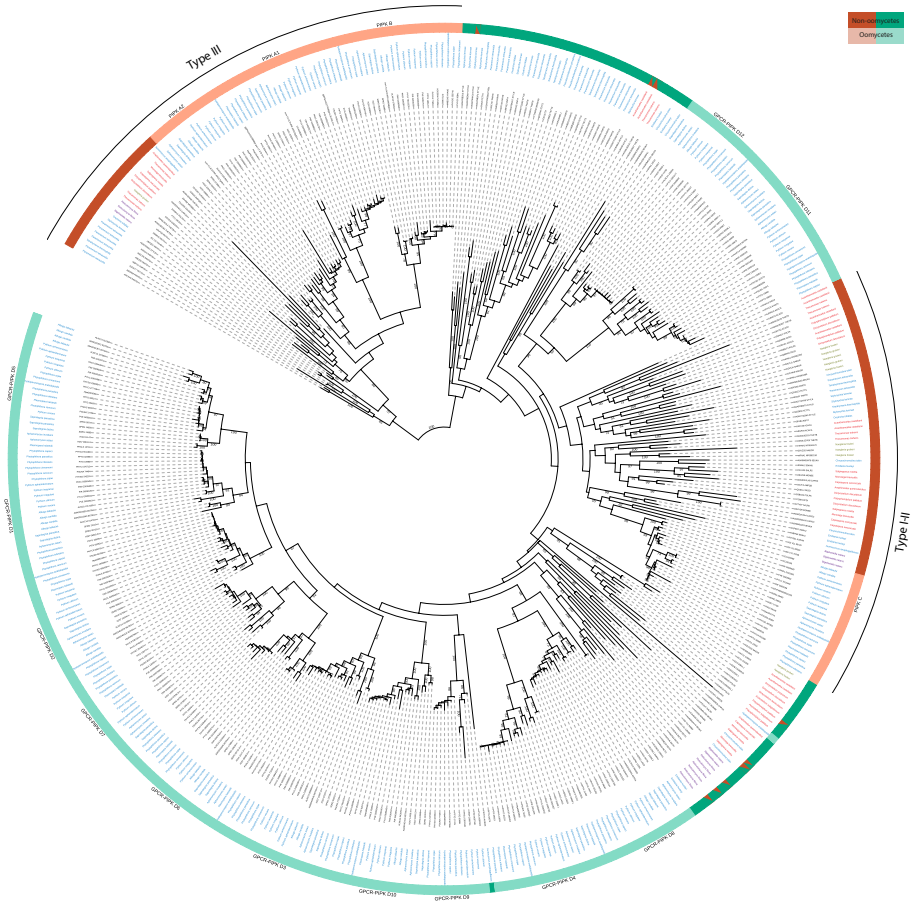

Figure S2.2 | Phylogenetic tree of type I, II, III, and IV PIPKs. The outer circle shows the classification of PIPKs based on domain composition, with orange representing type I, II, and III PIPKs and lime type IV PIPKs (i.e., GPCR-PIPKs). Split-color bars indicate truncated gene models. The color coding of the species names corresponds to the coding of the supergroup colors described for **Figure 2.1**. The numbers at the nodes represent bootstrap support percentages from RAxML (500 replicates). Bootstrap values of <50 are omitted.

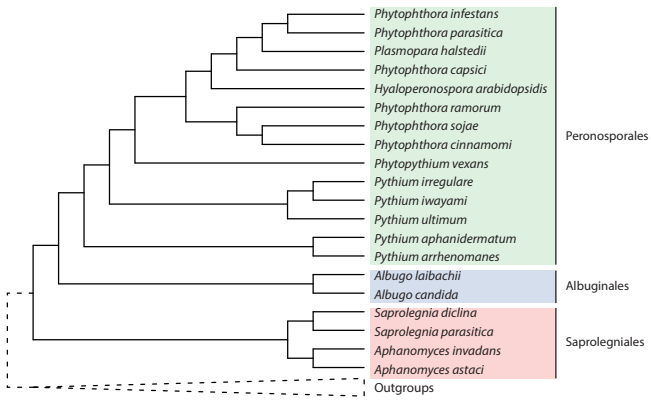

Figure S2.3 | Simplified phylogeny of oomycetes and related organisms based on the supertree as presented by McCarthy et al. (2017)

Supplementary tables

Table S2.1 | Overview of the number of GPCR-bigrams in all species included in this study and references to genome papers.

Supergroup	Taxon	Species	GPCR-PIPKs	GPCR-INPPs	GPCR-ACs	GPCR-PDEs	GPCR-TKLs	GPCR-APs	Genome paper
Excavates	Heterolobosea	*Naegleria fowleri*	1						(Zysset-Burri et al. 2014)
		Naegleria gruberi	1						(Fritz-Laylin et al. 2010)
Chromalveolates	Ciliates	*Oxytricha trifellax*	2						(Swart et al. 2013)
		Paramecium tetraurelia	15						(Aury et al. 2006)
		Tetrahymena thermophila	6						(Eisen et al. 2006)
		Tetrahymena borealis	1						1
		Stylonychia lemnae	6						(Aeschlimann et al. 2014)
		Pseudocohnilembus persalinus	2						(Xiong et al. 2015)
	Pelagophyceae	*Nannochloropsis gaditana*	7					(Radakovits et al. 2012)	
		Aureococcus anophagefferens	1						(Cobler et al. 2011)
	Oomycetes	*Albugo candida*	11	1	2		6	1	(Links et al. 2011)
		Albugo laibachii	11	1	4	1	8	1	(Kemen et al. 2011)
		Aphanomyces astaci	12	4	3		13	1	1
		Aphanomyces invadans	11	4	3	2	13	1	1
		Hyaloperonospora arabidopsidis	11	1	3		4	1	(Baxter et al. 2010)
		Phytophthora capsici	11	2	3		6	1	(Lamour et al. 2012)
		Phytophthora cinnamomi	12	4	7		16	1	(Studholme et al. 2016)
		Phytophthora infestans	12	7	4	3	17	1	(Haas et al. 2009)
		Phytophthora parasitica	12	4	6	2	18	1	1
		Phytophthora ramorum	11	3	7		13	1	(Tyler et al. 2006)
		Phytophthora sojae	12	5	7	2	14	1	(Tyler et al. 2006)
		Plasmopara halstedii	11	6	5		12	1	(Sharma et al. 2015)
		Pythium aphanidermatum	9	4	4	2	9	1	(Adhikari et al. 2013)
		Pythium arrhenomanes	9	4	8	2	11	1	(Adhikari et al. 2013)
		Pythium irregulare	11	3	6	2	202	1	(Adhikari et al. 2013)
		Pythium iwayamai	10	6	2	2	172	1	(Adhikari et al. 2013)
		Pythium ultimum	12	3	8	2	13	1	(Adhikari et al. 2013)
		Pythium vexans	9	4	6	2	13	1	(Adhikari et al. 2013)
		Saprolegnia diclina	12	6	3	3	16	1	1
		Saprolegnia parasitica	14	9	1	3	17	1	(Jiang et al. 2013)
	Haptophytes	*Chrysochromulina tobin*	4						(Hovde et al. 2015)
		Emiliania huxleyi	3						(Read et al. 2013)
Unikonts	Apusozoa	*Thecamonas trahens*	2						1
	Metazoa	*Amphimedon queenslandica*	1						(Srivastava et al. 2010)
	Choanoflagellates	*Capsaspora owczarzaki*	1						(Suga et al. 2013)
		Salpingoeca rosetta	1						(Fairclough et al. 2013)
		Monosiga brevicollis	1						(King et al. 2008)
	Dictyostelids	*Acytostelium subglobosum*	2						(Urushiharaet al. 2015)
		Dictyostelium discoideum	1				2		(Eichinger et al. 2005)
		Dictyostelium fasciculatum	1				1		(Heidel et al. 2011)
		Dictyostelium purpureum	1				1		(Sucgang et al. 2011)
		Polysphondylium pallidum	1				1		(Heidel et al. 2011)
	Lobosea	*Acanthamoeba castellanii*	2				2		(Clarke et al. 2013)
Rhizaria	Foraminifera	*Reticulomyxa filosa*	jan-43						(Glockner et al. 2014)
	Cercomonads	*Bigelowiella natans*	2						(Curtis et al. 2012)

Table S2.2 | Details of GPCR-PIPKs in oomycetes

Gene ID	Proposed name	Organism	Length (aa)	In tree (min)	In tree (max)
A0A024G3J2_9STRA	GPCR-PIPK D1A	*Albugo candida*	995	504	901
A0A024GGP6_9STRA	GPCR-PIPK D1B	*Albugo candida*	1027	524	916
A0A024G0E9_9STRA	GPCR-PIPK D2A	*Albugo candida*	852	500	836
A0A024GCM0_9STRA	GPCR-PIPK D2B	*Albugo candida*	820	471	811
A0A024GRJ8_9STRA	GPCR-PIPK D3	*Albugo candida*	893	378	887
A0A024G5F2_9STRA	GPCR-PIPK D5A	*Albugo candida*	864	490	811
A0A024GJE1_9STRA	GPCR-PIPK D5B	*Albugo candida*	994	640	959
A0A024GDI6_9STRA	GPCR-PIPK D6	*Albugo candida*	891	499	851
A0A024GMX6_9STRA	GPCR-PIPK D8	*Albugo candida*	928	384	733
A0A024G7D4_9STRA	GPCR-PIPK D10	*Albugo candida*	1646	377	778
A0A024GM15_9STRA	GPCR-PIPK D11	*Albugo candida*	1081	675	1007
ALNC14_111090	GPCR-PIPK D1	*Albugo laibachii*	1016	516	905
ALNC14_014740	GPCR-PIPK D2A	*Albugo laibachii*	916	581	910
ALNC14_017200	GPCR-PIPK D2B	*Albugo laibachii*	1384	1032	1368
ALNC14_009000	GPCR-PIPK D3	*Albugo laibachii*	835	375	829
ALNC14_012300	GPCR-PIPK D5A	*Albugo laibachii*	822	511	808
ALNC14_107060	GPCR-PIPK D5B	*Albugo laibachii*	902	548	867
ALNC14_011550	GPCR-PIPK D6	*Albugo laibachii*	916	524	876
ALNC14_069200	GPCR-PIPK D8	*Albugo laibachii*	790	380	716
ALNC14_043070	GPCR-PIPK D10	*Albugo laibachii*	929	572	925
ALNC14_046580	GPCR-PIPK D11	*Albugo laibachii*	738	334	666
ALNC14_105550	GPCR-PIPK D12	*Albugo laibachii*	709	382	696
H257_10334	GPCR-PIPK D1	*Aphanomyces astaci*	864	478	814
H257_05925.2	GPCR-PIPK D2	*Aphanomyces astaci*	924	459	843
H257_15597.2	GPCR-PIPK D3	*Aphanomyces astaci*	855	376	830
H257_16299.1	GPCR-PIPK D4	*Aphanomyces astaci*	868	368	792
H257_09611.2	GPCR-PIPK D5	*Aphanomyces astaci*	888	507	825
H257_05699.2	GPCR-PIPK D6	*Aphanomyces astaci*	927	529	879
H257_10507.2	GPCR-PIPK D7	*Aphanomyces astaci*	851	476	799
H257_15959.2	GPCR-PIPK D8	*Aphanomyces astaci*	838	343	724
H257_14336.4	GPCR-PIPK D10	*Aphanomyces astaci*	793	438	789
H257_00870	GPCR-PIPK D11A	*Aphanomyces astaci*	741	382	681
H257_00873.3	GPCR-PIPK D11B	*Aphanomyces astaci*	731	360	676
H257_00006.1	GPCR-PIPK D12	*Aphanomyces astaci*	697	377	681
H310_02759	GPCR-PIPK D1	*Aphanomyces invadans*	873	489	823
H310_07037	GPCR-PIPK D3	*Aphanomyces invadans*	826	361	808
H310_14231	GPCR-PIPK D4	*Aphanomyces invadans*	864	371	795
H310_11147	GPCR-PIPK D5	*Aphanomyces invadans*	869	487	807
H310_11127.4	GPCR-PIPK D6	*Aphanomyces invadans*	958	554	903
H310_07836.2	GPCR-PIPK D7	*Aphanomyces invadans*	867	496	814
H310_04755	GPCR-PIPK D8	*Aphanomyces invadans*	908	352	759
H310_11901.2	GPCR-PIPK D10	*Aphanomyces invadans*	849	445	844
H310_00967	GPCR-PIPK D11A	*Aphanomyces invadans*	735	369	685
H310_00968	GPCR-PIPK D11B	*Aphanomyces invadans*	736	378	676
H310_14760	GPCR-PIPK D12	*Aphanomyces invadans*	712	385	696
HpaG800146	GPCR-PIPK D1	*Hyaloperonospora arabidopsidis*	951	429	873
HpaG811351	GPCR-PIPK D3	*Hyaloperonospora arabidopsidis*	760	335	758
HpaG802846	GPCR-PIPK D4	*Hyaloperonospora arabidopsidis*	805	404	768
HpaG801064	GPCR-PIPK D5	*Hyaloperonospora arabidopsidis*	1029	479	799
HpaG802364	GPCR-PIPK D7	*Hyaloperonospora arabidopsidis*	1081	554	992
HpaG802934	GPCR-PIPK D8	*Hyaloperonospora arabidopsidis*	1013	386	791
HpaG802456	GPCR-PIPK D9	*Hyaloperonospora arabidopsidis*	1240	789	1213
HpaG804586	GPCR-PIPK D10	*Hyaloperonospora arabidopsidis*	928	513	907
HpaG809355	GPCR-PIPK D11	*Hyaloperonospora arabidopsidis*	816	407	721
HpaG804315	GPCR-PIPK D12	*Hyaloperonospora arabidopsidis*	741	382	721
HpaG814345	Not classified	*Hyaloperonospora arabidopsidis*	1411	547	1154
PHYCA_506791	GPCR-PIPK D1	*Phytophthora capsici*	1024	505	947
PHYCA_551190	GPCR-PIPK D2	*Phytophthora capsici*	938	552	915
PHYCA_527176	GPCR-PIPK D3	*Phytophthora capsici*	745	335	741
PHYCA_506037	GPCR-PIPK D4	*Phytophthora capsici*	806	404	768
PHYCA_541689	GPCR-PIPK D6	*Phytophthora capsici*	935	480	857
PHYCA_536734	GPCR-PIPK D7	*Phytophthora capsici*	1012	564	921
PHYCA_38287	GPCR-PIPK D8	*Phytophthora capsici*	1012	386	799
PHYCA_507566	GPCR-PIPK D9	*Phytophthora capsici*	947	496	919

Table S2.2 | Details of GPCR-PIPKs in oomycetes

Gene ID	Proposed name	Organism	Length (aa)	In tree (min)	In tree (max)
PHYCA_549299	GPCR-PIPK D10	*Phytophthora capsici*	699	294	686
PHYCA_575370	GPCR-PIPK D11	*Phytophthora capsici*	794	395	707
PHYCA_573663	GPCR-PIPK D12	*Phytophthora capsici*	737	381	720
PHYCI_105008	GPCR-PIPK D1	*Phytophthora cinnamomi*	1193	673	1116
PHYCI_376712	GPCR-PIPK D2	*Phytophthora cinnamomi*	939	551	916
PHYCI_269807	GPCR-PIPK D3	*Phytophthora cinnamomi*	758	332	754
PHYCI_91218	GPCR-PIPK D4	*Phytophthora cinnamomi*	805	404	768
PHYCI_277748	GPCR-PIPK D5	*Phytophthora cinnamomi*	920	552	871
PHYCI_285878	GPCR-PIPK D6	*Phytophthora cinnamomi*	874	408	791
PHYCI_97820	GPCR-PIPK D7	*Phytophthora cinnamomi*	1198	676	1104
PHYCI_481282	GPCR-PIPK D8	*Phytophthora cinnamomi*	1028	390	800
PHYCI_212799	GPCR-PIPK D9	*Phytophthora cinnamomi*	1244	794	1217
PHYCI_291554	GPCR-PIPK D10	*Phytophthora cinnamomi*	944	527	924
PHYCI_105811	GPCR-PIPK D11	*Phytophthora cinnamomi*	797	397	709
PHYCI_260267	GPCR-PIPK D12	*Phytophthora cinnamomi*	735	380	719
PITG_05282	GPCR-PIPK D1	*Phytophthora infestans*	1016	495	939
PITG_10980	GPCR-PIPK D2	*Phytophthora infestans*	934	553	909
PITG_05618	GPCR-PIPK D3	*Phytophthora infestans*	757	332	753
PITG_05519	GPCR-PIPK D4	*Phytophthora infestans*	807	405	769
PITG_00460	GPCR-PIPK D5	*Phytophthora infestans*	927	553	872
PITG_13511	GPCR-PIPK D6	*Phytophthora infestans*	950	492	869
PITG_13677	GPCR-PIPK D7	*Phytophthora infestans*	1241	722	1150
PITG_15475	GPCR-PIPK D8	*Phytophthora infestans*	1014	389	796
PITG_00896	GPCR-PIPK D9	*Phytophthora infestans*	1231	792	1204
PITG_02574	GPCR-PIPK D10	*Phytophthora infestans*	927	510	907
PITG_23066	GPCR-PIPK D11	*Phytophthora infestans*	796	400	712
PITG_20028	GPCR-PIPK D12	*Phytophthora infestans*	730	377	714
PPTG_18528	GPCR-PIPK D1	*Phytophthora parasitica*	1014	493	937
PPTG_02395	GPCR-PIPK D2	*Phytophthora parasitica*	934	553	909
PPTG_02787	GPCR-PIPK D3	*Phytophthora parasitica*	757	332	753
PPTG_02674	GPCR-PIPK D4	*Phytophthora parasitica*	853	451	815
PPTG_08317	GPCR-PIPK D5	*Phytophthora parasitica*	918	550	869
PPTG_10638	GPCR-PIPK D6	*Phytophthora parasitica*	938	486	857
PPTG_13077	GPCR-PIPK D7	*Phytophthora parasitica*	1238	723	1147
PPTG_11435	GPCR-PIPK D8	*Phytophthora parasitica*	1018	389	797
PPTG_17476	GPCR-PIPK D9	*Phytophthora parasitica*	1231	795	1204
PPTG_05314	GPCR-PIPK D10	*Phytophthora parasitica*	916	499	896
PPTG_09659	GPCR-PIPK D11	*Phytophthora parasitica*	795	399	711
PPTG_03738	GPCR-PIPK D12	*Phytophthora parasitica*	733	381	717
PSURA_80758	GPCR-PIPK D1	*Phytophthora ramorum*	1017	495	940
PSURA_74484	GPCR-PIPK D2	*Phytophthora ramorum*	1830	533	898
PSURA_73106	GPCR-PIPK D3	*Phytophthora ramorum*	557	324	554
PSURA_73182	GPCR-PIPK D4	*Phytophthora ramorum*	806	405	768
PSURA_72755	GPCR-PIPK D5	*Phytophthora ramorum*	1106	540	859
PSURA_96779	GPCR-PIPK D6	*Phytophthora ramorum*	976	352	693
PSURA_85104	GPCR-PIPK D7	*Phytophthora ramorum*	1234	731	1141
PSURA_77729	GPCR-PIPK D9	*Phytophthora ramorum*	1048	599	1020
PSURA_77535	GPCR-PIPK D10	*Phytophthora ramorum*	958	550	947
PSURA_72973	GPCR-PIPK D11	*Phytophthora ramorum*	800	402	712
PSURA_96917	GPCR-PIPK D12	*Phytophthora ramorum*	1282	927	1266
PHYSO_309429	GPCR-PIPK D1	*Phytophthora sojae*	1176	656	1099
PHYSO_543291	GPCR-PIPK D2	*Phytophthora sojae*	949	559	924
PHYSO_286433	GPCR-PIPK D3	*Phytophthora sojae*	757	332	753
PHYSO_286453	GPCR-PIPK D4	*Phytophthora sojae*	806	405	769
PHYSO_335695	GPCR-PIPK D5	*Phytophthora sojae*	921	553	872
PHYSO_533948	GPCR-PIPK D6	*Phytophthora sojae*	957	494	872
PHYSO_254487	GPCR-PIPK D7	*Phytophthora sojae*	1225	699	1131
PHYSO_297261	GPCR-PIPK D8	*Phytophthora sojae*	1030	392	802
PHYSO_322334	GPCR-PIPK D9	*Phytophthora sojae*	1245	795	1216
PHYSO_286311	GPCR-PIPK D10	*Phytophthora sojae*	944	529	927
PHYSO_287073	GPCR-PIPK D11	*Phytophthora sojae*	801	403	715
PHYSO_357778	GPCR-PIPK D12	*Phytophthora sojae*	737	382	721
PHALS_07480	GPCR-PIPK D1	*Plasmopara halstedii*	1011	493	934
PHALS_13711	GPCR-PIPK D2	*Plasmopara halstedii*	913	532	893

Table S2.2 | Details of GPCR-PIPKs in oomycetes

Gene ID	Proposed name	Organism	Length (aa)	In tree (min)	In tree (max)
PHALS_13328	GPCR-PIPK D3	*Plasmopara halstedii*	754	328	750
PHALS_10831	GPCR-PIPK D4	*Plasmopara halstedii*	797	395	759
PHALS_09337	GPCR-PIPK D5	*Plasmopara halstedii*	918	550	869
PHALS_12432	GPCR-PIPK D6	*Plasmopara halstedii*	929	482	855
PHALS_13026	GPCR-PIPK D7	*Plasmopara halstedii*	1239	724	1150
PHALS_01211	GPCR-PIPK D8	*Plasmopara halstedii*	996	390	794
PHALS_13990	GPCR-PIPK D10	*Plasmopara halstedii*	929	514	912
PHALS_04624	GPCR-PIPK D11	*Plasmopara halstedii*	799	401	704
PHALS_01082	GPCR-PIPK D12	*Plasmopara halstedii*	736	381	719
PAG1_G005942	GPCR-PIPK D1	*Pythium aphanidermatum*	975	480	898
PAG1_G006345	GPCR-PIPK D2	*Pythium aphanidermatum*	949	555	925
PAG1_G000538	GPCR-PIPK D3	*Pythium aphanidermatum*	792	345	788
PAG1_G006762	GPCR-PIPK D4	*Pythium aphanidermatum*	857	473	836
PAG1_G004464	GPCR-PIPK D5	*Pythium aphanidermatum*	938	555	883
PAG1_G005579	GPCR-PIPK D7	*Pythium aphanidermatum*	1188	607	1046
PAG1_G011183	GPCR-PIPK D8	*Pythium aphanidermatum*	963	383	740
PAG1_G011538	GPCR-PIPK D9	*Pythium aphanidermatum*	1080	776	1065
PAG1_G001667	GPCR-PIPK D10	*Pythium aphanidermatum*	1011	540	967
PAR_G008323	GPCR-PIPK D1	*Pythium arrhenomanes*	973	470	892
PAR_G005321	GPCR-PIPK D3	*Pythium arrhenomanes*	793	344	789
PAR_G001927	GPCR-PIPK D4	*Pythium arrhenomanes*	782	393	763
PAR_G001971	GPCR-PIPK D5	*Pythium arrhenomanes*	1008	554	882
PAR_G007543	GPCR-PIPK D6	*Pythium arrhenomanes*	955	555	910
PAR_G005872	GPCR-PIPK D7	*Pythium arrhenomanes*	1161	620	1081
PAR_G004575	GPCR-PIPK D8	*Pythium arrhenomanes*	999	387	748
PAR_G006704	GPCR-PIPK D9	*Pythium arrhenomanes*	920	562	886
PAR_G006155	GPCR-PIPK D11	*Pythium arrhenomanes*	764	357	670
PIR_G007963	GPCR-PIPK D1	*Pythium irregulare*	1027	514	948
PIR_G005128	GPCR-PIPK D2	*Pythium irregulare*	1003	617	987
PIR_G000755	GPCR-PIPK D3	*Pythium irregulare*	733	328	729
PIR_G001329	GPCR-PIPK D4	*Pythium irregulare*	807	409	789
PIR_G004315	GPCR-PIPK D5	*Pythium irregulare*	922	552	876
PIR_G010484	GPCR-PIPK D6	*Pythium irregulare*	1035	596	962
PIR_G005617	GPCR-PIPK D7	*Pythium irregulare*	1217	663	1083
PIR_G005327	GPCR-PIPK D8	*Pythium irregulare*	946	393	743
PIR_G003551	GPCR-PIPK D10	*Pythium irregulare*	2320	551	960
PIR_G000134	GPCR-PIPK D11	*Pythium irregulare*	751	343	653
PIR_G008692	GPCR-PIPK D12	*Pythium irregulare*	759	378	735
PIW_G002225	GPCR-PIPK D1	*Pythium iwayamai*	925	417	846
PIW_G001556	GPCR-PIPK D2	*Pythium iwayamai*	971	585	955
PIW_G000082	GPCR-PIPK D3	*Pythium iwayamai*	749	311	745
PIW_G005427	GPCR-PIPK D4	*Pythium iwayamai*	796	399	778
PIW_G009501	GPCR-PIPK D5	*Pythium iwayamai*	747	377	701
PIW_G007059	GPCR-PIPK D7	*Pythium iwayamai*	1042	486	913
PIW_G007346	GPCR-PIPK D9	*Pythium iwayamai*	1238	802	1184
PIW_G007017	GPCR-PIPK D10	*Pythium iwayamai*	939	533	925
PIW_G001360	GPCR-PIPK D11	*Pythium iwayamai*	772	346	674
PIW_G008266	GPCR-PIPK D12	*Pythium iwayamai*	767	388	743
PYU1_G013260	GPCR-PIPK D1	*Pythium ultimum*	986	472	905
PYU1_G005521	GPCR-PIPK D2	*Pythium ultimum*	987	603	973
PYU1_G005339	GPCR-PIPK D3	*Pythium ultimum*	768	335	764
PYU1_G005232	GPCR-PIPK D4	*Pythium ultimum*	783	402	765
PYU1_G004188	GPCR-PIPK D5	*Pythium ultimum*	920	548	872
PYU1_G008271	GPCR-PIPK D6	*Pythium ultimum*	871	436	800
PYU1_G008111	GPCR-PIPK D7	*Pythium ultimum*	1176	643	1055
PYU1_G007339	GPCR-PIPK D8	*Pythium ultimum*	967	365	733
PYU1_G002023	GPCR-PIPK D9	*Pythium ultimum*	1140	713	1094
PYU1_G008545	GPCR-PIPK D10	*Pythium ultimum*	948	532	930
PYU1_G009408	GPCR-PIPK D11	*Pythium ultimum*	771	365	679
PYU1_G001177	GPCR-PIPK D12	*Pythium ultimum*	739	369	710
PVE_G002231	GPCR-PIPK D1	*Pythium vexans*	1001	494	924
PVE_G002810	GPCR-PIPK D2	*Pythium vexans*	921	556	897
PVE_G002030	GPCR-PIPK D3	*Pythium vexans*	766	333	757
PVE_G002533	GPCR-PIPK D4	*Pythium vexans*	795	406	778

Table S2.2 | Details of GPCR-PIPKs in oomycetes

Gene ID	Proposed name	Organism	Length (aa)	In tree (min)	In tree (max)
PVE_G000411	GPCR-PIPK D5	*Pythium vexans*	836	453	791
PVE_G009494	GPCR-PIPK D7	*Pythium vexans*	1119	610	1024
PVE_G006124	GPCR-PIPK D8	*Pythium vexans*	821	395	757
PVE_G002942	GPCR-PIPK D10	*Pythium vexans*	4172	1579	2036
PVE_G001250	GPCR-PIPK D11	*Pythium vexans*	1140	378	662
SDRG_03333	GPCR-PIPK D1	*Saprolegnia diclina*	915	493	855
SDRG_00721	GPCR-PIPK D2	*Saprolegnia diclina*	855	466	834
SDRG_00401	GPCR-PIPK D3	*Saprolegnia diclina*	772	348	771
SDRG_03698.1	GPCR-PIPK D4	*Saprolegnia diclina*	857	354	768
SDRG_11885	GPCR-PIPK D5	*Saprolegnia diclina*	902	517	838
SDRG_05710.2	GPCR-PIPK D6	*Saprolegnia diclina*	844	427	775
SDRG_07592	GPCR-PIPK D7	*Saprolegnia diclina*	883	490	827
SDRG_14228	GPCR-PIPK D8	*Saprolegnia diclina*	746	339	667
SDRG_12324	GPCR-PIPK D10	*Saprolegnia diclina*	861	474	855
SDRG_00836.1	GPCR-PIPK D11A	*Saprolegnia diclina*	697	331	646
SDRG_00837.1	GPCR-PIPK D11B	*Saprolegnia diclina*	785	410	712
SDRG_05817	GPCR-PIPK D12	*Saprolegnia diclina*	698	382	684
SPRG_00503	GPCR-PIPK D1	*Saprolegnia parasitica*	914	492	854
SPRG_22110	GPCR-PIPK D2	*Saprolegnia parasitica*	753	362	730
SPRG_13728	GPCR-PIPK D3	*Saprolegnia parasitica*	765	341	764
SPRG_19929	GPCR-PIPK D4	*Saprolegnia parasitica*	858	357	771
SPRG_09727	GPCR-PIPK D5A	*Saprolegnia parasitica*	894	509	830
SPRG_14656	GPCR-PIPK D5B	*Saprolegnia parasitica*	630	261	566
SPRG_02629	GPCR-PIPK D6A	*Saprolegnia parasitica*	834	435	767
SPRG_17099	GPCR-PIPK D6B	*Saprolegnia parasitica*	724	309	657
SPRG_04701	GPCR-PIPK D7	*Saprolegnia parasitica*	714	491	686
SPRG_14055	GPCR-PIPK D8	*Saprolegnia parasitica*	745	339	666
SPRG_10998	GPCR-PIPK D10	*Saprolegnia parasitica*	842	475	836
SPRG_03031	GPCR-PIPK D11A	*Saprolegnia parasitica*	680	332	629
SPRG_03032	GPCR-PIPK D11B	*Saprolegnia parasitica*	672	348	650
SPRG_10518	GPCR-PIPK D12	*Saprolegnia parasitica*	696	380	682

Table S2.3 | Details GPCR-PIPKs in organisms other than oomycetes

Gene ID	Organism	Notes	Length (aa)	For tree (min)	For tree (max)
ACA1_120810	*Acanthamoeba castellanii*	LRxGI motif absent	855	347	851
ACA1_215300	*Acanthamoeba castellanii*		863	350	859
XM_012893031.1	*Acytostelium subglobosum*		630	332	602
XM_012903423	*Acytostelium subglobosum*		696	369	695
I1FNC1_AMPQE	*Amphimedon queenslandica*		824	419	823
F0YEY0_AURAN	*Aureococcus anophagefferens*		995	512	986
JGI_V11_86869	*Bigelowiella natans*		570	266	549
JGI_V11_128099	*Bigelowiella natans*		869	426	847
A0A0D2WMD5_CAPO3	*Capsaspora owczarzaki*		832	467	831
A0A0M0JVY0_9EUKA	*Chrysochromulina tobin*		889	533	860
A0A0M0JZS1_9EUKA	*Chrysochromulina tobin*		653	309	634
A0A0M0K846_9EUKA	*Chrysochromulina tobin*		1024	669	1022
A0A0M0LC85_9EUKA	*Chrysochromulina tobin*		861	501	786
DDB_G0283615	*Dictyostelium discoideum*		828	442	802
EGG23334.1	*Dictyostelium fasciculatum*	LRxGI motif present, but gap in gene model	544	223	543
EGC30811.1	*Dictyostelium purpureum*		817	511	816
R1B3W9_EMIHU	*Emiliania huxleyi*	Truncated gene model	428	92	314
R1C8C1_EMIHU	*Emiliania huxleyi*		839	406	723
R1CZI6_EMIHU	*Emiliania huxleyi*		673	325	638
A9UUR7_MONBE	*Monosiga brevicollis*		724	378	698
NF0081820	*Naegleria fowleri*		1203	740	1107
D2VZQ3_NAEGR	*Naegleria gruberi*		1044	607	967
J9F1E2_9SPIT	*Oxytricha trifallax*		799	477	797
J9HVM1_9SPIT	*Oxytricha trifallax*		632	293	615
A0BHU4_PARTE	*Paramecium tetraurelia*		734	430	734
A0BQ85_PARTE	*Paramecium tetraurelia*		728	423	728
A0C061_PARTE	*Paramecium tetraurelia*		719	413	718
A0C747_PARTE	*Paramecium tetraurelia*		647	364	646
A0CAY0_PARTE	*Paramecium tetraurelia*		706	407	705
A0CB17_PARTE	*Paramecium tetraurelia*	LRxGI motif absent	1061	743	1061
A0CVD9_PARTE	*Paramecium tetraurelia*		731	433	731
A0CVJ0_PARTE	*Paramecium tetraurelia*		692	399	688
A0D8U5_PARTE	*Paramecium tetraurelia*		723	425	723
A0D8Z3_PARTE	*Paramecium tetraurelia*		692	410	688
A0D9N1_PARTE	*Paramecium tetraurelia*	LRxGI motif absent	725	426	724
A0DRY7_PARTE	*Paramecium tetraurelia*	LRxGI motif absent	717	431	716
A0DW93_PARTE	*Paramecium tetraurelia*		711	411	711
A0E6X4_PARTE	*Paramecium tetraurelia*		706	407	705
GSPATP00004271001	*Paramecium tetraurelia*		636	353	635
D3AWU0_POLPA	*Polysphondylium pallidum*		671	277	643
KRX00481.1	*Pseudocohnilembus persalinus*		699	389	698

Table S2.3 | Details GPCR-PIPKs in organisms other than oomycetes

Gene ID	Organism	Notes	Length (aa)	For tree (min)	For tree (max)
KRX00482.1	*Pseudocohnilembus persalinus*		707	391	706
X6L9J3_RETFI	*Reticulomyxa filosa*	LRxGI motif present, but no GPCR	311	110	310
X6MDI8_RETFI	*Reticulomyxa filosa*	Not included in tree; only GPCR and LRxGI motif	470	-	-
F2U247_SALR5	*Salpingoeca rosetta*		1147	790	1146
A0A077ZQS6_STYLE	*Stylonychia lemnae*		774	402	752
A0A077ZXB4_STYLE	*Stylonychia lemnae*	LRxGI motif absent	1009	468	1008
A0A078ARL7_STYLE	*Stylonychia lemnae*		779	456	775
A0A078B2U3_STYLE	*Stylonychia lemnae*	LRxGI motif absent	874	287	804
A0A078BDF2_STYLE	*Stylonychia lemnae*	LRxGI motif absent	878	401	874
A0A078BDW7_STYLE	*Stylonychia lemnae*	LRxGI motif absent	849	265	803
EI9_01737	*Tetrahymena borealis*		795	456	791
I7M9D0_TETTS	*Tetrahymena thermophila*		747	444	746
I7MIV9_TETTS	*Tetrahymena thermophila*		408	67	404
Q23DH0_TETTS	*Tetrahymena thermophila*		775	441	771
Q23WQ3_TETTS	*Tetrahymena thermophila*		975	559	975
TTHERM_00530790	*Tetrahymena thermophila*	LRxGI motif absent	1201	866	1200
W7X9T0_TETTS	*Tetrahymena thermophila*		726	425	726
A0A0L0DB47_THETB	*Thecamonas trahens*		826	479	825
A0A0L0DRJ2_THETB	*Thecamonas trahens*		783	468	779

Supplementary tables available online

The following supplementary tables are available online at http://mbio.asm.org/content/9/1/e02119-17

Table	Table ID online	Content
S2.4	S2c	Details of oomycete type I, II, and III PIPKs
S2.5	S2d	Details of type I, II, and III PIPKs in species having one or more GPCR-PIPKs
S2.6	S3a	Inventory of GPCRs and GPCR-bigrams in *P. infestans*
S2.7	S3b	Details of GPCR-TKLs
S2.8	S3c	Details of GPCR-INPPs
S2.9	S3d	Details of GPCR-ACs
S2.10	S3e	Details of GPCR-PDEs
S2.11	S3f	Details of GPCR-ACs

Chapter 3

The G-protein γ subunit of *Phytophthora infestans* is involved in sporangial development

Johan van den Hoogen, Natalie Verbeek - de Kruif, Francine Govers

This chapter is published as: The G-protein γ subunit of *Phytophthora infestans* is involved in sporangial development (2018), *Fungal Genetics and Biology*. doi: 10.1016/j.fgb.2018.04.012

3.1 Abstract

The oomycete *Phytophthora infestans* is a notorious plant pathogen with potato and tomato as its primary hosts. Previous research showed that the heterotrimeric G-protein subunits Gα and Gβ have a role in zoospore motility and virulence, and sporangial development, respectively. Here, we present analyses of the gene encoding a Gγ subunit in *P. infestans*, *Pigpg1*. The overall similarity of PiGPG1 with non-oomycete Gγ subunits is low, with only the most conserved amino acids maintained, but similarity with its homologs in other oomycetes is high. *Pigpg1* is expressed in all life stages and shows a similar expression profile as the gene encoding the Gβ subunit, *Pigpb1*. To elucidate its function, transformants were generated in which *Pigpg1* is silenced or overexpressed and their phenotypes were analyzed. *Pigpg1*-silenced lines produce less sporangia, which are malformed. Altogether, the results show that PiGPG1 is crucial for proper sporangia development and zoosporogenesis. PiGPG1 is a functional Gγ, and likely forms a dimer with PiGPB1 that mediates signaling.

3.2 Introduction

G-protein signaling is an elementary signal transduction pathway that is essential for viability of all eukaryotes. The central elements of this signaling pathway are constituted by membrane-bound G-protein-coupled receptors (GPCRs) and associated guanidine-binding (G) proteins. G-proteins form a heterotrimeric complex, which consists of three subunits, α (Gα), β (Gβ), and γ (Gγ). A GPCR senses extracellular signals and changes conformation upon ligand binding, and this conformational change induces the dissociation of the G-protein complex from the receptor. In turn, the activated Gα and G$\beta\gamma$ subunits stimulate downstream effector proteins such as protein kinase C, adenylate cyclase, or ion channels, to evoke a cellular response (Dupre et al. 2009). Alternatively, GPCRs can propagate signals independently from G-proteins, through β-arrestins (Smith & Rajagopal 2016).

In higher eukaryotes such as mammalians, genes encoding proteins involved in G-protein signaling are usually present in large numbers. For example, humans have more than 800 GPCR genes, and 16 Gα, 5 Gβ, and 14 Gγ subunit genes (Fredriksson & Schioth 2005; Hillenbrand et al. 2015). In lower eukaryotes, these numbers are reduced. For example, the slime mold *Dictyostelium discoideum* has 55 GPCR genes, 12 Gα subunit genes, and only 2 and 1 encoding the Gβ and Gγ subunit, respectively (Bakthavatsalam et al. 2009). The yeast *Saccharomyces cerevisiae* has even less; three GPCR genes, and 2 Gα, 1 Gβ, and 1 Gγ subunit genes (Kraakman et al. 1999; Hoffman 2005; Overton et al. 2005). In fungi, G-protein signaling is crucial for several basal processes such as growth, development, and asexual and sexual reproduction (Versele et al. 2001; Xue et al. 2008). In addition, G-protein signaling is involved in virulence of several filamentous pathogens (Li et al. 2007). For example, in the rice blast fungus *Magnaporthe oryzae* subunits Gα, Gβ, and Gγ play a role in the regulation of appressorium formation, and knockout lines show a reduced level of pathogenicity or even a complete loss thereof (Liu & Dean 1997; Nishimura et al. 2003; Liang et al. 2006).

Our focus is on the filamentous plant pathogen *Phytophthora infestans*, the causal agent of late blight and the culprit of the Irish potato famine in the mid-19th century (Ribeiro 2013). *Phytophthora* spp. are classified as oomycetes, a diverse group of eukaryotic organisms comprising plant and animal pathogens as well as saprophytes (Erwin & Ribeiro 1996). Oomycetes occupy similar environmental niches as fungi but are evolutionary unrelated (Raffaele & Kamoun 2012). Since the first report on the importance of G-protein signaling in a fungal pathogen (Choi et al. 1995), the role of this signaling pathway has been studied in a broad range of fungal species (reviewed in (Li et al. 2007)). In oomycetes, research on G-protein signaling is limited to only a few species and all these studies point to a primary role in asexual development. *Pigpa1*, the *P. infestans* gene encoding a Gα subunit, was found to have a role in zoospore release and swimming behavior, and in chemotaxis (Latijnhouwers et al. 2004). Moreover, *Psgpa1* was shown to be involved in virulence of *P. infestans* on potato. Similar results were observed for *Psgpa1*, the *Pigpa1* homolog in the soybean pathogen

Phytophthora sojae (Hua et al. 2008). Stimulation of Gα using mastoparan, a peptide from wasp venom, was found to induce encystment of zoospores of *P. infestans* and *Aphanomyces cochlioides*, an oomycete causing root rot on several crops (Latijnhouwers et al. 2002; Islam et al. 2003). Transformants deficient in PiGPB1, a *P. infestans* Gβ subunit, had defects in sporangia production and mycelial growth, suggesting that the Gβ subunit is important for vegetative growth and sporulation (Latijnhouwers & Govers 2003). *Psgpr11*, a putative GPCR in *P. sojae*, was found to control zoospore development, and silenced transformants showed a reduced virulence on soybean (Wang et al. 2010). Apart from canonical GPCRs, oomycetes have several novel types of GPCRs in which a GPCR domain is fused to a catalytic domain (van den Hoogen et al. 2018). One type, named GPCR-PIPK, has a C-terminal phospholipid kinase domain and is present as a multigene family in *Phytophthora* with typically 12 members (Meijer & Govers 2006; van den Hoogen et al. 2018). Overexpression of *PiGK4*, one of 12 GPCR-PIPK genes in *P. infestans*, led to malformed elongated sporangia and defects in zoospore release (Hua et al. 2013). One GPCR-PIPK in *P. sojae*, i.e. PsGK4, was found to be involved in chemotaxis, while silencing of *PsGK5*, another member of the GPCR-PIPK gene family, resulted in defects in oospore formation (Yang et al. 2013).

In addition to these novel types of GPCRs *P. infestans* has a rather extensive set of putative GPCRs with 88 gene models predicted to encode a canonical GPCR (van den Hoogen et al. 2018). In contrast, only a single Gα subunit and a single Gβ subunit are described (Laxalt et al. 2002). Initially attempts to identify a *Phytophthora* gene encoding a Gγ subunit failed even when whole genome sequences of *Phytophthora* spp. became available (Tyler et al. 2006; Haas et al. 2009). Their small size, typically ranging in length from 70 to 110 amino acids, and high sequence divergence makes identification of Gγ subunits in unrelated taxa difficult. Using iterative hidden Markov model searches, Anantharaman and colleagues ultimately identified a putative Gγ subunit gene in *P. sojae* and *P. infestans* (Anantharaman et al. 2011).

In this study, we explored the role of the proposed *P. infestans* Gγ subunit gene, *Pigpg1*. We identified homologs in other oomycetes and show the significant distance of the conserved oomycete Gγ subunits to other eukaryotic Gγ subunits. To determine the function of PiGPG1, we generated *Pigpg1*-overexpression and *Pigpg1*-silenced lines and analyzed their phenotypes. The phenotypic defects in the *Pigpg1*-silenced transformants resemble those observed in previously studied *Pigpb1*-silenced transformants (Latijnhouwers & Govers 2003), suggesting that Gβ and Gγ behave similar as in other eukaryotes and function as a Gβγ dimer. Altogether, this study provides evidence for the validity of the proposed Gγ subunit gene model and its importance for asexual reproduction in *P. infestans*.

3.3 Results

P. infestans has one putative Gγ gene

The gene model proposed to encode a Gγ subunit is PITG_16898 (Anantharaman et al. 2011). The gene has one putative intron and is predicted to encode a protein of 71 amino acids (Fig. 1A). The protein sequence has similarity to a G-protein gamma-like domain (PF00631). Moreover, conserved motifs such as the Gβ-interacting DPLL/I motif (present as DPFL) (Trusov et al. 2012), and the C-terminal CAAX box (CSIL) (Higgins & Casey 1996) are present, pointing to a bona fide Gγ subunit (**Figure 3.1a**). Hence, the gene was named *Pigpg1*. To investigate the validity of the gene model, we utilized in-house RNAseq data and this confirmed the intron prediction. These results were validated by comparing the length of the *Pigpg1* PCR amplicons derived from genomic DNA and cDNA, and demonstrating the presence of the 72 bp intron (**Figure S3.1**). No *Pigpg1* homologs were found by BLAST analysis of the *P. infestans* T30-4 reference genome (Haas et al. 2009), pointing to a single gene encoding a Gγ subunit.

Oomycete Gγ subunits are strongly conserved

We analyzed 19 oomycete genomes for the presence of homologs of *Pigpg1*. This confirmed the presence of a single Gγ subunit gene in each of the assembled genomes, with the exception of *Hyaloperonospora arabidopsidis*, which has two copies (**Table S3.1**). All putative oomycete Gγ subunit genes have two exons, encoding a protein of 70 or 71 amino acids. In all the oomycete Gγ genes, canonical GT/AG intron boundaries are present. The intron length ranges from 41 to 92 bp and the intron sequences are not conserved (**Figure S3.2**).

To analyze the degree of conservation across oomycete Gγ subunits, we constructed a multiple sequence alignment of protein sequences of oomycete Gγ subunits. The Gγ subunits in the six *Phytophthora* species analyzed are nearly identical, with 60 out of 71 amino acids entirely conserved. The sequence identity among oomycete Gγ subunits is over 75% and shows a strong conservation of several amino acids (**Figure 3.1b**). All predicted oomycete Gγ subunits have the DPLL/I motif and CAAX box (**Figure 3.1b**), with the exception of one of the two *H. arabidopsis* copies. This gene product is unlikely to function as a Gγ and therefore the gene model is not included in the alignment.

Quarternary structure of the predicted Gβγ complex

To further validate the putative Gβγ complex of *P. infestans*, we examined the predicted quaternary structure. To do so, we first predicted the 3D structure of both PiGPB1 and PiGPG1 using SWISS-MODEL (Bordoli et al. 2009) and then structurally aligned the models (**Figure 3.1c**). The predicted quaternary structure resembles the stereotypical structure of

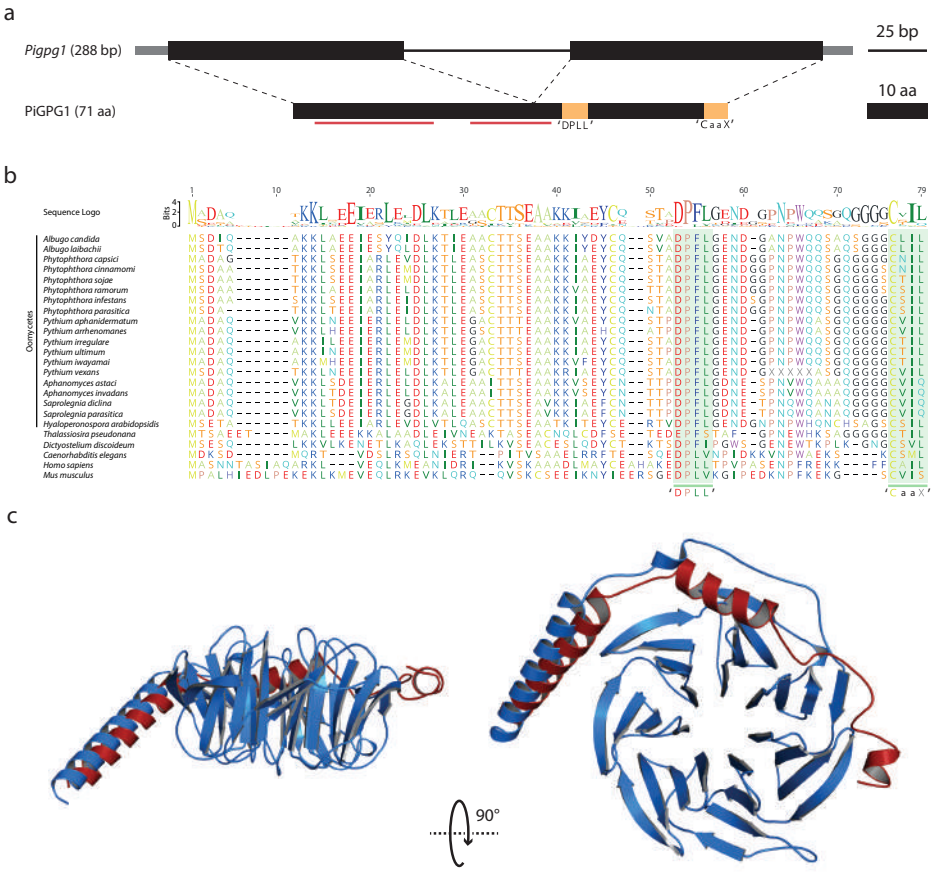

Figure 3.1 | a) Graphical representation of *Pigpg1* and the encoded protein PiGPG1. The gene (288 bp) has two exons (black bars) interrupted by one intron (black line). The grey bars depict the 5' and 3' UTR. The conserved motifs in PiGPG1 are highlighted in orange and the locations of predicted alpha-helices are underlined in red. **b)** Multiple sequence alignment of PiGPG1 homologs including 19 derived from oomycete species (black vertical bar), one from a diatom (*Thalassiosira pseudonana*) and four from unikonts (*Dictyostelium discoideum*, *Caenorhabditis elegans*, *Homo sapiens*, *Mus musculus*). Conserved motifs (DPLL, CAAX) are highlighted. Gene IDs of all included gene models are listed in Table S1. **c)** Predicted 3D model of the tertiary structure of the Gβγ dimer with PiGPB1 depicted in blue and PiGPG1 in red.

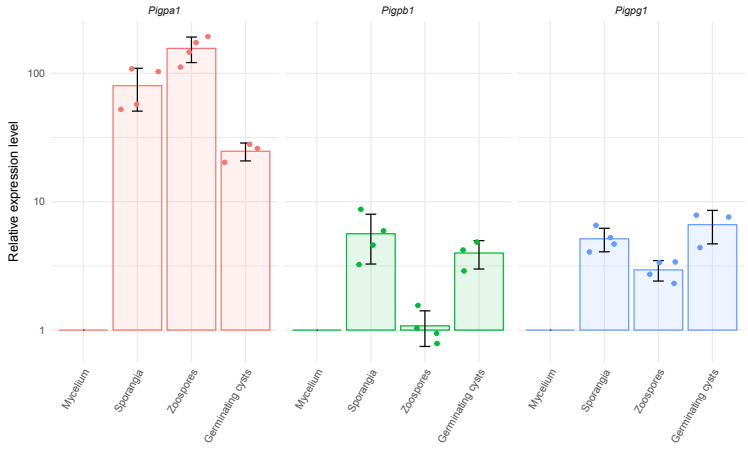

Figure 3.2 | Expression of *Pigpa1*, *Pigpb1*, and *Pigpg1* in mycelium, sporangia, zoospores, and germinating cysts. Expression is normalized to *PiActA* expression, and shown relative to expression in mycelium.

a G$\beta\gamma$ complex, where Gγ wraps around Gβ, interacting with the two α-helices at the C-terminus of Gβ (Oldham & Hamm 2006). This further underscores the validity of the gene model, and suggests that PiGPB1 and PiGPG1 can form a G$\beta\gamma$ dimer.

Pigpg1 is higher expressed in spores than in mycelium

Next, we analyzed the expression of *Pigpg1* during vegetative growth and asexual development. Analyses by qPCR showed that, relative to mycelium, expression of *Pigpg1* is induced in sporangia, zoospores, and germinating cysts (**Figure 3.2**). In this analysis, we also monitored the expression of *Pigpa1* and *Pigpb1* and this showed that *Pigpa1* expression is low in mycelium and upregulated in sporangia and zoospores whereas *Pigpb1* is upregulated in sporangia but not in zoospores (**Figure 3.2**). These results are in line with previous expression analyses based on Northern blot hybridizations (Laxalt et al. 2002). In that analysis *Pigpa1* transcripts were not detectable in mycelium and this may explain why the upregulation of *Pigpa1* in sporangia and zoospores measured by qPCR is so strong when compared to the expression levels in mycelium.

Transcriptional silencing and overexpression of *Pigpg1*

To obtain *P. infestans* lines with a reduced or increased expression of *Pigpg1* we introduced extra copies *Pigpg1* in the genome of *P. infestans* by PEG-mediated DNA transformation of a construct carrying a geneticin resistance gene (*nptII*) for selection and the genomic DNA sequence of *Pigpg1* in sense orientation regulated by a strong promoter (**Figure S3.3**).

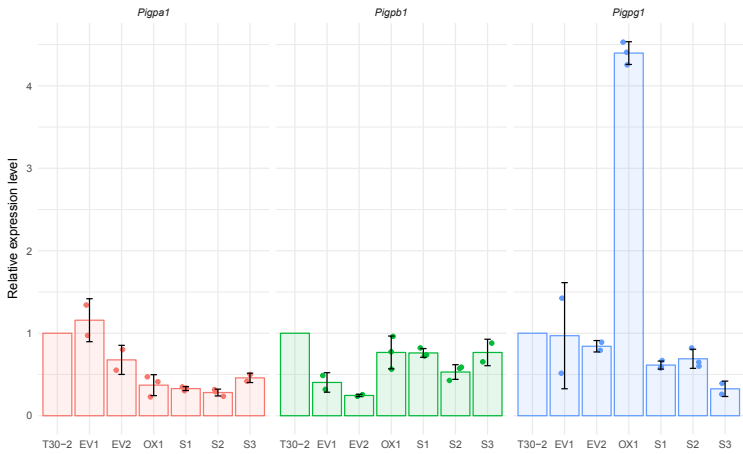

Figure 3.3 | Relative expression levels of *Pigpa1*, *Pigb1*, and *Pigpg1* in mycelium of the recipient strain (T30-2), the empty vector transformants (EV1 and EV2), the overexpression transformant (OX1) and the silenced transformants (S1, S2, and S3). The expression of each gene was calculated relative to *PiActA* and normalized to the expression in strain T30-2.

We obtained a total of 56 stable geneticin resistant lines. However, most of these lines showed severe growth defects, making them unusable for further analysis. A subset of four transformed lines without severe growth defects was selected for further analysis. As a control, DNA transformations were performed with an empty vector (EV). Two EV control lines were included for further analysis.

To assess whether the transformed lines showed altered expression levels of *Pigpg1*, we performed qPCRs on RNA obtained from mycelium. We observed three transformed lines in which *Pigpg1* expression was reduced (silenced transformants S1, S2, and S3), and one in which expression was increased (overexpression transformant OX1) (**Figure 3.3**).

To assess whether the expression of *Pigpa1* and *Pigpb1* was affected by silencing or overexpressing *Pigpg1*, we performed additional qPCRs. Overall, the transcript levels of *Pigpa1* were slightly reduced in comparison to the wild type recipient strain, not only in the *Pigpg1* silenced transformants S1, S2 and S3, but also in the overexpression transformant OX1. *Pigpb1* transcript levels seemed to be less affected.

PiGPG1 is not required for oospore formation

To assess whether PiGPG1 is involved in mating of *P. infestans*, we co-cultivated the wild type recipient strain T30-2, the *Pigpg1*-silenced transformants and the overexpression transformant (mating type A1) with a wild type strain of the opposite mating type (mating type A2). In all combinations, the number of oospores that was formed at the interface

was in the same range, and also the morphology of the oospores was comparable. This suggests that PiGPG1 is not required for oospore formation.

Mycelial growth is impaired by *Pigpg1*-overexpression

To assess whether *Pigpg1* has a role in vegetative growth, we analyzed the radial growth rate of the transformed lines on rye sucrose agar (RSA). The *Pigpg1*-silenced lines showed a growth rate similar to that of the EV lines, reaching a 7 to 8 cm diameter colony in 14 days (**Figure 3.4a**). In contrast, the *Pigpg1*-overexpression line OX1 consistently grew slower compared to the other lines (**Figure 3.4a**). OX1 also showed a more aerial and 'fluffy' phenotype in comparison to the empty vector control lines while the silenced lines displayed no obvious changes in morphology (**Figure 3.4b**).

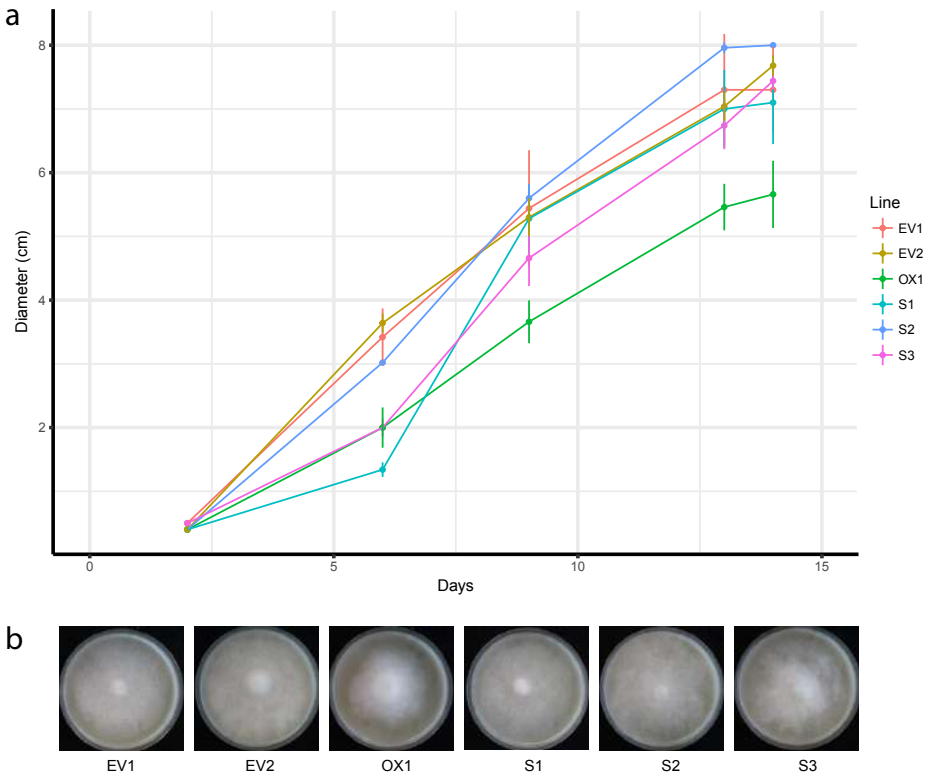

Figure 3.4 | a) Radial growth rate of empty vector control lines (EV), *Pigpg1* overexpression (OX) and *Pigpg1* silenced (S) lines. The graph is representative for three independent growth rate assays that each included five replicates per line. The diameter at d = 2 is the size of inoculation plug (ø 0.5 cm). EV lines did not show deviations from growth rates observed in the recipient strain T30-2. **b)** Morphology of EV, OX, and S lines, cultivated for 14 days on RSA at 18 °C

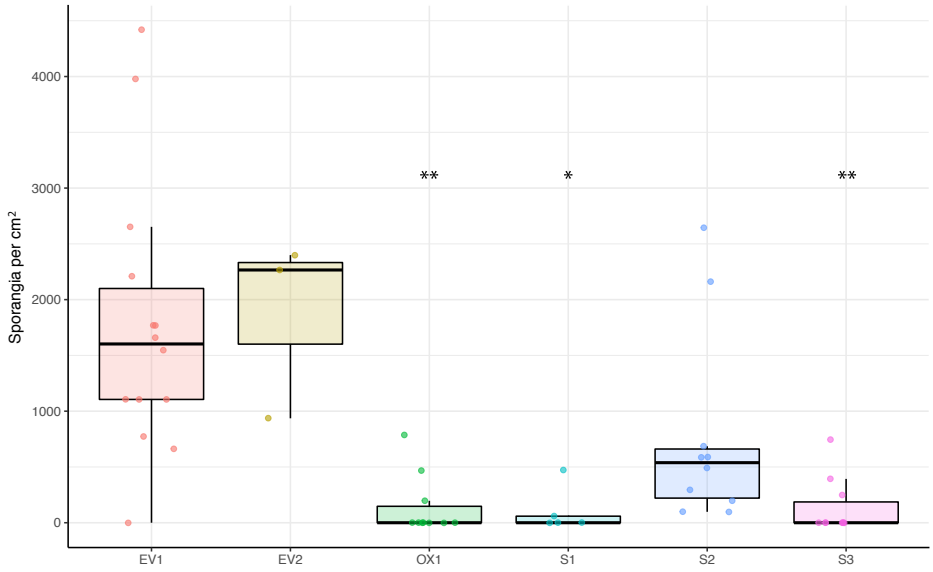

Figure 3.5 | Average number of sporangia per square centimeter of mycelium after 14-day growth on RSA. The total number of sporangia was set relative to the total area of the colony. Differences between the number of sporangia were evaluated with Wilcoxon signed-rank test (* $p<0.05$, ** $p<0.01$).

Pigpg1 silencing and overexpression affects sporangial development

To evaluate whether *Pigpg1*-silenced lines have defects in sporangial development, we analyzed the number of sporangia formed during cultivation on solid medium. Overall, in both *Pigpg1*-silenced and *Pigpg1*-overexpression lines, we observed a strong reduction in the number of sporangia compared to the control EV lines (**Figure 3.5**).

In wild type strains, *P. infestans* sporangia are ovoid, lemon-shaped. In *Pigpg1*-silenced lines we observed many sporangia with aberrant phenotypes (**Figure 3.6a**). Their shape was more elongated, and in many cases sporangia with oversized papillae were observed (**Figure 3.6a**). To assess whether the shape of the malformed sporangia of the silenced lines is significantly different from the normal shape as observed in the control lines, we measured length and width of the sporangia and determined the length-to-width (LW) ratio. Although no significant differences were observed in the length or width of sporangia (**Figures 3.6c, 3.6d, Table S3.2**) the LW ratio of sporangia of the silenced was significantly increased. In EV lines this LW ratio is on average 1.46±0.17, whereas in silenced lines the LW ratio is around 1.63±0.28 (**Figure 3.6b, Table S3.2**). In contrast, the sporangia of the overexpression line OX1 were more round shaped instead of oval (**Figure 3.6a**) and this is reflected in a slightly lower LW ratio of 1.37±0.16 (**Table S3.2**).

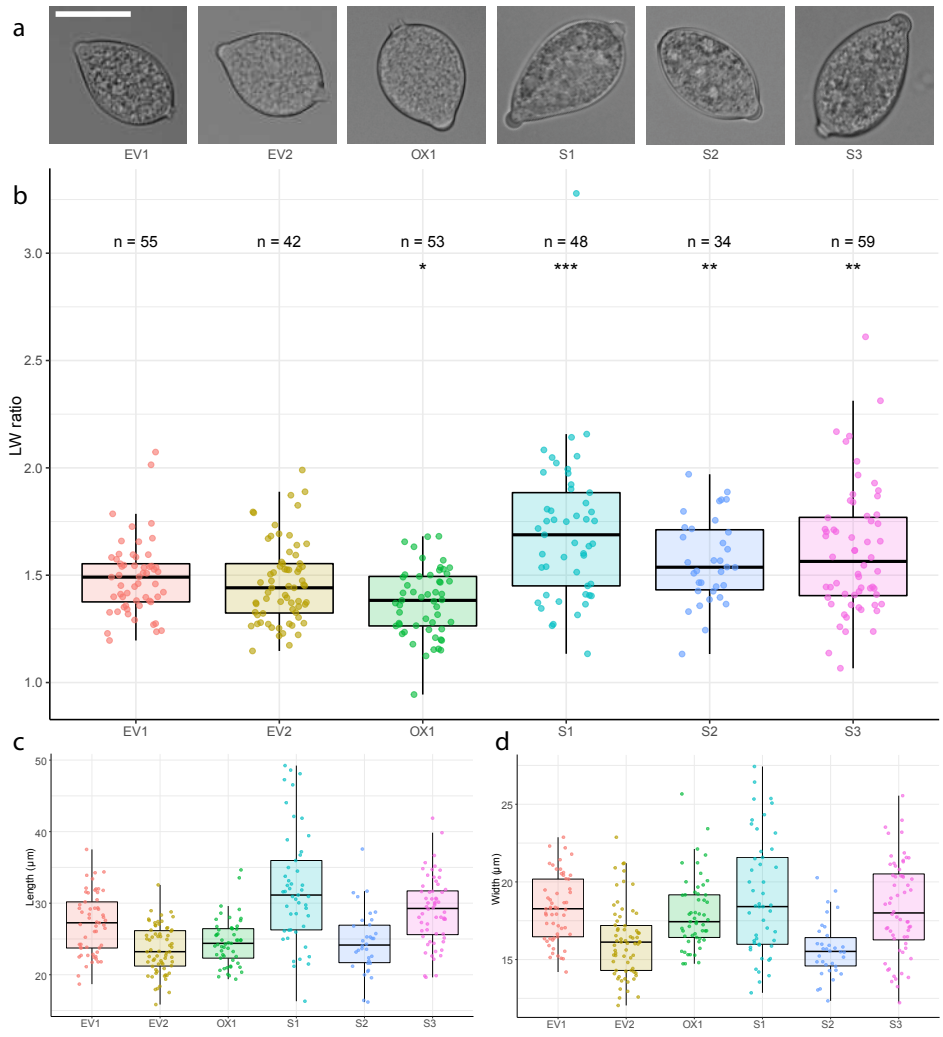

Figure 3.6 | a) Representative sporangia from control lines (EV1-3), the *Pigpg1*-overxpression line (OX1), and *Pigpg1*-silenced (S1-3) lines. Bar is 20 µm; **b)** Length-to-width (LW) ratios from at least 34 sporangia per line. Differences between LW ratios were evaluated with Wilcoxon signed-rank test (* p<0.05, ** p<0.01, *** p <0.001). The experiment was performed three times on independent samples of sporangia of each line, with similar results; Length **(c)** and width **(d)** of at least 34 sporangia per line.

3.4 Discussion

Previous studies on G-protein signaling in *P. infestans* dealt with the functional analyses of two the three subunits of the heterotrimeric G-protein complex, i.e. Gα and Gβ. In this study, we show that *P. infestans* has a functional Gγ subunit that plays a crucial role in asexual development of this plant pathogen. Transformed lines in which *Pigpg1* is silenced or overexpressed produce a reduced number of sporangia, and if produced, they display malformations. We also observed defects in the production of zoospores, but this phenotype was not always consistent and difficult to quantify. The relatively low sequence similarity of PiGPG1 to Gγ subunits previously identified in organisms from other taxa explains why Gγ subunit genes were not readily detected in oomycetes, neither by automatic genome annotation pipelines nor by manual inspection. The high degree of conservation of the Gγ subunit within oomycetes, together with the conserved Gα and Gβ subunits is a strong indication that oomycetes have a bona fide heterotrimeric G-protein complex.

Because of the elementary role of PiGPG1 in development we faced limitations in our experimental set-up employing gene silencing of *Pigpg1*. From the initial pool of *P. infestans* transformants, over 50 lines had severe growth defects and were not viable. In the few that could be maintained, transcriptional silencing of *Pigpg1* was relatively ineffective, with the lowest transcription levels down to approximately 35% of those observed in the recipient strain T30-2. It is not unlikely that the transformed lines, which we had to discard due to lack of viability, posed higher silencing efficiencies. Presumably, lower transcription levels of *Pigpg1* result in either severe growth defects or are lethal. Thus, we expect PiGPG1 to be essential for *P. infestans*.

The phenotypes of *Pigpg1*-silenced lines are similar to what was observed in *Pigpb1*-silenced lines, which also produce fewer sporangia than wild type, and those produced are malformed (Latijnhouwers & Govers 2003). Moreover, the single *Pigpg1*-overexpression line OX1 displayed 'fluffy', aerial mycelium, similar to *Pigpgb1*-silenced lines (Latijnhouwers & Govers 2003). These results are in line with the general consensus that Gβ and Gγ form a heterodimer that, as such, activates or suppresses downstream effectors in the G-protein signaling pathway. The Gβγ complex functionally acts as a monomer and only under denaturing conditions the subunits are dissociated (Clapham & Neer 1997). Compared to the Gβ subunit, Gγ is relatively small but nevertheless its role is essential. Its primary function is the localization of the Gβγ complex to the plasma membrane. Post-translational lipid modifications on the CAAX box at the C-terminus, such as isoprenylation, serve as a membrane anchor to aid membrane localization, which is a prerequisite for proper G-protein signaling (Zhang et al. 2001; Vogler et al. 2008; Mulligan et al. 2010).

Compared to higher eukaryotes, the versatility of G-protein signaling in oomycetes might appear limited. With only one single gene for each G-protein subunit, only one unique heterotrimeric G-protein complex can be formed. This is in sharp contrast to the vast numbers

of potential unique heterotrimers in higher eukaryotes. In humans, for example, a total of around 700 combinations is theoretically possible, and although not all these 700 are verified, many combinations have been observed, often as tissue specific heterotrimeric G-protein complexes or associated with certain developmental stages (Hillenbrand et al. 2015). Hence, it is likely that the single heterotrimeric G-protein complex in *P. infestans* has a much broader function in signaling than the more specialized heterotrimers in other organisms. Consequently, a deficiency in either one of the G-protein subunits will have profound effects. Indeed, severe phenotypes were observed in both *Pigpa1* and *Pigpb1* silenced transformants (Latijnhouwers & Govers 2003; Latijnhouwers et al. 2004), and as shown in this study, also upon *Pigpg1* silencing.

The observation that silencing or overexpressing *Pigpg1* has an effect on the expression level of *Pigpa1* and also *Pigpb1*, albeit to a lesser extent, indicates regulation of G-protein subunit genes via (post)transcriptional feedback. This presumed transcriptional feedback mechanism could in part explain the profound phenotypes that we observed. Supposedly not only G$\beta\gamma$ levels are reduced but also Gα. It has been reported that silencing or knock-out mutagenesis of a particular G-protein subunit gene can indeed lead to decreased levels of other subunits, illustrating their interdependency. In the filamentous fungus *Neurospora crassa*, reduced protein levels of Gα and Gβ were observed in Gγ deletion mutants (Krystofova & Borkovich 2005) and similar findings were reported for *S. cerevisiae* and mice (Hirschman et al. 1997; Schwindinger et al. 2004). Apart from the regulation on protein level, which occurs likely by an increased turnover rate, also the transcription rate of G-protein subunit genes can be affected. For example, in the chestnut blight fungus *Cryphonectria parasitica*, disruption of the Gβ subunit gene resulted in reduced mRNA levels of the gene encoding Gα (Kasahara et al. 2000).

G-proteins do not seem to be involved in the initial phases of sexual reproduction of *P. infestans*. In *Pigpg1* silenced and overexpression lines, we did not observe differences in the numbers of oospores that were formed, nor in their morphology. This is in accordance with previous observations that silencing of *Pigpgb1* did not affect oospore formation (Latijnhouwers & Govers 2003). In several fungi though, G-protein subunits play an important role in sexual reproduction. For example, in *S. cerevisiae* G$\beta\gamma$ subunits are essential for initiating downstream signaling upon recognition of the mating factor (Alvaro & Thorner 2016). In *Phytophthora* the molecular basis of sexual reproduction is still poorly understood. A recent study in *P. infestans* showed severe defects in oospore formation upon silencing of *PiLLP*, a gene encoding a loricin-like, glycine rich cell wall protein (Guo et al. 2017). In *P. sojae*, silencing of *PsGK5* severely affects oospore formation pointing to a role for a GPCR-PIPK as signaling component in mating (Yang et al. 2013). In view of the findings that reduction in either Gβ (Latijnhouwers & Govers 2003) or Gγ (this study) has no severe effects on oospore formation suggests that GPCR-PIPKs can act independently of the heterotrimeric G-protein complex. One of the proposed models for the mode of action of GPCR-PIPKs entails a direct activation of the PIPK domain through agonist binding on the GPCR domain (**this thesis, chapter 6**). In this case the agonist could be a mating hormone.

Phytophthora mating hormones have been identified but what their receptors are and how their synthesis is regulated is unknown (Harutyunyan et al. 2008).

The severe impairment in sporangial development and zoospore release in the *Pigpg1*-silenced and overexpression lines refrained us from testing the role of PiGPG1 in virulence of *P. infestans*. As none of the transformed lines produced sufficient sporangia or zoospores for the inoculation of potato leaves we made attempts to use mycelium as inoculum. We performed several trials, but were unable to determine whether the reduced infection efficiencies were due to poor quality of the inoculum or to reduced levels of PiGPG1.

Integrating the results of this study with previous findings lead us to conclude that *P. infestans* has a functional heterotrimeric G-protein complex with a vital role in asexual development. Although all three G-protein subunits are present, *P. infestans* only has a single gene for each subunit, a restriction that likely limits the flexibility in heterotrimeric G-protein signaling in this pathogen. The same holds for other oomycetes and this raises the question how these organisms deal with this. The most pressing question is whether all the 88 GPCRs, predicted to be present in *P. infestans* based on genome mining (van den Hoogen et al. 2018), are dependent on one heterotrimeric G-protein. This seems unlikely; it would be a kind of bottleneck severely reducing the variety of potential downstream signaling pathways that have to be in place in such a complex environment. Presumably, in oomycetes this bottleneck can be avoided by alternative signaling pathways. The variety of so-called GPCR-bigrams, i.e. GPCRs with a catalytic accessory domain such as the GPCR-PIPKs (van den Hoogen et al. 2018), offers ample opportunity for transmission of extracellular signals to the inside of the cell independent of the heterotrimeric G-protein. Alternatively, signaling through β-arrestins might be in play as well. Altogether, the intricate network underlying G-protein signaling in *Phytophthora* and other oomycetes is still a black box with many questions that remain to be answered.

3.5 Materials and Methods

Strains, culture conditions and life stages

P. infestans strain T30-2 (van der Lee et al. 2004) (A1 mating type) and all transgenic lines were grown routinely at 18 °C in the dark on rye agar medium supplemented with 2% sucrose (RSA) (Caten & Jinks 1968). RSA was supplemented 20 µg/ml vancomycin, 100 µg/ml ampicillin and 50 µg/ml amphotericin B, in addition with 2.5 µg/ml geneticin for the transformants. Prior to assays, transformant lines were cultivated on RSA without geneticin for two generations to rule out possible adverse effects of the selection compound. Sporangia were dislodged from sporulating mycelium in sterile milli-Q water by rubbing with a Drigalski spatula, and counted using a haemocytometer. Mycelial fragments were filtered out using a 50 µm nylon mesh. Zoospore release was induced by flooding sporulating mycelium with cold milli-Q water and incubation at 4°C for 2.5h. To obtain mycelium

free of sporangia for RNA isolation, mycelium was grown in liquid rye sucrose medium and washed multiple times in sterile milli-Q water, snap-frozen in liquid nitrogen and subsequently freeze-dried overnight. Mating assays were performed by cocultivating the T30-2 recipient strain or transformed lines, along with *P. infestans* strain 88133 (mating type A2). Oospores were observed at the interface of the two strains after 7 days.

RNA isolation and expression analyses

RNA was isolated using home-made TRIzol (Verdonk 2014) and cDNA was synthesized using M-MLV Reverse Transcriptase (Promega) according to manufacturer's instructions. qPCR was carried out on an ABI7300 PCR machine (Applied Biosystems) in combination with the SensiMix SYBR Hi-ROX kit (BioLine). The following qPCR conditions were used: an initial 95°C denaturation step for 10 seconds followed by denaturation for 15 seconds at 95°C, annealing for 60 seconds at 60°C, and extension at 72°C for 40 cycles. Melt curves were generated to evaluate the specificity of amplification. *ActA* (PITG_15117) was used as endogenous control. The fold change of expression was calculated using the delta-delta Ct method (Livak & Schmittgen 2001).

Microscopy

Microscopy was performed using a Nikon 90i microscope and analyzed using ImageJ (Schneider et al. 2012). The average length-to-width ratio of *Pigpg1*-silenced and *Pigpg1*-overexpressed sporangia were compared to the control lines using a Wilcoxon signed-rank test in R v3.3.2.

Plasmid construction and *P. infestans* transformations

To obtain a sense construct for the silencing and overexpression of the *P. infestans* Gγ subunit, the full-length sequence of PITG_16898 was amplified from gDNA of P. infestans isolate 88069 and cloned into the NotI and AatII sites of the vector pmCherry-N (Ah-Fong & Judelson 2011), resulting in plasmid pmCherry-Gγ. This plasmid and the empty vector pmCherry (as control) were used for DNA transformation of *P. infestans* strain T30-2. Stable transformants were generated using PEG/CaCl2-mediated protoplast transformation according to methods described previously (Ah-Fong et al. 2008), omitting the step of complexing circular plasmid DNA with Lipofectin. A total of 70 transformants was obtained, from which four were selected for analysis. All primers used in this study are listed in supplemental table S2.

Bioinformatic analyses

To predict the quaternary structure of the *P. infestans* Gβγ dimer, 3D models of G-protein subunits PiGPB1 (PITG_06376) and PiGPG1 (PITG_16898) were predicted using SWISS-MODEL (Bordoli et al. 2009). Next, the align feature in PyMOL (Schrodinger 2015) was used to align the subunits. Oomycete Gγ homologs were obtained by BLAST (Altschul et al. 1997) search on FungiDB (Stajich et al. 2012), using the PiGPG1 protein sequence as query. Protein sequences of putative homologs were analyzed in Geneious V9.1.4 (Kearse et al. 2012). Multiple sequence alignments were made using the MAFFT (Katoh & Standley 2013) plugin in Geneious.

3.6 Acknowledgements

We would like to thank Prof. Dr. Howard Judelson for kindly providing the pmCherry-N vector, Harold Meijer for support in the initial phase of the project, Paul Schaap for technical assistance, Pierre Moquet for helping with statistical analyses, and Julian Verdonk for providing home-made TRIzol reagent. This work was financially supported by the Division for Earth and Live Sciences (ALW) with financial aid from the Netherlands Organization for Scientific Research (NWO) in the framework of the ALW-JSTP programme (project number 833.13.002; J.H.; F.G) and by the Food-for-Thought campaign from the University Fund Wageningen (N.V.; F.G.). The authors declare no conflict of interest.

3.7 Supplemental files

Table S3.1 | Gγ subunit genes in oomycetes

Gene ID	Product description	Note	Organism	Length (aa)
evm.TU.AC2VRR_s00154g59	unspecified product		*Albugo candida*	70
ALNC14_027420	unspecified product		*Albugo laibachii*	70
H257_08527	unspecified product		*Aphanomyces astaci*	70
H310_08072	unspecified product		*Aphanomyces invadans*	70
Hpa_Gpg1	uncharacterized protein		*Hyaloperonospora arabidopsidis*	71
Hpa_Gpg2	uncharacterized protein	Pseudogene	*Hyaloperonospora arabidopsidis*	71
PHYCA_11944	unspecified product		*Phytophthora capsici*	71
PHYCI_226007	unspecified product		*Phytophthora cinnamomi*	71
PITG_16898	hypothetical protein		*Phytophthora infestans*	71
PPTG_12153	hypothetical protein		*Phytophthora parasitica*	70
PramPr-102_SC0012 - 495630-495361	N/A	Corrected	*Phytophthora ramorum*	71
PHYSO_288141	unspecified product	Corrected	*Phytophthora sojae*	71
PAG1_G009306	unspecified product		*Pythium aphanidermatum*	70
PAR_G013431	unspecified product		*Pythium arrhenomanes*	70
PIR_G005981	unspecified product		*Pythium irregulare*	70
PIW_G007690	unspecified product		*Pythium iwayamai*	70
PYU1_G009775	unspecified product		*Pythium ultimum*	70
PVE_G008653	unspecified product	Corrected	*Pythium vexans*	70
SDRG_05853	hypothetical protein		*Saprolegnia diclina*	70
SPRG_15045	hypothetical protein		*Saprolegnia parasitica*	70

Table S3.2 | Length and width measurements of *P. infestans* sporangia. Average length and width of sporangia isolated from control (EV), Pigpg1-overexpression (OE) and Pigpg1-silenced (S) lines, and length-to-width (LW) ratios. * p <0.05, ** p <0.01, *** p <0.001 using Wilcoxon signed-rank test.

Line	Average length (µm)	Average width (µm)	Average LW
EV1	27.13	18.28	1.49
EV2	23.53	16.20	1.46
OX1	24.53	17.96	1.37
S1	32.15	19.01	1.70*
S2	24.58	15.67	1.57*
S3	28.99	18.31	1.61*

Table S3.3 | Primers used in this study

Name	Sequence (5' - 3')	Purpose
Pigpa1_qF	CATGTACGATGTCGGTGGAC	Pigpa1 qPCR
Pigpa1_qR	GCCTCGATCATACGGTTTGT	Pigpa1 qPCR
Pigpb1_qF	GAGCCTCAAGGAGACGATTG	Pigpb1 qPCR
Pigpb1_qR	GCCAAAGTGGCCTTTCAATA	Pigpb1 qPCR
Pigpg1_qF	CGAGATCGACCTCAAGACG	Pigpg1 qPCR
Pigpg1_qR	GTACTCGGCGATTTTCTTGG	Pigpg1 qPCR
PiActA_qF	CATCAAGGAGAAGCTGACGTACA	PiActA qPCR
PiActA_qR	GACGACTCGGCGGCAG	PiActA qPCR
Pigpg1_NotI_F	TACAAGGCGGCCGCAATGTCCGACGCAGCCTCCAAG	Cloning Pigpg1 in pmCherryN
Pigpg1_AatII_R	GGTTAGACGTCCTACAAAATGCTACAACCGCCG	Cloning Pigpg1 in pmCherryN
Pigpg1_F	TATACCGGTATGTCCGACGCAGCCT	Full-length {Pigpg1 }gene product
Pigpg1_R	TATGCTAGCCAAAATGCTACAACCGC	Full-length {Pigpg1 }gene product

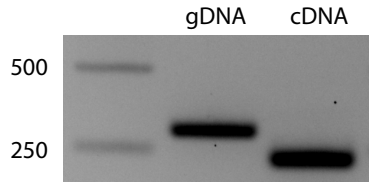

Figure S3.1 | The *P. infestans* Gγ subunit gene *Pigpg1* has one intron. The 72 bp intron present in PITG_16898 is spliced out during transcription. Amplicons of *Pigpg1* obtained by PCR with primers Pigpg1_F and Pigpg1_R and *P. infestans* T30-2 gDNA (expected size: 288 bp) and cDNA (expected size: 216 bp) as template.

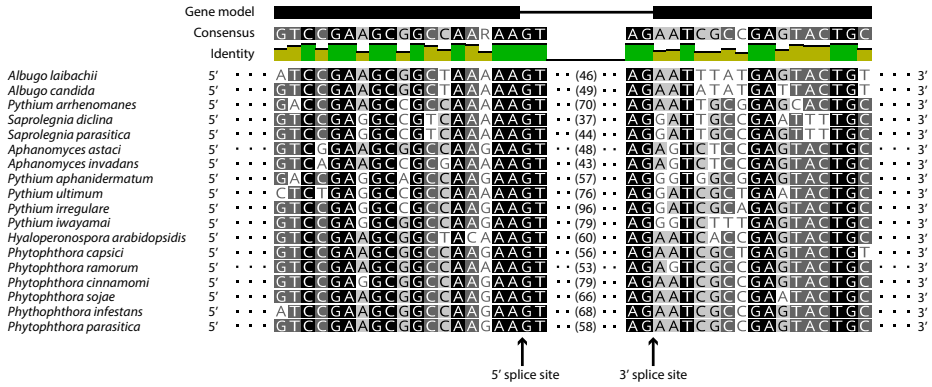

Figure S3.2 | The intron boundaries in oomycete Gγ subunit genes are conserved. GT/AG splice sites (indicated with arrows) are present in all sequences. All gene models have two exons (black bars) and one intron (black line). Numbers between brackets indicate intron lengths (GT/AG not included). Interpuncts (·) indicate truncated sequences.

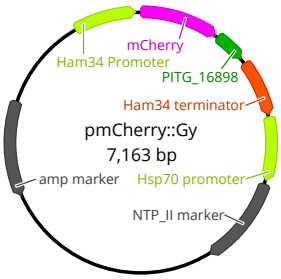

Figure S3.3 | Construct used for transformation of *P. infestans*. Integration in the genome can lead to transcriptional silencing and overexpression of *Pigpg1*.

Chapter 4

The microtubule cytoskeleton and motor proteins in *Phytophthora*

Johan van den Hoogen[#], Kiki Kots[#], Michiel Kasteel, Tijs Ketelaar, Francine Govers

[#] These authors contributed equally to the work presented

This chapter is in preparation for publication.

4.1 Abstract

The microtubule (MT) cytoskeleton is a system of intracellular filaments, that is able to quickly adapt different configurations. This process is regulated by microtubular dynamics and MT-associated proteins (MAPs). The MT cytoskeleton is shared by all eukaryotes and is involved in numerous cellular processes ranging from nuclear division to intracellular transport, but its role varies between organisms and cells. Here, we focus on the microtubule (MT) cytoskeleton in filamentous plant pathogens in the genus *Phytophthora*. We made an inventory of α- and β-tubulin proteins, the building blocks of microtubules in oomycetes, and also catalogued MAPs in *Phytophthora infestans*. This resulted in 186 putative MAPs that are divided over all major MAP classes and include some unique dynein and kinesin types, some with accessory domains not found elsewhere. Live cell imaging of transgenic *Phytophthora palmivora* lines carrying an ectopically integrated GFP-α-tubulin fusion gene provided insight in the spatio-temporal organization of the MT cytoskeleton in *Phytophthora*. These lines enabled us to monitor the *in vivo* mitotic dynamics for the first time in any oomycete. Additionally, we tested the effect of the microtubule depolymerizing drug oryzalin on the GFP-tubulin tagged lines and used oryzalin as a tool to study the consequences of microtubule depolymerization on hyphal growth and polarity. Altogether, this study provides a basis for future research on MTs and MAPs in *Phytophthora* and a first glimpse of the dynamics of the MT cytoskeleton in an oomycete.

4.2 Introduction

The cytoskeleton is a well-organized, dynamic system of intracellular filaments, shared across the three domains of life (Wickstead & Gull 2011). It has a myriad of roles, for example in processes that provide structural rigidity to cells or allow for polarized cell growth and cell movement. Main components of the eukaryotic cytoskeleton are filamentous actin, microtubules, and intermediate filaments. This study focuses on the microtubule (MT) cytoskeleton in *Phytophthora*. *Phytophthora* spp. are filamentous plant pathogens that belong to the oomycetes, organisms that together with, among others, brown algae and diatoms belong to the Stramenopiles. They are only distantly related to unikonts, a supergroup that harbors another important class of filamentous plant pathogens, namely fungi (Koonin 2010; Lévesque 2011). Though numerous free-living saprophytic oomycetes exist, many oomycetes are pathogenic, mainly on plants but also on animals, insects, or microbes (Govers & Gijzen 2006). Our prime interest is *Phytophthora*, a genus comprising over 120 species which are all plant pathogens (Kroon et al. 2012). One of the most notorious species is the late blight pathogen *Phytophthora infestans*, the culprit of the Irish potato famine in the mid-19th century (Fry 2008). But even now, *P. infestans* is problematic for potato production worldwide. For disease control farmers heavily rely on chemical crop protection, spraying every 5-7 days. Another well-known species is *Phytophthora palmivora*, the causal agent of black pod in cacao. It can infect over 170 plant species mainly in the (sub)tropics, including cacao, citrus, rubber, coconut, and oil palm (Torres et al. 2016).

To gain a better understanding of the cell biology of these pathogens and to identify novel drug targets, our research focusses on the cytoskeleton of *Phytophthora*. Our previous studies using live cell imaging of the actin cytoskeleton in *P. infestans*, showed some novel actin configurations including actin asters at the site of plant cell penetration and immobile cortical actin dots (Meijer et al. 2014; Kots et al. 2016). These so-called actin plaques appear similar to actin patches in fungi, but whereas actin patches are relatively short-lived, with turnover rates around 10 seconds (Smith et al. 2001), actin plaques in *P. infestans* have a much longer lifetime of approximately 75 minutes (Meijer et al. 2014). Moreover, unlike actin patches, actin plaques are probably not involved in endocytosis (Meijer et al. 2014). Because of the presence of these unique actin structures, and the central role of the actin cytoskeleton in growth and development, it was hypothesized that actin plaques hold promise as potential drug target (Meijer et al. 2014). Here we take a similar approach, focusing on the MT cytoskeleton of *Phytophthora*. By addressing issues related to its organization and dynamics we aim to identify features that can potentially be exploited for designing alternative control agents.

The MT cytoskeleton is crucial for nuclear division, intracellular transport, and flagellar movement. MTs are hollow, polymeric, 25 nm wide tubes assembled from protofilaments, heterodimers that are composed of α- and β-tubulin (**Figure 4.1**) (Desai & Mitchison 1997). All heterodimers are incorporated in the same orientation, with the β-tubulin monomer pointing towards the plus (+), and the α-tubulin towards the minus (-) end

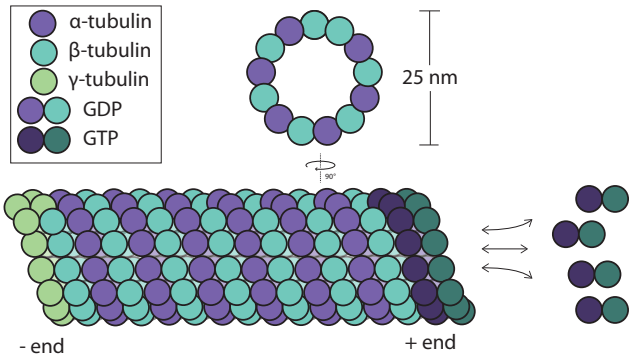

Figure 4.1 | Schematic representation of a microtubule filament. Protofilaments containing GTP-bound tubulin are continuously assembled and disassembled at the + end. The rate of GTP hydrolysis on GTP-bound tubulin protofilaments dictates the stability of the MT + end.

of the MT (Desai & Mitchison 1997). This orientation of the heterodimers determines the intrinsic polarity of the protofilaments. Rather than being a static structure, MTs are constantly growing and shrinking through a process known as dynamic instability, which is driven by GTP hydrolysis. Under physiological conditions, this process occurs at the + end of MTs. In its growing, polymerizing state, a MT contains a so-called GTP-cap, consisting of GTP-bound tubulin protofilaments. If the rate of GTP hydrolysis is higher than the incorporation of GTP-bound tubulin protofilaments, the GTP-cap is lost and the MT rapidly depolymerizes during a so-called catastrophe. At a certain point the MT is 'rescued', switching back from shrinking to growth. This dynamic instability primarily occurs at the + end, while at the - end γ-tubulin serves as a stabilizer and nucleator of MTs.

So-called motor proteins, such as kinesin and dynein, 'walk' along MTs, directed by the orientation of the protofilaments. By this movement, motor proteins are able to, for example, transport cargo or building the tension between MT pairs and the central MTs to generate the force flagellar movement. In eukaryotes, the MT cytoskeleton and motor protein movement are essential for spindle formation and functioning of the spindle during mitosis (Xiang & Plamann 2003). In filamentous fungi, the MT cytoskeleton is involved in nuclear positioning, involving the motor proteins dynein and kinesin (Xiang & Fischer 2004; Gibeaux et al. 2017). In mammalian cells, dynein and kinesin movement along MTs is crucial for transport in neurons, covering large distances (Maday et al. 2014). Another motor protein type is myosin, which transports cargo along actin filaments. Interestingly, *Phytophthora* appears to have an expansive and diverse array of this motor protein, more diverse than in any other organism, with some myosin types composed of domain combinations that are not found in organisms from other taxa (Richards & Cavalier-Smith 2005). Whether this implies extended functions for myosins in *Phytophthora* is not known, as none of these myosins have been further characterized.

Studies focused at comparative analysis of the MT cytoskeleton in a range of organisms, have identified several *Phytophthora* genes encoding components of the MT cytoskeleton, and proteins associated with it, including α-, β-, and γ-tubulin subunits, kinesins, and dyneins (Richardson et al. 2006; Wickstead & Gull 2011; Kollmar 2016). However, a complete and detailed inventory of MT proteins in an oomycete is as of yet not available. Hence, we set out to analyze the *P. infestans* genome for genes encode proteins with sequence similarity to proteins known to be part of the MT cytoskeleton. To assess whether oomycetes have unique features in their repertoire of MT-associated proteins (MAPs), we classified putative microtubule motor proteins and other MAPs in *P. infestans*. These include novel subfamilies of the motor proteins dynein and kinesin, which are unique for oomycetes. Moreover, some kinesins with unique accessory domains were identified. To test the hypothesis that MTs in oomycetes play a role in nuclear positioning in coenocytic hyphae (Heath & Kaminskyj 1989), we set out to visualize the MTs in *Phytophthora* by live cell imaging. We generated *P. palmivora* transformants expressing fluorescently labeled α-tubulin subunits, an approach that has been successfully implemented to visualize the MT cytoskeleton in a wide range of organisms, as reviewed by Goodson et al. (2010). We exploited these transformants to follow the development of the mitotic spindle and to monitor the dynamics of cytoplasmic MTs polymerizing from the Microtubule Organizing Centers (MTOCs). This is the first study in which the MT cytoskeleton in an oomycete has been visualized by live cell imaging. Altogether, this study gives us a unique insight in the MT dynamics in *Phytophthora* and provides an important basis for future research on the oomycete MT cytoskeleton.

4.3 Results and Discussion

A genome-wide inventory of oomycete microtubule proteins

To create an inventory of tubulin encoding genes in oomycetes, we first screened the *P. infestans* genome. We identified five gene models predicted to encode an α-tubulin subunit, and one gene model to encode a β-tubulin subunit. We named these genes *PiTubA1-5* and *PiTubB1*, respectively (**Tables S4.1, S4.2**). Subsequently, the *P. infestans* gene models were used as a query to identify homologs in other oomycetes. In general, most oomycetes have three to five genes encoding a α-tubulin subunit and a single β-tubulin gene (**Tables S4.1, S4.2**). At the protein level, oomycete α- and β-tubulins are highly similar; α-tubulin subunits display 91.5% pairwise identity, and β-tubulins are essentially identical exhibiting 99.4% pairwise identity.

Many oomycete α-tubulin genes are poorly annotated and the low number of identified genes in some species is likely due to a poor coverage and/or annotation of the genome sequences. In particular in *Pythium* spp., many α-tubulin gene models are incorrect resulting in truncated proteins (**Table S4.1**). Consequently, it is difficult to define the exact number of genes encoding α-subunits. However, in *Pythium ultimum* three full-length protein

models are present. Consequently, we presume that this is the number of α-subunit genes in *Pythium* spp. In *Albugo* and *Aphanomyces* spp., we were only able to detect two α-tubulin coding genes (**Table S4.1**).

Generally speaking, these numbers are in line with the gene copy numbers found for other organisms. The ciliate *Tetrahymena thermophila*, which just as oomycetes belongs to the eukaryotic supergroup chromalveolates, contains a single α-tubulin gene and two β-tubulin genes (Smith et al. 2004). Whereas lower fungi in the divisions Zygomycota and Chytridiomycota have up to five α- and β-tubulin coding genes, higher fungi often have less with ascomycetes and basidiomycetes containing only one and two α- or β-tubulin genes (Zhao et al. 2014). In plants, tubulin encoding genes underwent duplication events, resulting in up to 20 β-tubulin genes in flowering plants (Breviario et al. 2013).

Functional classification of putative *P. infestans* microtubule-associated proteins

With the aim of providing a comprehensive overview of MT-associated motor proteins and other MAPs in *P. infestans*, we extended our search. To this end, we used a combination of Blast, HMM, and keyword searches, including motor proteins and other MAPs previously described in fungi (Xiang & Plamann 2003) and plants (Krtkova et al. 2016) as queries. This resulted in a total of 186 gene models, which were classified into relevant (sub)families based on sequence homology to known MAPs. An overview of the MAPs identified in *P. infestans* is provided in **Table 4.1**, and all putative MAP encoding genes are listed in **Table S4.3**.

The inventory includes members of all major classes of described MAPs, such as the motor proteins dynein and kinesin, while genes encoding augmin subunits seem absent (discussed in detail below). Several MT plus end binding proteins were identified (**Table S4.3**), which have important roles in several processes such as protein localization and regulating MT dynamics. Also, proteins involved in MT nucleation are present, including 6 γ-tubulins and a homolog of TPX2 (Targeting protein for Xklp2) (**Table S4.3**). Furthermore, MT- and centrosome-associated protein kinases, tubulin assembly proteins, and kinetochore and centromere-associated proteins are found. We have also included a number of previously identified intraflagellar transport proteins (Judelson et al. 2012).

Oomycetes contain unique kinesins

We identified a total of 58 *P. infestans* genes encoding putative kinesins (**Table S4.3**). Most of these could be classified in existing subfamilies, according to similarity to members of described kinesin families in other eukaryotes. In accordance with earlier analyses in *Phytophthora sojae* (Wickstead et al. 2010), two *P. infestans* kinesins were found to be divergent from other eukaryotic kinesins. In a phylogenetic reconstruction, we found that one of these kinesins groups with several ciliate and protozoan kinesins, which are also

Table 4.1 | Microtubule subunits and microtubule associated proteins (MAPs) in *P. infestans*

Family	Subfamily	Number of genes
Tubulin	Alpha	5
	Beta	1
	Gamma	1
Other subunits	SPC97/98	5
	FtsZ	3
MT+ end binding proteins	EB1	1
	CLASP	1
	MOR1/MAP215	1
Kinesins	KIN family	61
Dynein	Light chain	15
	Intermediate chain	4
	Heavy chain	20
	Dynein regulatory complex protein	2
Protein kinases	Aurora kinase	4
	Other tubulin-related kinases	5
Other MAPs	Katanin	4
	Chaperones	3
	TTL	3
	Interflagellar transport proteins	18
	Kinetochore	10
	Centromere	9
	TPX2	1
	MAP65 (Ase1, PRC1)	1
	RIB43a	1
	TRAF3IP	3
	Tubulin-related WD-repeat proteins	3
	Dynamin	3
	Memo-like	1
	SF-assemblin	1
Not found	Augmin	

not classifiable in previously described subfamilies.

In *P. sojae* and *Phytophthora ramorum*, several kinesins with oomycete specific domain combinations are reported (Richardson et al. 2006). However, some of these are likely a result of misannotation as they are not found in other oomycetes. For example, in *P. sojae* and *P. ramorum*, the genomic regions containing the genes predicted to encode kinesins with a N-terminal endonuclease/exonuclease/phosphatase domain (Richardson et al. 2006), are syntenic to regions in other *Phytophthora* spp. where the domains are annotated as individual genes. Consequently, it is unlikely that such proteins exist. Nonetheless, we are confident that a kinesin with a ZZ-type Zinc Finger domain, a protein domain combination not observed in other eukaryotes, is present in *P. infestans* (**Table S4.3**) and in other Peronosporalean oomycetes. Similarly, some oomycete myosins, actin-related motor proteins, have a FYVE-type Zinc Finger domain (Richards & Cavalier-Smith 2005; Seidl et al. 2011).

In addition, we identified two kinesins with transmembrane domains, and one kinesin with a major facilitator superfamily (MFS) domain (**Table S4.3**). Even though these proteins contain unique accessory domains, their kinesin domains show similarity to other eukaryotic kinesins. Hence, it is likely that the accessory domains were acquired later in evolution. What role, if any, these accessory domains have in the functioning of these oomycete-specific kinesins is unclear and remains to be investigated.

Dynein light chain subunits are expressed in spores

We identified a total of 39 dynein subunit encoding genes in *P. infestans*. These include 15 dynein light chain (DLC) subunits, 5 dynein intermediate chain (DIC) subunits, and 20 dynein heavy chain (DHC) subunits (**Table S4.3**). Three DHC subunits belong to oomycete-specific classes: DHC14, DHC15, and DHC16 (Kollmar 2016). Genes encoding DHC14, DHC15, and DHC16 subunits are present as single copy genes in all oomycetes. Using in-house RNAseq data (C. Schoina et al., unpublished), we analyzed the expression profile of dynein subunit genes in *P. infestans*. This showed that nearly all DLC encoding genes are upregulated in sporangia, with 12 out of 14 detected DLC genes having this expression profile (**Table S4.3**). In sporangia, zoospores are formed, which explains the upregulation of DLC subunit genes. During zoosporogenesis, flagella are formed, in which dynein is crucial for exerting movement. DIC and DHC subunit genes have a less pronounced expression profile.

Peronosporalean oomycetes do not encode augmin subunits

In *P. infestans*, we did not detect any genes homologous to augmin encoding genes. In fact, we have not been able to identify augmin encoding genes in any Peronosporalean oomycetes, including species from the genera *Phytophthora*, *Hyaloperonopspora*, *Peronospora*,

and *Plasmopara* **Figure S4.1**. In contrast, a single gene homologous to augmin subunit 4 (Aug4) is present in species from the genera *Albugo*, *Pythium*, *Aphanomyces*, and *Saprolegnia* **Table S4.4**. Searches using putative oomycete Aug4 subunits as query in Peronosporeles, did not result in significant hits. Hence, we conclude that at least one augmin subunit gene was present in basal oomycetes and that it was lost during evolution.

Augmin subunits form a protein complex binding to spindle MTs, and by recruitment of γ-tubulin promote centrosome-independent MT generation in spindles (Goshima et al. 2008). In higher metazoans, the complex consists of eight subunits (Lawo et al. 2009), but genes encoding the subunits are not detected in yeast or *Caenorhabditis elegans* (Kamasaki et al. 2013; Edzuka et al. 2014). The absence of augmin dictates that centrosomes are present in oomycetes, which is in agreement with earlier findings that in *Saprolegnia ferax* centrosomes with centrioles are present (Heath & Greenwood 1968). Also in brown algae and diatoms, which are close phylogenetic relatives of oomycetes, microtubule organizing centres (MTOCs) are found (Azimzadeh 2014). However, in contrast to these close relatives, mitosis in oomycetes is closed, meaning that the nuclear membrane remains intact throughout nuclear division. Closed or partially closed mitosis occurs in many lower eukaryotes (reviewed by Heath (1980). In oomycetes, the occurrence of closed mitosis can be linked to an evolutionary advantage to their coenocytic life style. In syncytia, many nuclei are present in a common cytoplasm and during mitosis it is vital that genetic material does not get mixed among different nuclei. One way to assure this is to contain each spindle within their own nuclear envelope (De Souza & Osmani 2007). This strategy can also be found in many other coenocytes, among which the malaria parasite *Plasmodium* (Gerald et al. 2011), the filamentous fungus *Neurospora crassa* (Gladfelter 2006), and the algae *Boergesenia forbessi* (Itagaki & Ogawa 1994) and *Vaucheria terrestris* (Takahashi et al. 2003).

Introduction of a GFP-α-tubulin fusion gene in *Phytophthora palmivora*

To generate transgenic *Phytophthora* lines expressing GFP-tagged tubulin we transformed *P. infestans* with constructs carrying GFP-α-tubulin fusion genes, one based on tubulin subunit TubA2 and the other on TubA5 (**Figure S4.2**). However, despite considerable effort, no suitable transgenic *P. infestans* lines were obtained. None of the transformants that grew on selective medium showed fluorescence suggesting that the DNA transformation was successful but that either the fusion gene was not expressed or the GFP-α-tubulin fusion protein was unstable. We then transformed *P. palmivora* (strain 6390) using the same constructs and obtained a total of five transformants with a detectable fluorescent signal. The lines were designated GFP-TubA2#1,-3,-4 and GFP-TubA5#1,-2; in which TubA2 and TubA5 refer to the α-tubulin gene that is introduced in the respective line. Both constructs were found to label the same population of MTs (Figure S4.3). In all lines, GFP labelled tubulin was observed and recorded. However, only in two lines, GFP-TubA2#1 and GFP-TubA5#1, the fluorescence was maintained in single zoospore cultures generated

from the initial transformants. In the three other lines (GFP-TubA2#2-3 and GFP-TubA5#2-3) fluorescence was lost within several weeks. Possibly the transformation was not stable, or the transformed lines displayed silencing of the constructs. To assess whether the transformation or the expression of the transgene had unexpected adverse effects in GFP-TubA2#1 and GFP-TubA5#1, we monitored the viability and general growth morphology of the lines. In none of these transformed lines phenotypic defects were observed, and colony expansion rate was not affected (**Figure S4.4**).

Live cell imaging of the MT cytoskeleton during nuclear division

We first analyzed all the transformed lines, i.e. GFP-TubA2#1,-3,-4 and GFP-TubA5#1-2, by microscopy and confirmed that they all showed the same MT organization. The results shown hereafter are obtained from one of the six lines, i.e. GFP-TubA2#1. In the GFP-TubA labeled lines we observed that during interphase, cytoplasmic MTs (**Figure 4.2a**) radiate from Microtubule Organizing Centers (MTOCs). This is in line with previous studies by Heath and Greenwood (1970) who showed by transmission electron microscopy that in oomycetes the MTOCs are similar to those found in animals and brown algae (Katsaros et al. 2006), with each MTOC being associated with a nucleus in interphase and containing two tubular centrioles (Heath & Greenwood 1970). Here we were able to observe MT dynamics in the cytoplasm (**Figure 4.2b**). The MTs in *P. palmivora* show dynamic instability, growing and shrinking alternately and besides we observe MT-MT interactions between antiparallel MTs, originating from different MTOCs.

Shortly before nuclear division, the MTOC duplicates and the two daughter MTOCs position themselves on opposite sides of the nucleus. Subsequently, an intranuclear spindle is formed between the MTOCs (**Figure 4.2c**). As the division proceeds, we can see that the MTOCs move apart. However, the MTOCs remain connected by MTs for some time after nuclear division is completed, possibly preventing collision of the two daughter nuclei. Although this suggests that MTs play a role in nuclear positioning further studies are needed to prove this hypothesis.

Oryzalin-mediated depolymerisation of MTs

As a next step, we tested the sensitivity of *Phytophthora* MTs to the microtubule depolymerizing drug oryzalin. Oryzalin, commercially available as an herbicide, has a strong binding affinity to plant α-tubulin, while having no affinity for mammalian tubulin (Hugdahl & Morejohn 1993; Anthony et al. 1998). By direct binding to α-tubulin, oryzalin prevents polymerization and promotes depolymerization of plant microtubules (Strachan & Hess 1983). Next to being effective against plant tubulin, oryzalin was also reported to work against protozoan parasites (Hugdahl & Morejohn 1993). In literature we could not find any studies in which this drug was tested for activity against oomycetes. To test the sensitivity of *P. palmivora* to oryzalin, we exposed germinating cysts (GFP-TubA2#1) to different

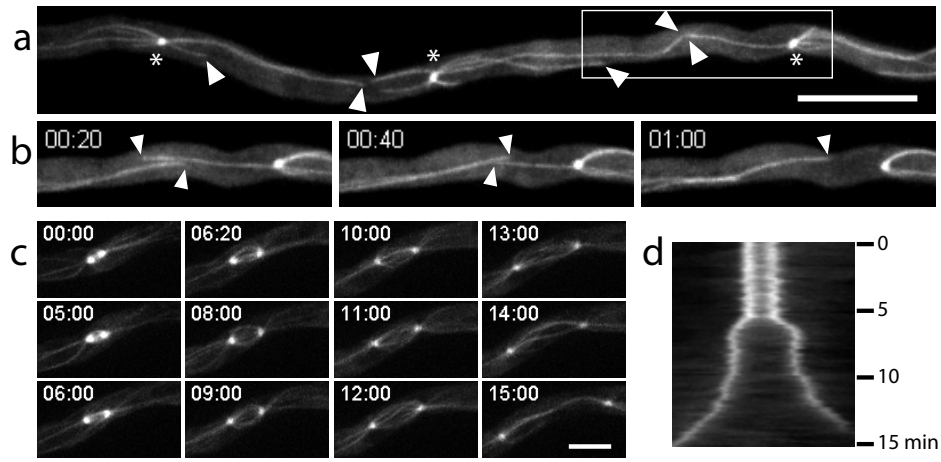

Figure 4.2 | Microtubules in *P. palmivora* hyphae. a) Internuclear MTs with MTOCs (*) and growing or shrinking plus ends (arrowheads) indicated. Scale bar: 10 µm. **b)** Detail of the box in **a)** showing MT dynamics. **c)** Mitotic spindle over time. Scale bar: 5 µm. **d)** Kymograph of spindle in **c)** showing the MTOC moving apart over time. Time is in min:sec.

concentrations of oryzalin. MT depolymerization could clearly be observed at oryzalin concentrations of 2.5 µM and higher (**Figure 4.3a, 4.3b**). In contrast, the MTOCs, and sometimes the MTs in the spindle, were not affected by oryzalin treatment up to 10 µM (**Figure 4.3c**). Since dynamic microtubules are reported to be more sensitive to oryzalin than static ones (Strachan & Hess 1983), we presume that oomycete MTOCs and possibly also the spindle MTs are relatively static.

4.4 Conclusion

Altogether, this work provides an important basis for future research on the MT cytoskeleton of *Phytophthora* and that of other oomycetes. The MAP inventory provides a comprehensive overview of both universal and oomycete-specific features of proteins putatively interacting with MTs, and is a useful resource for future studies. For example, the novel kinesin and dynein types are intriguing. Do they have a specific role that is unique for oomycetes and if so, are they potential drug targets? Likewise, the *P. palmivora* lines with fluorescently labeled tubulin may serve as an important tool for further unraveling the dynamics of the *Phytophthora* MT cytoskeleton and its role in hyphal growth, development and plant infection. Ultimately, they can help in the identification of oomycete-specific drug targets by testing the sensitivity to chemicals targeting the MT cytoskeleton.

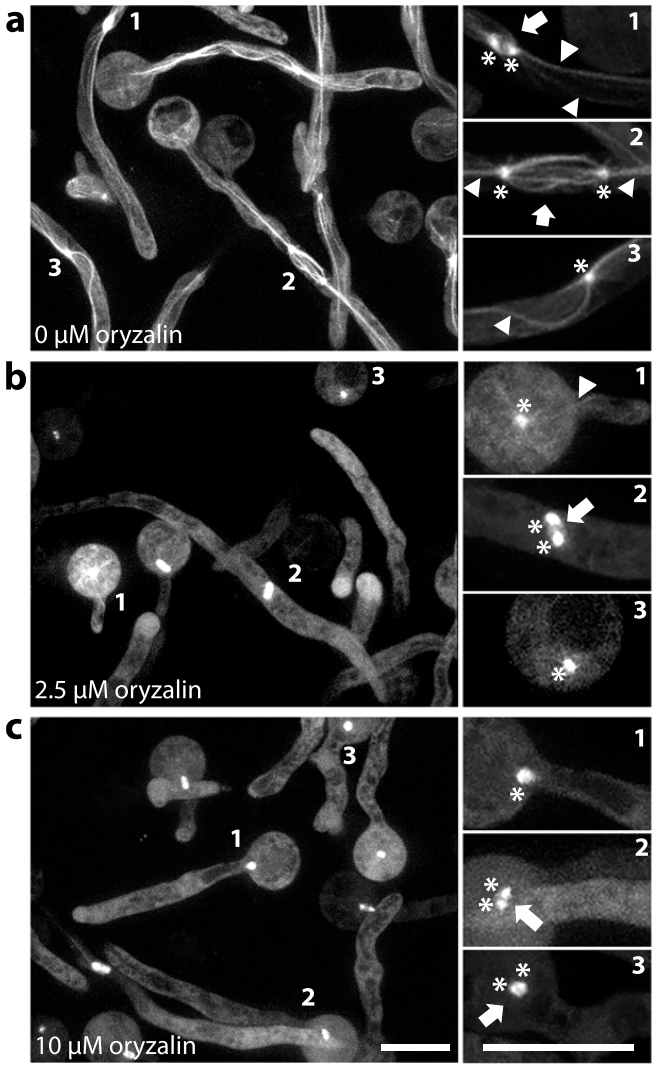

Figure 4.3 | MT organization in germinating cysts treated with oryzalin. The right panels zoom in on hypha indicated by numbers in the left panels. Free cytoplasmic MTs (arrowheads), MTOCs (*) and spindles (arrows) are indicated. **a)** Untreated germinating cysts with intact MT cytoskeleton. 1) early spindle, 2) late spindle and 3) a single nucleus with one MTOC. **b)** Germinated cysts treated with 2.5 µM oryzalin. 1) and 3) show a single MTOC and 2) an early spindle. **c)** Germinated cysts treated with 10 µM oryzalin. 1) a single MTOC, 2) early spindle and 3) a pair of MTOCs. Scale bars: 10 µm.

4.5 Materials and methods

Search strategies

The genome of *P. infestans* strain T30-4 (Haas et al. 2009) was screened for genes encoding α- and β-tubulin subunits by BLAST search using previously annotated genes from *P. sojae* and *P. ramorum*. In addition, 19 oomycete species (FigureS3) were analyzed for homologs using BLAST and orthology searches on FungiDB (Stajich et al. 2012). Protein domains were predicted using SMART (Letunic et al. 2015) and InterProScan (Jones et al. 2014).

Kinesin and dynein heavy chain classification

P. infestans kinesins and dynein heavy chain (DHC) subunits were categorized according to previously described kinesin and DHC families (Wickstead et al. 2010; Kollmar 2016) based on sequence similarity. To this end, a multiple sequence alignment was made of putative *P. infestans* kinesins and 1188 eukaryotic kinesin protein sequences (Wickstead et al. 2010) using MAFFT v7 (Katoh & Standley 2013) and resources available from the CIPRES Science Gateway (Miller et al. 2010). Next, alignment positions that contained more than 25% gaps were trimmed using TrimAL (Capella-Gutierrez et al. 2009). A phylogenetic tree was reconstructed using the WAG amino acid substitution model with gamma model of rate heterogeneity, and bootstrapping (100 replicates) was performed with rapid bootstrap analyses on RAxML v8 (Stamatakis 2014). A similar approach was used for DHC subunits, were 3540 eukaryotic DHC subunits and 19 putative *P. infestans* DHC subunits were included in the tree. All DHC sequences were obtained from CyMoBase (Odronitz & Kollmar 2006). Putative *P. infestans* kinesins not readily categorized were annotated as 'ungrouped'. Protein domains were predicted using InterProScan (Jones et al. 2014).

Strains, culture conditions and life stages

P. palmivora strain P6390 (McHau & Coffey 1994) was routinely grown on 10% V8 medium (10% V8 juice, 1 g/l CaCO3, 1.5% technical agar) containing 20 µg/ml vancomycin, 100 µg/ml ampicillin and 50 µg/ml amphotericin B at 25 °C under continuous light. For selection of transgenic lines the medium was supplemented with 25 µg/ml geneticin. To induce sporulation, plates were sealed with surgical tape (3M Micropore). For zoospore release, 4 to 6 day old plates were flooded with cold sterile tap water (10 ml per plate) and incubated in the light for 20 to 40 minutes. Zoospores were encysted by vigorous shaking for 5 minutes, subsequently 500 µl cyst suspension was pipetted in 35 mm glass bottom dishes (MatTek, Ashland, USA) and cysts were allowed to germinate for 2 hours before microscopic imaging. For the oryzalin assay, cysts where supplemented with desired concentration of oryzalin (10mM in DMSO stock). MT organization was observed using a Roper (Evry, France) Spinning Disc Confocal System on a Nikon Eclipse Ti microscope using a 100×

Plan apo oil immersion objective (NA 1.4) and a 491 nm laserline. Z-stacks were collected with 0.5 µm Z-intervals. Images were analyzed using FIJI (https://imagej.net/Fiji).

Plasmid construction and transformations

To obtain N-terminally GFP-tagged constructs for expression in *P. palmivora*, α-tubulin genes *PiTubA2* (PITG_07960) and *PiTubA5* (PITG_07999) were amplified from *P. infestans* strain NL88069 genomic DNA using primers PITG_07960_NotI_F, PITG_07960_AscI_R, PITG_07999_NotI_F, and PITG_07999_AscI_R (Table S5). Next, the respective PCR amplicons were cloned in pGFP-N (Ah-Fong & Judelson 2011) using the restriction sites NotI and AscI, resulting in constructs pGFP-07960 and pGFP-07999 (Figure S1). Stable transformants of *P. palmivora* were generated using PEG/CaCl2-mediated protoplast transformation using a modified version of earlier described methods (van West et al. 1999). Germinating sporangia (105/ml) were incubated on a large petri dish (ø 15 cm) containing 25 ml 10% V8 broth for 18 h at 28°C in the dark. Mycelia were washed in MQ to remove sporangia and incubated in 0.8 M mannitol for 10 min to induce plasmolysis, and subsequently protoplasted by incubation in protoplasting buffer [0.4 M mannitol, 20 mM KCl, 20 mM MES pH 5.7, 10 mM CaCl2, 5 mg/ml CELLULYSIN (Sigma-Aldrich) and 10 mg/ml Lysing Enzymes from *Trichoderma harzianum* (Sigma-Aldrich)] for 30-45 minutes at room temperature in the dark. After removing residual mycelial fragments by filtration (50 µm mesh), protoplasts were pelleted by centrifugation (4 minutes, 700 g). The protoplasts were resuspended in MT buffer (1 M mannitol, 10 mM Tris-HCl pH 7.5) and after a second centrifugation step in MTC buffer (MT + 25 mM CaCl2), then diluted with MTC to 1·106 - 5·106 protoplasts per ml. 700 µl of the protoplast suspension was mixed with 30 µg circular plasmid DNA in 50 µl MQ. After incubation for 10 minutes at room temperature, 700 µl of freshly prepared PEG solution (50% PEG-3350, 10 mM Tris-HCl pH 7.5, 25 mM CaCl2, sterilized by filtration) was slowly added to the DNA-protoplast mixture. Protoplasts were regenerated overnight at 28°C in 25 ml rye sucrose medium (Caten & Jinks 1968) containing 1 M mannitol, without antibiotics. Regenerated protoplasts were pelleted by centrifugation (5 minutes, 1000 g), resuspended, and plated on selective plates containing 25 µg/ml geneticin. Plates were incubated at 28°C in the dark. Colonies appeared within 4 days.

4.6 Acknowledgements

We thank Howard Judelson for kindly providing the vector pGFP-N, Harold Meijer for his contribution in the initial phase of this study, and Sander Rodenburg for advice on bioinformatic analyses.

4.7 Supplemental files

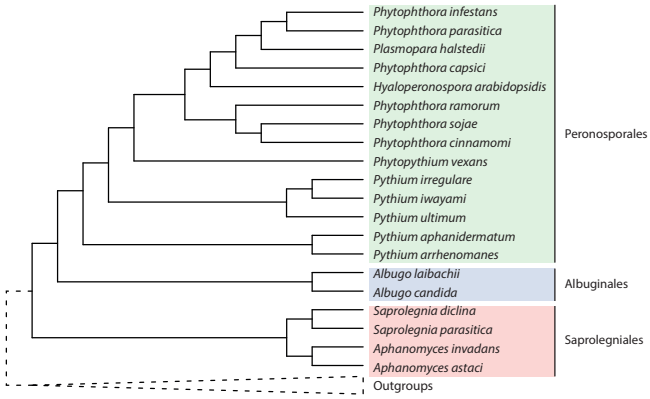

Figure S4.1 | Simplified phylogeny of oomycetes and related organisms based on the supertree as presented by McCarthy and Fitzpatrick (2017).

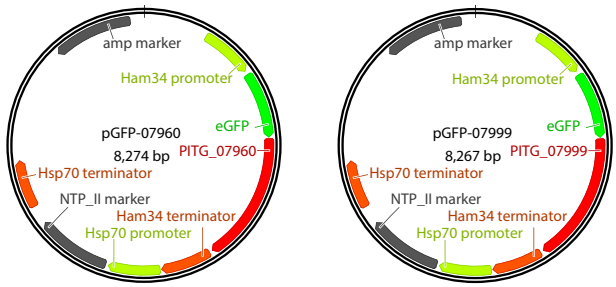

Figure S4.2 | Constructs encoding N-terminally GFP-tagged P. infestans α-tubulins PITG_07960 (pGFP-07960) and PITG_07999 (pGFP-07999).

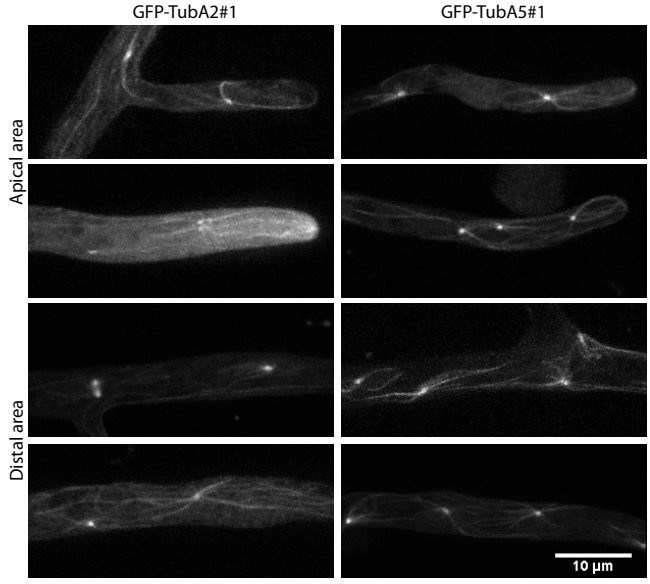

Figure S4.3 | Both GFP-PiTubA2 and GFP-PiTubA5 label the same population of MTs. In all lines MTOCs, spindles, and internuclear MTs were observed in all areas of the hyphae.

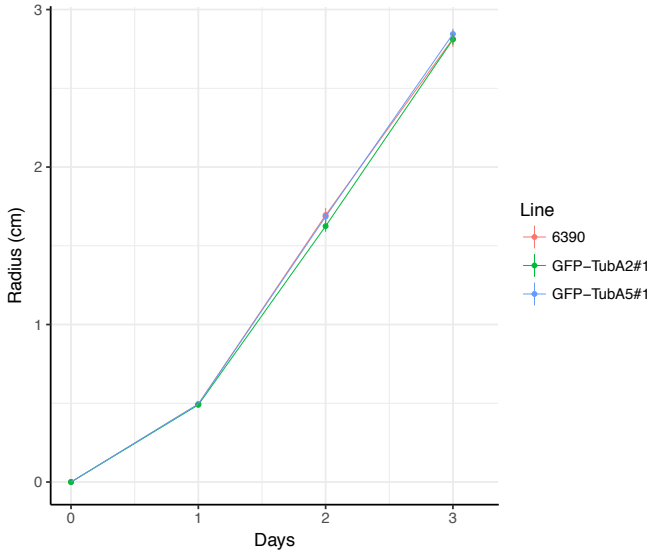

Figure S4.4 | Radial growth rate of *P. palmivora* recipient strain P6390 (6390) and two GFP-tubulin strains (GFP-TubA2#1 and GFP-TubA5#1). The graph is representative for three independent growth rate assays that each included five replicates per line. Error bars represent standard deviations.

Table S4.1 | Details of oomycete a-tubulin genes

Gene ID	Product description	Organism	Notes	Length (aa)
evm.TU.AC2VRR_s00248g27	unspecified product	*Albugo candida*		449
evm.TU.AC2VRR_s00248g139	unspecified product	*Albugo candida*		453
ALNC14_062890	unspecified product	*Albugo laibachii*		449
CCA24429	splicing factor putative	*Albugo laibachii*	corrected, truncated	436
H257_08698	tubulin alpha chain	*Aphanomyces astaci*		453
H257_15887	tubulin alpha chain	*Aphanomyces astaci*		453
H257_08697	tubulin alpha chain	*Aphanomyces astaci*	corrected	454
H310_12120	tubulin alpha chain	*Aphanomyces invadans*	truncated	362
H310_08859	tubulin alpha chain	*Aphanomyces invadans*		453
HpaG803637	unspecified product	*Hyaloperonospora arabidopsidis*		451
HpaG803651	unspecified product	*Hyaloperonospora arabidopsidis*		452
PHYCA_511272	alpha tubulin 1	*Phytophthora capsici*		452
PHYCA_530856	tubulin alpha-2 chain-like	*Phytophthora capsici*	gap in gene model	429
PHYCA_107024	tubulin alpha-4 chain-like	*Phytophthora capsici*		452
PHYCA_511275	tubulin alpha-3 chain	*Phytophthora capsici*	truncated	410
PHYCA_575859	tubulin alpha-5 chain	*Phytophthora capsici*		450
PHYCI_89449	Alpha tubulin	*Phytophthora cinnamomi*		452
PHYCI_111102	unspecified product	*Phytophthora cinnamomi*	truncated	340
PHYCI_233998	unspecified product	*Phytophthora cinnamomi*		453
PITG_07960	alpha-tubulin, putative	*Phytophthora infestans*		453
PITG_07999	alpha-tubulin, putative	*Phytophthora infestans*		453
PITG_07949	alpha-tubulin, putative	*Phytophthora infestans*		454
PITG_07996	alpha-tubulin	*Phytophthora infestans*		453
PITG_07961	cleavage induced tubulin alpha chain	*Phytophthora infestans*	corrected	453
PPTG_08465	tubulin alpha chain	*Phytophthora parasitica*		452
PPTG_08466	tubulin alpha chain	*Phytophthora parasitica*		452
PPTG_08498	tubulin alpha chain	*Phytophthora parasitica*		453
PPTG_08506	tubulin alpha chain	*Phytophthora parasitica*		453
PPTG_08453	tubulin alpha chain	*Phytophthora parasitica*		454
PSURA_72478	Alpha tubulin	*Phytophthora ramorum*	truncated	322
PSURA_51050	Alpha tubulin	*Phytophthora ramorum*		450
PSURA_72335	Alpha tubulin	*Phytophthora ramorum*		450
PSURA_71889	Alpha tubulin	*Phytophthora ramorum*		452
PSURA_71894	Alpha tubulin	*Phytophthora ramorum*		453

Table S4.1 | Details of oomycete a-tubulin genes

Gene ID	Product description	Organism	Notes	Length (aa)
PSURA_51154	unspecified product	*Phytophthora ramorum*		446
PSURA_71890	unspecified product	*Phytophthora ramorum*		452
PHYSODRAFT_338144	hypothetical protein	*Phytophthora sojae*	gap in gene model	438
PHYSODRAFT_288901	hypothetical protein	*Phytophthora sojae*		441
PHYSODRAFT_288898	hypothetical protein	*Phytophthora sojae*		452
PHYSODRAFT_565438	hypothetical protein	*Phytophthora sojae*		452
PHYSODRAFT_356026	hypothetical protein	*Phytophthora sojae*		453
PHYSODRAFT_528260	hypothetical protein	*Phytophthora sojae*		453
Phal02670	tubulin alpha chain	*Plasmopara halstedii*	corrected	296
Phal02671	tubulin alpha chain	*Plasmopara halstedii*	corrected	303
Phal08353	tubulin alpha chain	*Plasmopara halstedii*		453
Phal13640	tubulin alpha chain	*Plasmopara halstedii*	corrected, truncated	136
PAG1_G000452	Alpha-tubulin	*Pythium aphanidermatum*		434
PAG1_G000713	Protein F44F4.11	*Pythium aphanidermatum*	truncated	83
PAR_G009305	Alpha-tubulin	*Pythium arrhenomanes*	truncated	50
PIR_G008598	Alpha-tubulin	*Pythium irregulare*	corrected, truncated	413
PIW_G013767	Alpha-tubulin	*Pythium iwayamai*	truncated	41
PIW_G003138	Alpha-tubulin	*Pythium iwayamai*	truncated	56
PIW_G012562	Alpha-tubulin	*Pythium iwayamai*	truncated	153
PIW_G014282	Alpha-tubulin	*Pythium iwayamai*	truncated	178
PYU1_G011143	unspecified product	*Pythium ultimum*		451
PYU1_G011167	unspecified product	*Pythium ultimum*		452
PYU1_G011535	unspecified product	*Pythium ultimum*		453
PVE_G008283	Alpha tubulin	*Pythium vexans*	gap in gene model	426
PVE_G010441	Alpha-tubulin	*Pythium vexans*	truncated	73
PVE_G010138	Alpha-tubulin	*Pythium vexans*	truncated	140
PVE_G010242	Alpha-tubulin	*Pythium vexans*	truncated	150
PVE_G010239	Alpha-tubulin	*Pythium vexans*	gap in gene model	334
SDRG_17410	tubulin alpha	*Saprolegnia diclina*	truncated	273
SDRG_02711	tubulin alpha	*Saprolegnia diclina*	truncated	299
SDRG_11427	tubulin alpha chain	*Saprolegnia diclina*		449
SDRG_11949	tubulin alpha chain	*Saprolegnia diclina*		451
SDRG_11948	tubulin alpha chain	*Saprolegnia diclina*		453
SPRG_09506	hypothetical protein	*Saprolegnia parasitica*	truncated	186

Table S4.1 | Details of oomycete a-tubulin genes

Gene ID	Product description	Organism	Notes	Length (aa)
SPRG_07894	tubulin alpha-1 chain	*Saprolegnia parasitica*		450
SPRG_04481	tubulin alpha chain	*Saprolegnia parasitica*		451
SPRG_04482	tubulin alpha chain	*Saprolegnia parasitica*		453
SPRG_09503	tubulin alpha chain	*Saprolegnia parasitica*		453

Table S4.2 | Details of oomycete β-tubulin genes

Gene ID	Product description	Species	Notes	Length (aa)
evm.TU.AC2VRR_s00054g80	unspecified product	*Albugo candida*		446
CCA17899	Tubulin beta chain putative	*Albugo laibachii*	Fragment	381
H257_01711	tubulin beta chain	*Aphanomyces astaci*		446
H310_03943	tubulin beta chain	*Aphanomyces invadans*		446
HpaP814031	Beta-tubulin	*Hyaloperonospora arabidopsidis*		446
PHYCA_576734	beta-tubulin	*Phytophthora capsici*		446
PHYCI_418545	unspecified product	*Phytophthora cinnamomi*		446
PITG_00156	beta-tubulin	*Phytophthora infestans*		446
PPTG_15113	tubulin beta chain	*Phytophthora parasitica*		446
PSURA_72114	Beta tubulin	*Phytophthora ramorum*		446
PHYSODRAFT_507388	hypothetical protein	*Phytophthora sojae*		446
Phal03888	beta- partial	*Plasmopara halstedii*	Corrected	447
PAG1_G000598	Beta-tubulin	*Pythium aphanidermatum*		446
PAR_G000681	Beta-tubulin	*Pythium arrhenomanes*		446
PIR_G007881	Beta-tubulin	*Pythium irregulare*		446
PIW_G014483	Beta-tubulin	*Pythium iwayamai*	Fragment	127
PIW_G007163	Beta-tubulin	*Pythium iwayamai*	Fragment, corrected	133
PIW_G006543	Beta-tubulin	*Pythium iwayamai*	Fragment, corrected	154
PUG3_G000817	Beta-tubulin	*Pythium ultimum*		446
PVE_G004943	Beta-tubulin	*Pythium vexans*		446
SDRG_08123	tubulin beta chain	*Saprolegnia diclina*		446
SPRG_09415	tubulin beta chain	*Saprolegnia parasitica*		446

Table S4.3 | Details of microtubule-associated proteins (MAPs) in *P. infestans*. All MAPs are clustered according to predicted function and/or subcellular localization (**grey rows**). Expression profiles are based on RNAseq data of *P. infestans* strain 88069 (C. Schoina et al., unpublished data).

Family	Subfamily	Proposed name	Gene ID	Product description	Expression profile	Notes
Tubulin subunits						
Alpha tubulin		PiTubA1	PITG_07949	alpha-tubulin, putative	up in zsp	
		PiTubA2	PITG_07960	alpha-tubulin, putative	down in spor	
		PiTubA3	PITG_07961	cleavage induced tubulin alpha chain	up in zsp	
		PiTubA4	PITG_07996	alpha-tubulin	up in spor	
		PiTubA5	PITG_07999	alpha-tubulin, putative	up in spor	
Beta tubulin		PiTubB1	PITG_00156	beta-tubulin	up in spor	
Microtubule organizing centers & nucleation factors						
Gamma tubulin		PiTubG1	PITG_14807	tubulin gamma chain	up in myc	
		PiTubG2	PITG_01154	gamma-tubulin complex component	down in spor	
		PiTubG3	PITG_11106	gamma-tubulin complex component	down in spor	
		PiTubG4	PITG_00634	gamma-tubulin complex component	down in spor/zsp	
		PiTubG5	PITG_18463	hypothetical protein	down in spor	
		PiTubG6	PITG_14022	conserved hypothetical protein	down in spor	
TPX2		PiTPX2	PITG_08093	conserved hypothetical protein	down in spor	
Other filaments						
FtsZ/cryptic tubulin		PiFtsZ1	PITG_18788	tubulin/FtsZ family	up in myc	
		PiFtsZ2	PITG_19212	tubulin/FtsZ family protein	down in spor	
		PiFtsZ3	PITG_00509	Delta tubulin, putative	up in myc	
striated MT-associated fibers		PiSFA1	PITG_01027	SF-assemblin, putative	up in zsp	
MT+ end binding proteins						
EB1		PiEB1	PITG_14584	microtubule-associated protein EB1	up in myc	
CLASP		PiCLASP	PITG_05233	CLIP-associating protein, putative	down in spor	
MOR1/MAP215		PiMOR1	PITG_14441	cytoskeleton-associated protein, putative	up in gc	
Katanin		PiKatp60-1	PITG_12195	katanin p60 ATPase-containing subunit	up in myc	
		PiKatp60-2	PITG_21068	katanin p60 ATPase-containing subunit A	up in spor	
		PiKatp60-3	PITG_23128	katanin p80 subunit	down in spor	
		PiKatp80	PITG_06132	katanin p60 ATPase-containing subunit	up in zsp	
Motor proteins						
Kinesin	KIF1	PiKIF1A	PITG_00204	kinesin heavy chain, putative	down in spor	ZZ-type Zinc finger
	KIF1	PiKIF1B	PITG_06859	kinesin-like protein	up in spor	
	KIF1	PiKIF1C	PITG_10881	kinesin-like protein	up in myc	
	KIF2	PiKIF2A	PITG_00111	kinesin-like protein	down in zsp	
	KIF2	PiKIF2B	PITG_03858	kinesin-like protein	down in spor	
	KIF2	PiKIF2C	PITG_08423	kinesin-like protein	up in zsp	
	KIF2	PiKIF2D	PITG_08458	kinesin-like protein	up in spor	
	KIF2	PiKIF2E	PITG_12987	kinesin-like protein	up in gc	
	KIF3	PiKIF3A	PITG_02343	kinesin-like protein	down in zsp	
	KIF3	PiKIF3B	PITG_02538	conserved hypothetical protein	up in zsp	
	KIF3	PiKIF3C	PITG_12262	kinesin-like protein	up in zsp	
	KIF3	PiKIF3D	PITG_12263	kinesin-like protein	up in zsp	

Table S4.3 | Details of microtubule-associated proteins (MAPs) in *P. infestans*. All MAPs are clustered according to predicted function and/or subcellular localization (**grey rows**). Expression profiles are based on RNAseq data of *P. infestans* strain 88069 (C. Schoina et al., unpublished data).

Family	Subfamily	Proposed name	Gene ID	Product description	Expression profile	Notes
	KIF 4/10	PiKIF4/10A	PITG_00152	kinesin-like protein	down in spor/zsp	
	KIF 4/10	PiKIF4/10B	PITG_03064	kinesin-like protein	down in zsp	
	KIF 4/10	PiKIF4/10C	PITG_20348	kinesin-like protein	up in gc	
	KIF 4/10	PiKIF4/10D	PITG_20349	kinesin-like protein	down in spor	
	KIF 5	PiKIF5	PITG_00226	kinesin-like protein	down in spor	MFS domain
	KIF 6	PiKIF6A	PITG_19553	conserved hypothetical protein	down in spor	
	KIF 6	PiKIF6B	PITG_20287	kinesin-like protein	up in gc	Transmembrane domains
	KIF 7	PiKIF7A	PITG_07125	kinesin-like protein	down in spor	Transmembrane domains
	KIF 7	PiKIF7B	PITG_10520	kinesin-like protein	up in gc	
	KIF 7	PiKIF7C	PITG_18579	kinesin-like protein	up in gc	
	KIF 8	PiKIF8	PITG_00860	kinesin-like protein	down in spor/zsp	
	KIF 9	PiKIF9A	PITG_08424	kinesin-like protein	up in spor	
	KIF 9	PiKIF9B	PITG_13923	kinesin-like protein	up in zsp	
	KIF 9	PiKIF9C	PITG_14188	kinesin-like protein KIF6	up in spor	
	KIF 9	PiKIF9D	PITG_15530	kinesin-like protein KIF9	up in zsp	
	KIF 9	PiKIF9E	PITG_21476	conserved hypothetical protein		
	KIF 13	PiKIF13A	PITG_03756	kinesin-like protein	up in myc	
	KIF 13	PiKIF13B	PITG_06856	kinesin-like protein	up in myc	
	KIF 13	PiKIF13C	PITG_15042	sporangia-induced kinesin-like protein	up in zsp	
	KIF 13	PiKIF13D	PITG_16513	conserved hypothetical protein	up in spor	
	KIF 14	PiKIF14A	PITG_00188	kinesin-like protein	down in spor	
	KIF 14	PiKIF14B	PITG_00620	kinesin-like protein	up in zsp	
	KIF 14	PiKIF14C	PITG_00666	kinesin-like protein	up in zsp	
	KIF 14	PiKIF14D	PITG_03872	kinesin-like protein	down in spor	
	KIF 14	PiKIF14E	PITG_08046	kinesin-like protein	up in spor	
	KIF 14	PiKIF14F	PITG_09344	kinesin-like protein	up in zsp	
	KIF 14	PiKIF14G	PITG_10514	kinesin-like protein	up in myc	
	KIF 14	PiKIF14H	PITG_18624	kinesin-like protein	up in gc	
	KIF 14	PiKIF14I	PITG_19351	kinesin-like protein	up in gc	
	KIF 15	PiKIF15A	PITG_00078	kinesin-like protein	up in gc	
	KIF 15	PiKIF15B	PITG_10859	kinesin-like protein	down in spor	
	KIF 16	PiKIF16A	PITG_03657	kinesin-like protein	up in zsp	
	KIF 16	PiKIF16C	PITG_19554	kinesin-like protein		
	KIF 16	PiKIF16D	PITG_20283	kinesin-like protein	down in zsp	
	KIF 17	PiKIF17	PITG_02421	kinesin-like protein	up in spor	
	KIF 19	PiKIF19	PITG_08916	kinesin-like protein	up in spor	
	KIF 20	PiKIF20A	PITG_01850	kinesin-like protein	down in spor	
	KIF 20	PiKIF20B	PITG_03701	kinesin-like protein	up in myc	
	KIF 20	PiKIF20C	PITG_04888	kinesin-like protein	down in spor	
	KIF 20	PiKIF20D	PITG_06666	kinesin-like protein	up in zsp	
	KIF X5	PiKIFX5A	PITG_10474	hypothetical protein	up in zsp	
	KIF X5	PiKIFX5B	PITG_10475	kinesin-like protein	up in zsp	
	KIF X8	PiKIFX8	PITG_05224	conserved hypothetical protein	up in gc	
	KIF X11	PiKIFX11	PITG_12579	kinesin-like protein	down in spor/zsp	

Table S4.3 | Details of microtubule-associated proteins (MAPs) in *P. infestans*. All MAPs are clustered according to predicted function and/or subcellular localization (**grey rows**). Expression profiles are based on RNAseq data of *P. infestans* strain 88069 (C. Schoina et al., unpublished data).

Family	Subfamily	Proposed name	Gene ID	Product description	Expression profile	Notes
	orphan	PiKIForph1	PITG_11652	conserved hypothetical protein	up in gc	Oomcyete specific
	orphan	PiKIForph2	PITG_03859	conserved hypothetical protein	up in zsp	Chromalveolate/Excavate specific
Dynein	Light chain	PiDLC1	PITG_04721	Dynein light chain/pantothenate kinase	up in spor	
	Light chain	PiDLC2	PITG_09030	dynein light chain, putative	up in spor	
	Light chain	PiDLC3	PITG_16973	dynein light chain	up in spor	
	Light chain	PiDLC4	PITG_04706	unspecified product		
	Light chain	PiDLC5	PITG_05682	Putative uncharacterized protein	up in spor	Truncated gene model
	Light chain, Tctex-1	PiTcTex-1-1	PITG_02342	conserved hypothetical protein	up in spor	
	Light chain, Tctex-1	PiTcTex-1-2	PITG_02108	dynein light chain-like protein	up in spor	
	Light chain, Tctex-1	PiTcTex-1-3	PITG_09704	dynein light chain Tctex-type	down in zsp	
	Light chain, Tctex-1	PiTcTex-1-4	PITG_05518	hypothetical protein	down in zsp	
	Light chain, Tctex-1	PiTcTex-1-5	PITG_07793	Outer Dynein Arm Light Chain 2	up in spor	
	Light chain, roadblock/LC7	PiLC7-1	PITG_08352	conserved hypothetical protein	up in spor	
	Light chain, roadblock/LC7	PiLC7-2	PITG_16429	conserved hypothetical protein	up in spor	
	Light chain, roadblock/LC7	PiLC7-3	PITG_18659	conserved hypothetical protein	up in spor	
	Light chain, roadblock/LC7	PiLC7-4	PITG_09567	conserved hypothetical protein	up in spor	
	Light chain, roadblock/LC7	PiLC7-5	PITG_12754	Dynein light chain 2B	up in spor	
	Intermediate chain	PiDIC1	PITG_01997	Dynein 1 light intermediate chain	up in myc	
	Intermediate chain	PiDIC2	PITG_16492	conserved hypothetical protein	up in myc	
	Intermediate chain	PiDIC3	PITG_22517	dynein heavy chain	up in zsp	
	Intermediate chain	PiDIC4	PITG_19149	Putative uncharacterized protein	down in spor	
	Heavy chain - DHC1	PiDHC1	PITG_02526	dynein heavy chain	up in myc	
	Heavy chain - DHC2	PiDHC2	PITG_13968	dynein heavy chain	up in gc	
	Heavy chain - DHC3	PiDHC3A	PITG_15967	dynein heavy chain, outer arm	up in myc	
	Heavy chain - DHC3	PiDHC3B	PITG_05922	dynein heavy chain	down in zsp	
	Heavy chain - DHC4	PiDHC4A	PITG_03423	dynein heavy chain	up in spor	
	Heavy chain - DHC4	PiDHC4B	PITG_12577	sporangia induced dynein heavy chain	down in spor	
	Heavy chain - DHC4	PiDHC4C	PITG_01852	dynein heavy chain	up in myc	
	Heavy chain - DHC4	PiDHC4D	PITG_15625	dynein heavy chain	down in spor/zsp	
	Heavy chain - DHC5	PiDHC5	PITG_01717	dynein heavy chain	up in myc	
	Heavy chain - DHC7	PiDHC6	PITG_03180	dynein heavy chain	up in myc	
	Heavy chain - DHC7	PiDHC7A	PITG_11437	axonemal dynein heavy chain	up in gc	
	Heavy chain - DHC7	PiDHC7B	PITG_03488	dynein heavy chain	up in zsp	
	Heavy chain - DHC8	PiDHC8A	PITG_03018	sporangia induced dynein heavy chain	down in spor	
	Heavy chain - DHC8	PiDHC8B	PITG_01088	sporangia induced dynein heavy chain	down in spor	
	Heavy chain - DHC9	PiDHC9A	PITG_01326	dynein heavy chain	up in myc	
	Heavy chain - DHC9	PiDHC9B	PITG_08295	dynein heavy chain	down in spor	
	Heavy chain - DHC9	PiDHC9C	PITG_00998	dynein heavy chain	up in myc	
	Heavy chain - DHC14	PiDHC14	PITG_03444	dynein heavy chain	up in zsp	Oomycete-specific
	Heavy chain - DHC15	PiDHC15	PITG_08507	Dynein heavy chain-like protein	up in myc	Oomycete-specific, corrected
	Heavy chain - DHC16	PiDHC16	PITG_17408	dynein heavy chain	up in myc	Oomycete-specific
	Dynein regulatory complex protein		PITG_17342	Sporangia Induced Dynein Regulatory Complex Protein	up in spor	
			PITG_04697	Putative uncharacterized protein	up in zsp	

Table S4.3 | Details of microtubule-associated proteins (MAPs) in *P. infestans*. All MAPs are clustered according to predicted function and/or subcellular localization (**grey rows**). Expression profiles are based on RNAseq data of *P. infestans* strain 88069 (C. Schoina et al., unpublished data).

Family	Subfamily	Proposed name	Gene ID	Product description	Expression profile	Notes
Protein kinases						
	MT-related protein kinases		PITG_19450	Cell division protein kinase 2	up in myc	
			PITG_18073	Cell division protein kinase	down in spor	
			PITG_19459	Protein kinase	down in spor	
			PITG_11253	Serine/threonine protein kinase	up in spor	
			PITG_05364	Putative uncharacterized protein	up in gc	
	Aurora kinase	PiAur-1	PITG_16977	Aurora-like protein kinase	down in spor	
		PiAur-2	PITG_05483	Protein kinase, putative	down in spor	
		PiAur-3	PITG_19456	Protein kinase, putative	down in spor	
		PiAur-4	PITG_00115	Protein kinase, putative	down in spor	
Tubulin assembly						
Chaperones		PiChap1	PITG_14614	Tubulin-specific chaperone C, putative	down in spor/zsp	
		PiChap2	PITG_16797	Tubulin-specific chaperone D, putative	up in myc	
		PiChap3	PITG_16735	Putative uncharacterized protein	up in spor	
Polyglutamylases		PiPGS1	PITG_02721	tubulin polyglutamylase, putative	up in zsp	
		PiPGS2	PITG_03077	tubulin polyglutamylase, putative	up in zsp	
Tyrosine ligase		PiTTL1	PITG_08756	tubulin-tyrosine ligase family	up in spor	
Interflagellar transport proteins						
		PiIFT20	PITG_06949	Intraflagellar Transport Protein 20	up in spor	
		PiIFT22	PITG_09137	Putative uncharacterized protein	up in spor	
		PiIFT25	PITG_04711	Putative uncharacterized protein	up in spor	
		PiIFT27	PITG_20749	Putative uncharacterized protein	up in spor	
		PiIFT43	PITG_11983	Putative uncharacterized protein	up in spor	
		PiIFT46	PITG_14226	Putative uncharacterized protein	up in spor	
		PiIFT52	PITG_20745	Intraflagellar Transport Protein 52	down in zsp	
		PiIFT57	PITG_16112	Intraflagellar Transport Protein 57	up in spor	
		PiIFT72/74	PITG_11472	Intraflagellar Transport Protein 72/74	up in spor	
		PiIFT80	PITG_18714	Intraflagellar Transport protein 80	up in spor	
		PiIFT81	PITG_06106	Intraflagellar Transport Protein 81	down in zsp	
		PiIFT88	PITG_10094	Intraflagellar Transport Protein 88	up in gc	
		PiIFT121	PITG_13766	WD repeat protein 35	up in spor	
		PiIFT122	PITG_10664	Intraflagellar Transport Protein 122	up in zsp	
		PiIFT139	PITG_10096	Putative uncharacterized protein	up in gc	
		PiIFT140	PITG_03309	Intraflagellar Transport Protein 140	up in spor	
		PiIFT144	PITG_18065	Putative uncharacterized protein	up in spor	
		PiIFT172	PITG_20212	Intraflagellar transport protein 172	up in spor	
Kinetochore						
			PITG_00651	centromere/kinetochore protein, putative	up in myc	
			PITG_03918	conserved hypothetical protein	up in gc	
			PITG_05311	kinetochore protein NUF2-like protein	down in spor/zsp	
			PITG_05567	Kinetochore protein NDC80	up in gc	
			PITG_06914	conserved hypothetical protein	up in gc	
			PITG_17081	Voltage-gated Ion Channel (VIC) Superfamily	up in myc	
			PITG_15240	Putative uncharacterized protein	up in gc	

Table S4.3 | Details of microtubule-associated proteins (MAPs) in *P. infestans*. All MAPs are clustered according to predicted function and/or subcellular localization (**grey rows**). Expression profiles are based on RNAseq data of *P. infestans* strain 88069 (C. Schoina et al., unpublished data).

Family	Subfamily	Proposed name	Gene ID	Product description	Expression profile	Notes
			PITG_09827	Mitotic checkpoint protein, putative	down in spor/zsp	
			PITG_10233	Putative uncharacterized protein	up in gc	
			PITG_01293	Putative uncharacterized protein	down in spor	
Centromere						
			PITG_06277	conserved hypothetical protein	up in gc	
			PITG_09614	conserved hypothetical protein	up in gc	
			PITG_11136	conserved hypothetical protein	down in zsp	
			PITG_12723	conserved hypothetical protein	up in spor	
			PITG_12840	conserved hypothetical protein	up in myc	
			PITG_12841	conserved hypothetical protein	up in zsp	
			PITG_15175	conserved hypothetical protein	up in myc	
			PITG_17861	conserved hypothetical protein	up in spor	
			PITG_14021	Putative uncharacterized protein	up in spor	
Other MT-associated proteins						
MAP65			PITG_01921	conserved hypothetical protein	down in spor	
RIB43a			PITG_02163	RIB43a flagellar protofilament ribbon protein	up in spor	
TRAF3IP			PITG_19387	TRAF3-interacting protein, putative	up in myc	
			PITG_10084	Putative uncharacterized protein	up in spor	
			PITG_12594	TRAF3-interacting protein, putative	down in spor/zsp	
WD-repeat			PITG_11403	WD domain-containing protein	up in myc	
			PITG_00797	WD domain-containing protein	down in zsp	
			PITG_13618	WD repeat protein pop3	down in spor/zsp	
Dynamin			PITG_11454	Dynamin	up in spor	
			PITG_00183	Dynamin-2	down in spor	
			PITG_08837	Interferon-induced GTP-binding protein Mx	up in zsp	

Table S4.4 | Details of augmin subunit encoding genes in oomycetes.

Gene ID	Product description	Organism	Length (aa)
ALNC14_022390	unspecified product	*Albugo laibachii*	285
H257_11484	hypothetical protein	*Aphanomyces astaci*	315
H310_06484	hypothetical protein	*Aphanomices invadans*	303
PAG1_G011123	hypothetical protein	*Pythium aphanidermatum*	173
PIR_G010251	unspecified product	*Pythium irregulare*	309
PIW_G008869	unspecified product	*Pythium iwayamai*	120
PVE_G008681	unspecified product	*Pythium vexans*	273
PYU1_G003699	unspecified product	*Pythium ultimum*	120
SDRG_08716	hypothetical protein	*Saprolegnia diclina*	293
SPRG_19876	hypothetical protein	*Saprolegnia parasitica*	293

Table S4.5 | Primers used in this study

Name	Target gene	Sequence (5' - 3')
PITG_07960_NotI_F	PITG_07960 (*P. infestans*)	GTGCGGCCGCAGGCGCGCCTCGTGAAATTCTCTCCATTCACCTCGGC
PITG_07960_AscI_R	PITG_07960 (*P. infestans*)	ACGATGGCGCGCCCAGCACGCAAAATGCTTAGTACTCCTC
PITG_07999_NotI_F	PITG_07999 (*P. infestans*)	GTGCGGCCGCAGGCGCGCCTCGTGAGGTCATCTCCATCCACC
PITG_07999_AscI_R	PITG_07999 (*P. infestans*)	ACGATGGCGCGCCGAGTCTGCCTAGTACTCCTCGC

Chapter 5

Towards CRISPR/Cas9 genome editing in *P. infestans*

Johan van den Hoogen, Francine Govers

A modified version of this chapter is available on bioRxiv as: Attempts to implement CRISPR/Cas9 for genome editing in the oomycete *Phytophthora infestans*, doi:10.1101/274829

List of abbreviations

CRISPR	clustered regularly interspaced short palindromic repeats
Cas9	CRISPR-associated protein 9
DSB	double-strand break
gRNA	guide RNA
HDR	homology-directed repair
IVT	*in vitro* transcription
KO	Knock-out
NHEJ	non-homologous end-joining
NLS	nuclear localization sequence
PAM	protospacer adjacent motif
RNP	ribonucleoprotein
ssODN	single-stranded oligodeoxynucleotide
T7EI	T7 endonuclease I

5.1 Abstract

Few techniques have revolutionized the molecular biology field as much as genome editing using CRISPR/Cas9. Recently, a CRISPR/Cas9 system has been developed for *Phytophthora sojae*, and since then it has been employed in two other *Phytophthora* spp. Here, we report our progress on efforts to establish the system in *Phytophthora infestans*. Using the original constructs as developed for *P. sojae*, we did not obtain any transformants displaying a mutagenized target gene. We made several modifications to the CRISPR/Cas9 system to pinpoint the reason for failure and also explored the delivery of pre-assembled ribonucleoprotein complexes.

5.2 Introduction

The oomycete *Phytophthora infestans*, the causal agent of potato and tomato late blight, is an economically important plant pathogen that is difficult to control (Kamoun et al. 2015). Current efforts to identify and functionally analyze genes important for virulence, are hampered by a limited molecular toolbox. Gene knock-outs (KOs) or gene deletions are not possible via homologous recombination, as transgenes are integrated randomly via non-homologous end-joining (NHEJ) (Judelson 1997; Fang & Tyler 2016). Moreover, *P. infestans* is diploid and heterothallic. Generating sexual progeny is quite challenging and as a result studies based on genetic analyses are scarce (Govers & Gijzen 2006; Fry 2008). Consequently, to date, functional gene studies in oomycetes primarily rely on gene silencing and overexpression. DNA transformation of the target gene in *P. infestans* can lead to homology dependent gene silencing or overexpression (van West et al. 1999). By fusing a fluorescent tag to the target gene, the overexpression transformants can also be exploited for investigating the subcellular localization of the encoded protein. However, due to the random integration of transgenes and varying levels of silencing and overexpression efficiency, phenotypes often vary between transformed lines, experiments, and labs (Fang & Tyler 2016).

Recently, a CRISPR/Cas9 genome editing system has been developed for *Phytophthora sojae* (Fang & Tyler 2016). This provides an important addition to the molecular toolbox for oomycetes, and makes it up to par with other research areas. For genome editing based on CRISPR/Cas systems, a nuclease, e.g. Cas9, is targeted to the desired DNA sequence by a so-called synthetic guide RNA (gRNA). The 20-nucleotide protospacer directs Cas9 to a specific target DNA site, which must be immediately 5' of a protospacer adjacent motif (PAM) sequence (Ran et al. 2013). When Cas9 is directed to the target site a double-stranded break (DSB) is induced, which can be repaired either by the NHEJ repair mechanism, or via homology-directed repair (HDR) in case a repair template is available (Ran et al. 2013). Because of its low fidelity, NHEJ often leads to insertions or deletions (indels) in the repaired target gene, which can lead to frame shift mutations. HDR, on the other hand, can be exploited to introduce specific modifications such as base substitutions, insertions, or gene deletions.

So far, the *P. sojae* CRISPR/Cas9 system has been successfully used to mutagenize several genes in *P. sojae* (Fang & Tyler 2016; Ma et al. 2017), *Phytophthora capsici* (B.M. Tyler, personal communication), and *Phytophthora palmivora* (Gumtow et al. 2017). However, as of to date, no one has reported successful implementation of the system in *P. infestans*. Here, we present a case study for the effectuation of CRISPR/Cas9 for targeted genome editing in *P. infestans*. We chose to target three genes in *P. infestans* for a proof-of-principle study of CRISPR/Cas9-based genome editing in this organism.

The first target, *Avr1*, encodes an RXLR effector protein recognized by the cognate receptor protein R1 in potato. Recognition of AVR1 by R1 provides resistance to potato, while *P.*

infestans strains lacking *Avr1* are virulent on potato cultivars harboring resistance gene *R1*. Moreover, R1 fails to recognize several mutated forms of AVR1 (Du et al. 2018). Hence, *P. infestans Avr1* KO lines are expected to gain virulence on *R1* potato, providing a clear phenotype compared to non-edited lines. The second target, *PiTubA2*, is one of the five α-tubulin encoding genes in *P. infestans* (**Chapter 4**). Our aim was to modify the endogenous *PiTub2A* gene in such a way that it encodes a fusion protein that has a GFP tag fused to the N-terminus of PiTUBA2. We therefore designed a HDR construct for gene knock-in at the endogenous *PiTubA2* locus. A PiTubA2-GFP knock-in line would be ideal for live cell imaging of the microtubule cytoskeleton in *P. infestans*, as it lacks possible non-desirable side effects associated with overexpression and/or ectopic integration of the transgene. The third target, *PiAP5*, encodes an aspartic protease (AP) with an C-terminal GPCR domain (Kay et al. 2011), a protein which is unique for oomycetes (Van den Hoogen et al. 2018) (**Chapter 2**). To study to what extent the GPCR domain is important for functioning of the AP domain, we aimed at targeting Cas9 to the central region of the gene that separates the parts encoding the AP domain and the GPCR domain. An indel in this region should result in a truncated protein, which contains the N-terminal AP domain but lacks the C-terminal GPCR domain.

In the initial setup of our experiments, we used the CRISPR/Cas9 system as developed by Fang and Tyler (2016). In this system, the expression of Cas9 is driven by the strong constitutive *Bremia lactucae* Ham34 promoter and the expression of the gRNA by the *P. sojae* RPL41 promoter. The RPL41 promoter was chosen because the U6 small nuclear RNA promoters typically used in CRISPR/Cas9 systems, did not yield any detectable transcript (Fang et al. 2017). To ensure correct release of the gRNA from the transcript, the gRNA sequence was flanked with a hammerhead and a hepatitis delta virus (HDV) ribozyme at the 5' and 3' side, respectively (Fang et al. 2017).

This chapter summarizes an extensive experimental effort pursuing the application of a CRISPR/ Cas9 system for targeted mutagenesis in *P. infestans* and concludes with suggestions for future directions.

5.3 Results and discussion

Experimental setup: design of gRNAs

The first, and perhaps most critical step of setting up a CRISPR/Cas9 experiment, is the design of the gRNAs. The genes of interest were screened for target sites using NGG as the PAM. All gRNAs were scored for on-target activity according to Doench *et al*. (Doench et al. 2014) and for off-targets interactions according to Hsu *et al*. (Hsu et al. 2013). The top 10 best scoring protospacers were manually curated using BLAST analysis on the *P. infestans* reference genome and predictions of the secondary RNA structure of the corresponding gRNAs. For *Avr1*, we selected the three best scoring gRNAs (**Figure 5.1a**), i.e. no predicted

off-target interactions and no strong secondary RNA structure. For *PiTubA2* and *PiAP5* we selected the highest scoring gRNA (**Figure 5.1b**, **5.1c**).

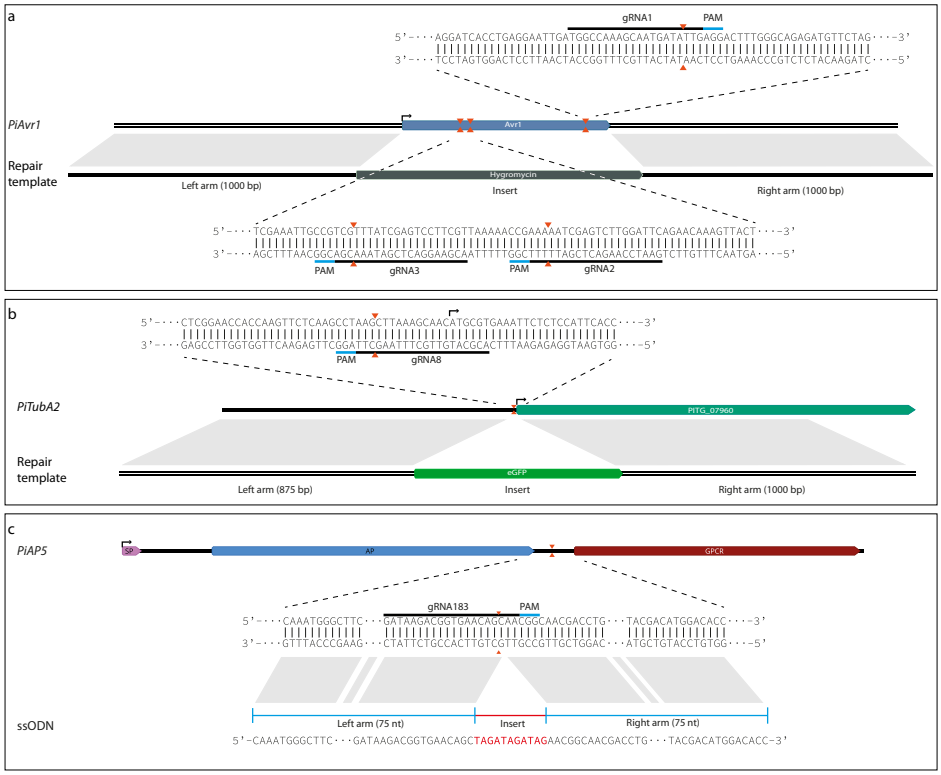

Figure 5.1 | CRISPR loci and HDR constructs for **(a)** *PiAvr1*, **(b)** *PiTubA1*, and **(c)** *PiAP5*. Orange arrowheads indicate expected DSB sites upon Cas9 nuclease activity; black arrows indicate start codons (ATG); grey blocks mark homologous regions between the genes and the HDR constructs (referred to as repair template or ssODN); interpuncts (·) represent cropped sequences; PAM: Protospacer Adjacent Motif.

HDR constructs

To employ the HDR repair pathway for targeted mutagenesis, we used a similar approach as previously used in *P. sojae*. This implies cotransformations of three plasmids, i.e., two plasmids with sequences encoding Cas9 and gRNA, respectively, and the third one containing the HDR repair template (Fang & Tyler 2016).

For *Avr1* we designed a construct to replace the coding region with *HygB*, a hygromycin-B resistance gene (**Figure 5.1a**). The inserts were flanked by a 1 kb right flanking arm and a 875 bp left flanking arm that are complementary to the target site for recombination. The reason for the shorter left flanking arm is a ~380 bp region in the genome assembly, that is not accessible for sequencing. We opted to use the largest possible flanking region, i.e.

875 bp (**Figure 5.1a**). For *PiTubA2* we designed a construct to knock-in GFP just before the start codon of the open reading frame (**Figure 5.1b**). The repair template was designed as such that the PAM would be disrupted upon HDR repair.

For a number of organisms, higher efficiency of HDR repair has been reported when making use of single-stranded oligodeoxynucleotides (ssODN) as repair template, instead of plasmid DNA (Chen et al. 2011). We designed a ssODN repair template for *AP5*, comprising an 11 bp insert flanked by two 75 nt homology arms. The insert is designed in such a way that there is a stop codon (TAG) in each of the three open reading frames (**Figure 5.1c**). Further, the ssODN and gRNA were designed as such, that introduction of the 11 bp construct would disrupt the protospacer and consequently withhold Cas9 from further processing the target site. The expected protein product from the truncated gene contains the AP domain but lacks the GPCR domain.

Testing the detection limit

We next examined the sensitivity of our screening methods. To do so, we simulated the situation that an unknown fraction of transformants contains a Cas9-induced mutation. This is expected to be the case in a sample from pooled transformants after transformation; screening these for mutations can give an idea about the efficiency of targeted mutagenesis. First, we constructed an *Avr1* amplicon (ΔAvr1) containing the 29 bp deletion that is expected after Cas9 cleavage at sites gRNA2 and gRNA3 (**Figure S5.1a**). Next, varying molar ratios of *Avr1* and ΔAvr1 amplicons were annealed and incubated with T7 endonuclease I (T7EI), which is an enzyme that specifically digests mispaired DNA. We found that the detection limit is just over a molar ratio of 95:5 (i.e. 5% mutated amplicons) (**Figure S5.1b**).

In parallel, PCR amplicons were sequenced. When sequencing an amplicon that is obtained from a PCR on a pool of transformants of which a certain fraction underwent CRISPR-induced mutagenesis, the resulting sequence chromatogram will contain a certain amount of 'noise', or background signals. These aberrant chromatogram peaks reflect the approximate frequency of amplicons with an indel, which can be estimated with an analysis tool such as TIDE (Brinkman et al. 2014). TIDE quantifies the editing efficacy by calculating the statistical probability of finding background signals in the chromatogram of a sample compared to finding them in a reference sequence chromatogram. A range of molar ratios of *Avr1*:ΔAvr1 was sequenced, and by using T30-2 *Avr1* as a reference, we analyzed the sequence chromatograms for mismatches. We found the lowest statistically significant detection at a molar ratio of 998:2 (i.e. 0.2% of the sequences having the deletion) (**Figure S5.1c**).

These detection limits are well below the observed frequencies of CRISPR-induced mutations in *P. sojae*, where up to 80% of the analyzed transformants have undergone NHEJ (Y.F.

Fang, personal communication). Assuming that the CRISPR/Cas9 system is functional in *P. infestans*, our detection assays are sufficiently sensitive to reveal induced mutations. It should be noted however, that in the simulations described above only a single mutation (i.e. a 29 bp deletion) was present. In an actual sample of pooled transformed *P. infestans* protoplasts, a mix of differently sized indels is expected and the detection limit will be higher. Nonetheless, we assume that our detection assays are sufficiently sensitive to detect CRISPR-induced mutations in pooled *P. infestans* transformed protoplasts.

In vitro activity assay

To examine the functionality of the designed gRNAs, we performed an *in vitro* cleavage assay of target DNA. This assay can give an indication of the *in vivo* efficacy of the gRNA for Cas9 activity. We used purified Cas9 protein and *in vitro* transcribed gRNA in equimolar amounts, in combination with a PCR product as target DNA. We observed Cas9 activity on *Avr1* using gRNA1 and gRNA3 (**Figure 5.2a**). In contrast, gRNA2 failed to direct Cas9 to the target site (**Figure 5.2a**). Examination of the sequence revealed a mistake in the design of the initial construct. When corrected gRNA2 also showed activity (not shown). We did not observe Cas9 activity on *PiTubA2* using gRNA8, nor on *PiAP5* using gRNA183 (**Figure 5.2b**). In contrast to the initial gRNA2 on *Avr1*, we could not detect mistakes in the design of these two gRNAs. Consequently, judging from their inability to guide Cas9 *in vitro*, it is likely that also the *in vivo* efficacies of gRNA8 and gRNA183 are limited. Other gRNAs for these target genes may have an increased activity, but due to time constraints we have not been able to test alternative gRNAs for *PiTubA2* and *PiAP5*.

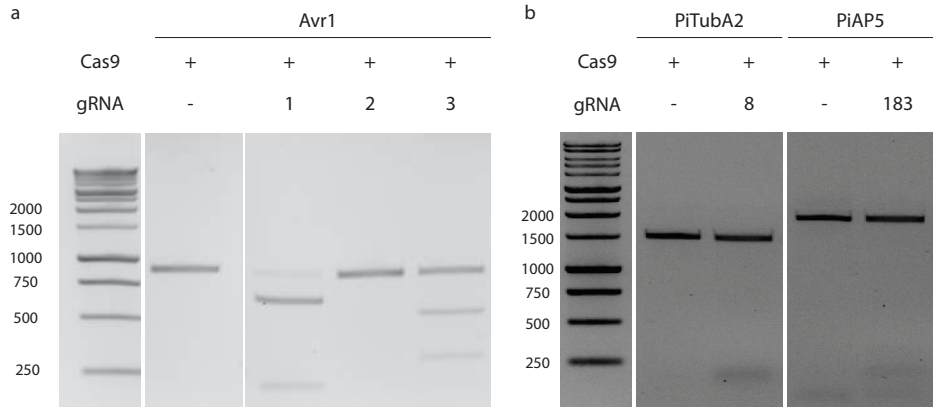

Figure 5.2 | In vivo cleavage assay. **a)** gRNAs 1, 2, and 3 with Avr1 as target DNA. **b)** gRNA8 with PiTubA2 as target DNA (**right**) and gRNA183 with PiAP5 as target DNA (**left**).

In vivo CRISPR/Cas9 in *P. infestans*

Next, we set out to test the *in vivo* editing efficacy of the system. To this end, we first cloned the respective gRNAs into the expression plasmid pYF2.3-gRNA (Fang & Tyler 2016). We performed several transformations of *P. infestans* with plasmids pYF2.2-Cas9 and pYF2.3-gRNA and obtained numerous transformants resistant to the selection antibiotic geneticin. In these transformants, the presence of indels as a result of the presumed Cas9 activity was monitored by T7EI digestion and sequencing analysis. However, contrary to expectations set by the positive results of the use of CRISPR/Cas9 in *P. sojae*, *P. capsici*, and *P. palmivora*, the analyses did not reveal any lines in which the target gene was mutagenized. In some cases, the sequence chromatogram showed ambiguities near the target site, raising the hope that the mutagenesis was successful. More detailed analysis however, revealed that these lines were identical to the recipient isolate and should be considered as false-positives. Further trials focused at targeting *Avr1* included transformations combining two or three gRNA-expressing vectors along with Cas9, but in all cases the results were negative.

In order to induce specific mutations in *P. infestans*, we performed experiments where plasmid DNA containing a HDR repair template for *Avr1* was co-transformed with the CRISPR/Cas9 constructs. Even though several hygromycin-B resistant colonies were obtained, and the presence of *HygB* could be detected by PCR on genomic DNA, we were not able to detect integration of the transgene at the endogenous genomic locus. Possibly, the hygromycin-B resistance gene was integrated ectopically, or resistance was conferred by transcription from non-integrated plasmid DNA. Similarly, we did not obtain transformed lines with GFP-encoding sequences inserted at the 5' end of *PitubA2*, or *PiAP5*-mutants with the stop codon insertion.

For the target genes *PiTubA1* and *PiAP5* only a single gRNA was used. This and the fact the both gRNAs did not prove to be effective in the *in vitro* activity assay, are most likely the reasons for the absence of observable Cas9 activity. However, also in the case of *Avr1* as target gene, where all three gRNAs proved functional *in vitro*, Cas9 activity appeared to be absent.

An obvious explanation for failure is poor expression of Cas9. To assess the expression level of Cas9, reverse-transcription PCR was performed on RNA isolated from mycelium of transformed lines. In several lines expression of Cas9 could be detected (**Figure S5.2**). Consequently, it is unlikely that lack of expression of Cas9 is the prime reason for failure of the system. As yet, we have not monitored the presence of the gRNA transcripts. Altogether, these findings led us to conclude that the CRISPR/Cas9 system in *P. infestans* is not functioning, at least not up to the expected efficiency.

Modifications to the CRISPR/Cas9 system

It is hard to pinpoint the main cause for failure of the system, as multiple factors may have a role. Hence, we set out to make modifications at different steps in the process. Below we describe several modifications and alternative approaches in an effort to effectuate the CRISPR/Cas9 system in *P. infestans*.

Alternative vectors

In the original *P. sojae* CRISPR/Cas9 system, there is no selectable resistance marker present on the plasmid encoding the gRNA. However, in practice, cotransformations of plasmids usually result in integration of both plasmids (R. Weide, personal communication). Consequently, geneticin-resistant colonies are expected to also have incorporated the gRNA plasmid. Nevertheless, we decided to test whether we would be able to observe CRISPR/Cas9 activity by using a gRNA-encoding plasmid containing *HygB* as a resistance marker. To do so, we introduced the *HygB* in pYF2.3-gRNA-Ribo, replacing *eGFP* from the vector and yielding pJH2.4-gRNA-Ribo-Hyg (**Figure S5.3**). In this vector backbone, the respective gRNAs for the three target genes were cloned. Along with the Cas9 encoding plasmid, the resulting plasmids were used for cotransformations of *P. infestans*. Even though we obtained numerous hygromycin-B-resistant tranformants, in none of the screened transformants we could detect mutagenized target genes.

In another attempt, we cloned the gRNA expression components in pYF2.2-Cas9, resulting in the 'all-in-one' vector pJH2.5-Cas9-gRNA (**Figure S5.3**). Numerous geneticin-resistant transformants were obtained and PCR analysis confirmed the presence of the Cas9 and gRNA genes. Unfortunately, no mutagenized target genes were observed. Further, we constructed a vector containing both gRNA2 and gRNA3 (both targeting *Avr1*), but also here we did not obtain transformed lines with the expected deletion between the two target sites.

Nuclear localization sequence

Nuclear localization of Cas9 is essential. Oomycetes contain distinct nuclear localization sequence (NLS) signals, and commonly used mammalian NLS signals are not efficient in *P. sojae* (Fang & Tyler 2016; Fang et al. 2017). To overcome this, Fang & Tyler (2016) fused a synthetic NLS derived from a *P. sojae* bZIP transcription factor (TF) to Cas9. This NLS, further referred to as PsNLS, showed strong nuclear localization in *P. sojae* (Fang et al. 2017), and it is expected that it will perform likewise in *P. infestans*. To test the nuclear localization of Cas9, we obtained several transformed *P. infestans* lines carrying a PsNLS-Cas9-GFP fusion construct but unfortunately, for unknown reasons none of these lines showed fluorescence. Hence, we were unable to determine the localization of Cas9 in *P. infestans*. Anticipating that PsNLS is not able to target Cas9 to the nucleus in *P. infestans*, we

set out to test a different NLS. Using a BLAST search, we identified the *P. infestans* homolog of the *P. sojae* bZIP TF, from which the NLS was obtained. This gene, PITG_11668, encodes a TF that was previously shown to have strong nuclear localization in *P. infestans* (Gamboa-Melendez et al. 2013). Next, we replaced the *P. sojae* NLS in vectors pYF2.3-PsNLS-Cas9 and pYF2.3-PsNLS-Cas9-GFP with the NLS region of PITG_11668 (PiNLS) to obtain the vectors pJH2.6-PiNLS-Cas9 and pJH2.6-PiNLS-Cas9-GFP, respectively (**Figure S5.3**). In addition, PiNLS was cloned N-terminally of GFP in the basic expression vector pGFP-N (Ah-Fong & Judelson 2011), to obtain pGFP-PiNLS-GFP (**Figure S5.3**). Next, these constructs were used for transformation of *P. infestans*. We performed cotransformations of pJH2.6-PiNLS-Cas9 along with gRNAs for *Avr1*, *PiTubA2*, or *PiAP5* carried by vectors pYF2.3-gRNA or pJH2.4-gRNA-Hyg. Unfortunately, for none of the combinations we did obtain transformed lines in which we could observe Cas9 activity, nor did we obtain transformed lines exhibiting a fluorescent signal.

gRNA expression

In the *P. sojae* CRISPR/Cas9 system, expression of the ribozyme-gRNA construct as well as that of *nptII*, the gene providing geneticin resistance, is driven by p*Ps*RPL41, the promoter of the *P. sojae* ribosomal gene *Ps*RPL41. Thus, geneticin-resistant transformants should in principle express the ribozyme-gRNA construct. However, in the numerous geneticin-resistant transformants that we have obtained, we did not observe CRISPR/Cas9 activity. Consequently, we questioned whether the promoter of *Ps*RPL41 is active in *P. infestans*. In an earlier study performed in *P. infestans*, the expression stability of the *P. infestans* ortholog of p*Ps*RPL41 was found to be inferior to other *P. infestans* and *P. capsici* ribosomal promoters (Poidevin et al. 2015). p*Ps*RPL41 was not evaluated. To assess whether the use of a different promoter driving the expression of the ribozyme-gRNA construct could improve CRISPR/Cas9 activity, we opted to use the *P. capsici* S9 promoter (p*Pc*S9). The expression of this promoter was found to provide high and stable expression in *P. infestans* (Poidevin et al. 2015). To replace p*Ps*RPL41 with p*Pc*S9, the promotor was PCR amplified from pTOR-S9 (Poidevin et al. 2015) and cloned into EcoRI/NheI sites of pYF2.3-gRNA-Ribo. However, an unexpected NheI site at approximately 150 bp upstream of the 3' end of the promoter sequence, gave rise to a truncated insert, as the same restriction enzyme is used for gRNA insertion. To circumvent this problem p*Pc*S9 and the gRNA can be introduced into the vector backbone by Gibson assembly but due to time constraints we have not been able to obtain a suitable construct with p*Pc*S9 for transformation of *P. infestans*.

Delivery of ribonucleoprotein (RNP) complexes

In several organisms it has been shown that the delivery of Cas9 protein-gRNA ribonucleoproteins (RNPs) complexes is an efficient method for inducing targeted genome editing events, including numerous plant species (Woo et al. 2015), the nematode *Caenorhabditis elegans* (Cho et al. 2013), filamentous fungi and yeast (Pohl et al. 2016; Grahl et al. 2017),

protozoa (Soares Medeiros et al. 2017), and also in human cell lines (Ramakrishna et al. 2014). Moreover, it was found to result in genome editing with substantially higher specificity compared to DNA transformation (Zuris et al. 2015). From a technical perspective, the use of RNP complexes may have several advantages over a 'regular' CRISPR system where both components are delivered as plasmid DNA and integrated into the genome. Firstly, the genome-editing efficiency of Cas9 using RNP complexes does not rely on the transcription rate by the host, as both components are preassembled *in vitro* prior to delivery into cells. In *Phytophthora* spp., integration of foreign DNA occurs randomly, and it is plausible that integration in a 'silent' part of the genome results in reduced transcription rates. The integration can also lead to disruption of genes, when the transgene is inserted in an open reading frame. Secondly, and more importantly, transgene expression of Cas9 can have adverse effects and can even lead to cell death due to toxicity (Jiang et al. 2014; Kim et al. 2014; Peng et al. 2014). The use of RNP complexes of CRISPR-induced mutations might (partially) alleviate this issue, as after some time the RNP complexes are degraded, reducing chances for side effects.

To our knowledge, the use of RNP complexes for targeted genome editing has not been explored in oomycetes. To assess whether RNP complexes can be used for targeted genome editing in *P. infestans*, we used a modified protocol for PEG-mediated protoplast transformation, substituting plasmid DNA with pre-assembled RNP complexes. In parallel, one sample was co-transfected with the *Avr1* HDR construct (**Figure 5.1a**), which has *HygB* as a selectable marker. After transfection, regenerated protoplasts were analyzed by a T7EI assay and sequencing. These analyses showed all samples to be identical to control transformants, with no significantly overrepresented aberrant background signals in the sequence chromatograms. Moreover, we could not confirm the integration of *HygB* at the target locus, not even in transformants that were hygromycin-B resistant.

The experimental setup of direct delivery of RNP complexes has some limitations, most importantly the lack of selection. Whereas in a regular plasmid-based transformation experiment the introduced plasmid contains a resistance gene to a selection antibiotic, protein transfection does not yield antibiotic resistant colonies and hence also non-transfected protoplasts will regenerate. Consequently, in our experiments transfected protoplasts might have been overshadowed by non-transfected protoplasts. Moreover, despite careful preparation of the starting material, some residual sporangia may have been present in the protoplast suspension and these also readily overgrow regenerating protoplasts.

Another potential limitation is the nuclear localization of the RNP complexes. The Cas9 protein used in this experiment contains two Simian virus 40 (SV40) T antigen NLS tags, one at the N-terminus and the other at the C-terminus. The SV40 NLS is a well-studied monopartite NLS tag consisting of several basic amino acids (Lange et al. 2007), and has been shown to localize fusion gene products to the nucleus of *P. sojae*, albeit with a reduced efficiency compared to other NLS tags (Fang et al. 2017). Hence, it is expected that the RNP complexes used in this study are localized to the nucleus. Still, the use of a Cas9

protein equipped with a *Phytophthora* specific NLS tag might increase the efficiency (Fang et al. 2017). Since such Cas9 proteins are not commercially available they would have to be produced in-house.

5.4 Conclusions and future outlook

Contrary to expectations set by the successful application of the CRISPR/Cas9 system for targeted genome editing in *P. sojae*, *P. capsici* (B.M. Tyler, personal communication), and *P. palmivora* (Gumtow et al. 2017), we have as yet not been able to implement the system in *P. infestans*. The same holds for colleagues elsewhere who are also experiencing difficulties in effectuating the CRISPR/Cas9 system for use in *P. infestans* (personal communication). It is, however, hard to pinpoint the cause for failure of the system. Likely, it is an additive effect of several suboptimal conditions, such as Cas9 or gRNA expression levels, Cas9 localization, or the incubation temperature. Fang and Tyler (2016) who established the system in *P. sojae* also faced numerous challenges and made substantial modifications in the initial CRISPR/Cas9 procedure to get it to work in *P. sojae*. For *P. palmivora* (Gumtow et al. 2017) choose *Agrobacterium*-mediated transformation (AMT) to implement the CRISPR/Cas9 system. Whereas protoplast transformation typically results in multiple integration events of the transgene(s), AMT usually gives rise to only one or two integrations of the transgene in the genome (Vijn & Govers 2003). A higher transgene copy number easily results in altered expression levels due to homology-dependent gene silencing or overexpression of the transgene. However, *P. infestans* transformants resulting from AMT rarely show silencing or overexpression of the target gene (P.J.I. van de Vondervoort, unpublished data), a phenomenon that might be due to the low integration rate. Overall, generating transformants via AMT is less laborious and requires less starting materials than PEG mediated protoplast transformations. We are currently exploring the use of AMT for integration of the CRISPR/Cas9 components in *P. infestans*.

A clear difference between *P. infestans* and the three *Phytophthora* spp. in which CRISPR-induced mutations are observed, is their growth temperature. Whereas *P. infestans* is typically incubated at 18°C, the other three species are grown at 25°C. The Cas9 isoform used in the *P. sojae* CRISPR/Cas9 system is a human codon optimized gene from *Streptococcus pyogenes* (SpCas9), an organism which grows at 37°C. Hence, it is anticipated that the activity of SpCas9 is reduced at decreased temperatures. Indeed, *Arabidopsis thaliana* plants exposed to heat stress (37°C for 30 h) showed much higher rates of targeted mutagenesis by CRISPR/Cas9 compared to plants grown continuously at the standard temperature of 22°C (Le Blanc et al. 2017). On the other hand CRISPR/Cas9 has been employed in salmon eggs at temperatures as low as 6°C (Edvardsen et al. 2014), making it unlikely that the incubation temperature is the sole reason for absence of Cas9 activity in *P. infestans*. Still, incubating potential *P. infestans* transformants at elevated temperatures or exposing them to heat stress, might improve the efficiency of the system and is worth to try. This would require some pilot experiments for determining the right temperature and time of

exposure to the heat shock. When *P. infestans* is cultivated at 28°C it dies within 24 hours, but possibly a shorter exposure at elevated temperatures is sufficient to obtain higher frequencies of CRISPR-induced mutations. Another possible modification to the system which might be considered, is the use of a different nuclease. *S. pyogenes* Cas9 (SpCas9) is a relatively large protein which might hamper nuclear import. For a smaller isoform, such as Cas9 from *Staphylococcus aureus* (SaCas9), with approximately three quarters of the size of SpCas9 (Ran et al. 2015), it might be easier to find its way to the nucleus. In the protozoa *Trypanosoma cruzi*, delivery of RNP complexes of SaCas9 and gRNA resulted in gene edits, while SpCas9 did not (Soares Medeiros et al. 2017). Likewise, RNP complexes with SaCas9 could be more effective in *P. infestans* compared to those with SpCas9. Also for plasmid-based delivery of the CRISPR/Cas9 components, the smaller gene size of *SaCas9* might improve integration. However, SaCas9 recognizes a different PAM than SpCas9 (NNGRRT vs. NGG)> Hence, different gRNAs have to be designed when utilizing this nuclease, and there is likely a lower frequency of the PAM in the sequence of the target gene. Another nuclease to consider is Cpf1 (also known as Cas12a). Whereas SpCas9 creates DSB breaks with 'blunt' ends, Cpf1 introduces a staggered DSB break with a 4 or 5 nt 5' overhang (Zetsche et al. 2015). These cohesive ('sticky') ends can increase the frequency of HDR repair. Moreover, on certain positions, Cpf1 is sensitive to single-base mismatches in the protospacer, reducing the frequency of off-target cleavage (Kleinstiver et al. 2016). However, its T-rich PAM (TTTN) may limit the number of target sites in *P. infestans*, which has a GC content of 51

We trust that, with dedicated effort, developing a CRISPR/Cas system for *P. infestans* is attainable. Future work should focus on systematic analysis of factors limiting the efficiency of the system. When these limitations are identified and overcome, targeted mutagenesis in *P. infestans* might be within reach.

5.5 Materials and methods

Strains, culture conditions and transformations

P. infestans strain T30-2 (van der Lee et al. 2001) and all transgenic lines were routinely grown at 18 °C in the dark on rye agar medium supplemented with 2% sucrose (RSA) (Caten & Jinks 1968). RSA was supplemented with 20 µg/ml vancomycin, 100 µg/ml ampicillin and 50 µg/ml amphotericin B, and in addition, for transformed lines with 2.5 µg/ml G418. Transient and stable transformants of *P. infestans* were generated using PEG/CaCl2-mediated protoplast transformation and zoospore electroporation. Protoplast transformation was performed according to methods described previously (Ah-Fong et al. 2008), omitting the step of complexing circular plasmid DNA with Lipofectin in protoplast transformation. Zoospore electroporation was performed following protocols available.

gRNA design

Sequences for target genes were downloaded from FungiDB (Stajich et al. 2012). The full-length gene products were PCR amplified and subsequently validated by sequencing (Eurofins, Ebersberg, Germany). Next, the sequence was screened for CRISPR sites using NGG as PAM on Geneious R9.1.4 (Kearse et al. 2012). The resulting sites were scored for on-target activity according to Doench *et al*. (Doench et al. 2014), and for off-target interactions according to Hsu et al. (2013). The top 10 best scoring CRISPR sites were manually curated using BLAST analysis on the *P. infestans* reference genome and predictions of secondary RNA structure of the corresponding gRNAs using RNAstructure (Reuter & Mathews 2010).

gRNAs for *Avr1* and *PiTubA1* were ordered as sense and antisense PAGE-purified oligos (Integrated DNA Technologies) and subsequently annealed and ligated into pYF2.3-gRNA-Ribo-EV, as described by Fang and Tyler (2016), using BsaI and NheI-HF (New England Biolabs). For *PiAP5* and *PpAP5*, 283 bp constructs transcribing the ribozyme-gRNA insert flanked by two 30 bp overlaps, were designed and ordered as gBlocks (Integrated DNA Technologies). Next, the fragments were inserted into pYF2.3-gRNA-Ribo-EV by Gibson assembly using the NEBuilder HiFi kit (New England Biolabs Inc).

Constructs

The hygromycin-B resistance gene was amplified from pGFP-H (Ah-Fong & Judelson 2011) using primers Hyg_AflII_F and Hyg_ApaI_R, and the resulting amplicon was cloned into pYF2.3-gRNA-Ribo using AflI and ApaI (New England Biolabs), yielding pJH2.4-Hyg-gRNA. To constitute the 'all-in-one' vector pJH2.5-Cas9-gRNA, the gRNA expressing construct from pYF2.3-gRNA (containing the RPL41 promoter, gRNA insert, and Hsp70 terminator) was inserted into pYF2.2-Cas9 using EcoRI (Promega). A dual-gRNA vector encoding Avr1-targeting gRNA2 and gRNA3 was constructed by inserting the ribozyme-gRNA3 construct into pYF2.3-gRNA2 by Gibson assembly. The amplicon containing the insert was made using primers gRNA3_Gibson_F and gRNA3_Gibson_R. The NLS region from PITG_11668 was inserted at the N-terminus of GFP, the PCR amplicon was cloned into the AgeI and NheI sites of pGFP-N (Ah-Fong & Judelson 2011), yielding pGFP-PiNLS-GFP. To obtain pJH2.6-PiNLS-Cas9 and pJH2.6-PiNLS-Cas9-GFP, the NLS region from PITG_11668 was inserted into the SacII and SpeI sites of pYF2.2-PsNLS-Cas9 and pYF2.2-PsNLS-Cas9-GFP. ΔAvr1 was constructed by overlap extension PCR using primers Avr1_del_F and Avr1_del_R. All primers used in this study are listed in Table S5.1.

Cas9 *in vitro* activity assay

To obtain template DNA for *in vitro* transcription (IVT), a PCR was performed with a T7 promoter-fused forward primer (marked with extension _pT7_F) and the primer sgRNA_Col_R, using plasmid DNA containing the respective gRNAs as template. Next, gRNA was transcribed with T7 RNA polymerase using MEGAshortscript T7 kit (Thermo Fischer Scientific). IVT was allowed to proceed for 4 h, after which RNA was purified by phenol/chloroform and ethanol precipitation, and analyzed on agarose gel. Target DNA was amplified using the respective primers for full-length PCR products of *Avr1*, *PiTubA2*, and *PiAP5*. SpCas9 nuclease was purchased (New England Biolabs). The assay was performed according to manufacturer's instructions.

Molecular analysis of transformants

Genomic DNA (gDNA) was extracted from pooled or individual *P. infestans* transformants according to methods described previously (Fang & Tyler 2016), with modifications. Pooled transformants, 24-48 h after transformation, were pelleted by centrifugation, resuspended in 500 mL of gDNA extraction buffer (200 mM Tris, pH 8.0, 200 mM NaCl, 25 mM EDTA, pH 8.0, 2% SDS, plus 0.1 mg/mL RNase A added prior to use) and sheared by vigorous pipetting. For individual transformants, approximately 250 µl of *P. infestans* mycelium was frozen in liquid nitrogen, freeze-dried, and ground to a powder using a Retsch Mixer Mill MM 400 and metal beads (ø 3 mm) for 30 seconds at 30 Hz. Subsequently, the powder was resuspended in 500 µl of gDNA extraction buffer. DNA was recovered by phenol/chloroform extraction and isopropanol precipitation. RNA was isolated using home-made TRIzol (Verdonk 2014), and cDNA was synthesized using M-MLV Reverse Transcriptase (Promega) according to manufacturer's instructions. RT-PCR was performed using primers Cas9_RT_F and Cas9_RT_R.

All PCR amplifications were conducted using Q5 high-fidelity DNA polymerase (New England Biolabs). Nested PCR was performed using diluted (1000x) PCR products as a DNA template. PCR amplicons were purified using the NucleoSpin Gel and PCR Clean-up kit (Macherey-Nagel). Sequence analysis was performed at Eurofins.

T7EI assay

The efficiency of the CRISPR/Cas9 system was tested with T7 endonuclease I (T7EI) (New England Biolabs), using gDNA isolated from pooled transformants as template. First, the target gene was amplified from gDNA using primers amplifying the full-length sequence of the respective target genes (Table S1). Next, purified amplicons were annealed in a thermocycler using the following conditions: 95°C for 5 min, ramp down to 85°C at -2 °C/s, ramp down to 20°C at -0.1 °C/s, hold at room temperature. The T7EI cleavage assay was

performed according to manufacturer's instructions and analyzed by gel electrophoresis.

RNP assembly and transfection

Ribonucleoprotein complexes (RNPs) of Cas9 (EnGen Cas9 NLS, New England Biolabs) and gRNAs were prepared immediately before transfections. After IVT, gRNAs were refolded by heating at 90°C for 5 min and cooling to room temperature over the course of 12 h. To preassemble RNPs, equimolar amounts of Cas9 (120 pmol) and gRNA (120 pmol) were incubated at 25°C for 10 min. Next, RNPs (10 µl) were incubated with an equal volume of lipofectin for 5 min at room temperature and added to a 100 µl protoplast suspension (2 x 106/ml). After 5 minutes, 120 µl freshly prepared PEG solution (50% PEG-3350, 10 mM CaCl2, 10 mM Tris-HCl pH7.5) was added slowly. After incubation for 5 min at room temperature the volume was adjusted to 10 ml with regeneration medium (RSM + 1 M mannitol, without antibiotics) and protoplasts were regenerated for 48 h at 22°C. Next, regenerated protoplasts were collected by centrifugation, from which a sample was taken for gDNA extraction, while the remainder was plated on RSA plates. Protoplasts co-transfected with a HDR construct were plated on RSA plates supplemented with 25 mg/ml hygromycin-B. Colonies appeared on non-selective plates after two days, or after four days on selective plates. Individual colonies were transferred to new plates as soon as they appeared and cultured for further analysis.

5.6 Supplementary files

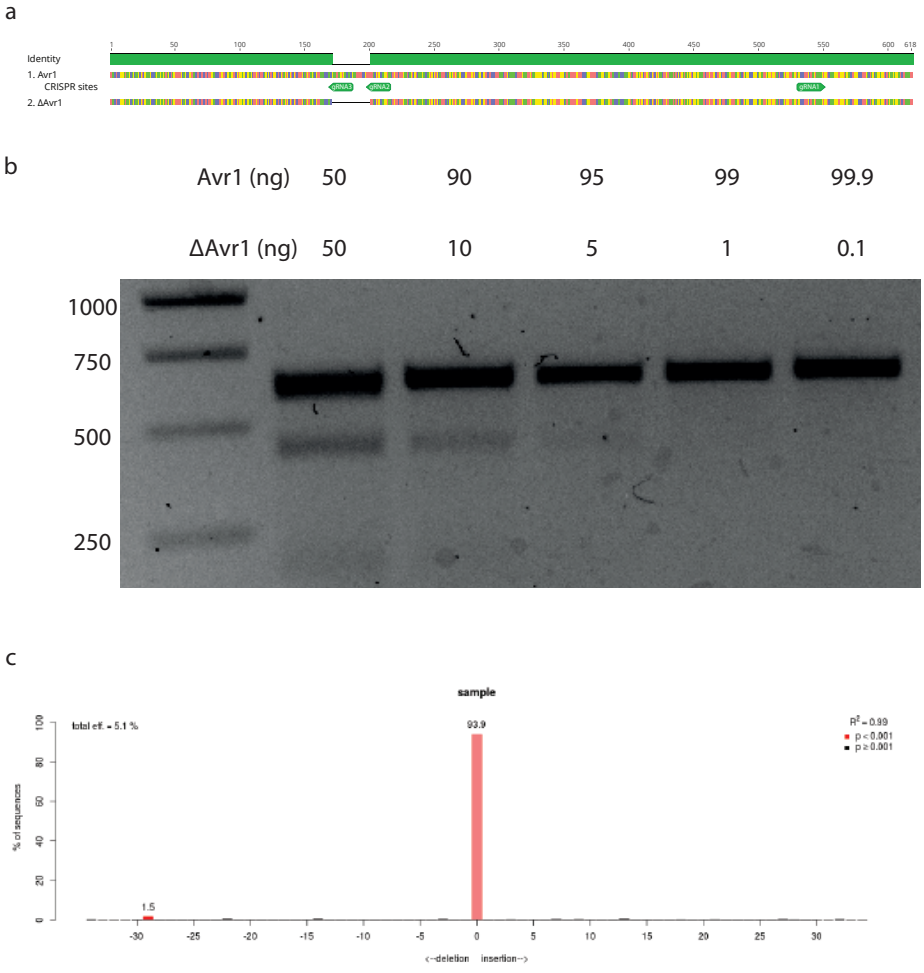

Figure S5.1 | Detection limit assays. a) PCR amplicons used for the detection limit assays. ΔAvr1 contains a 29 bp deletion. **b)** T7EI assay. Varying amounts of Avr1 and ΔAvr1 PCR amplicons were annealed and digested by T7EI. **c)** Example output from TIDE, confirming the presence of the 29 bp deletion in ΔAvr1 (left red bar). Here, a sequence chromatogram obtained from sequencing a molar ratio of 998:2 Avr1:ΔAvr1 was compared to a sequence chromatogram of Avr1. The predicted frequency of chromatograms with a deletion (1.5%) deviates from the actual molar ratio of Avr1:ΔAvr1 (0.2%).

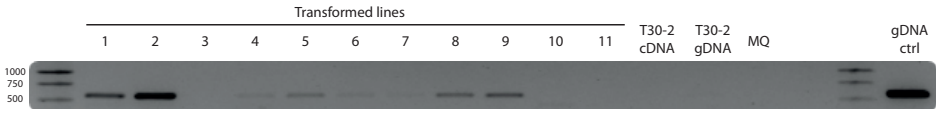

Figure S5.2 | Expression analysis of Cas9 in 11 selected transformed lines. cDNA and genomic DNA (gDNA) of *P. infestans* strain T30-2 were used as negative control and gDNA from a *P. infestans* Cas9 transformant as positive control.

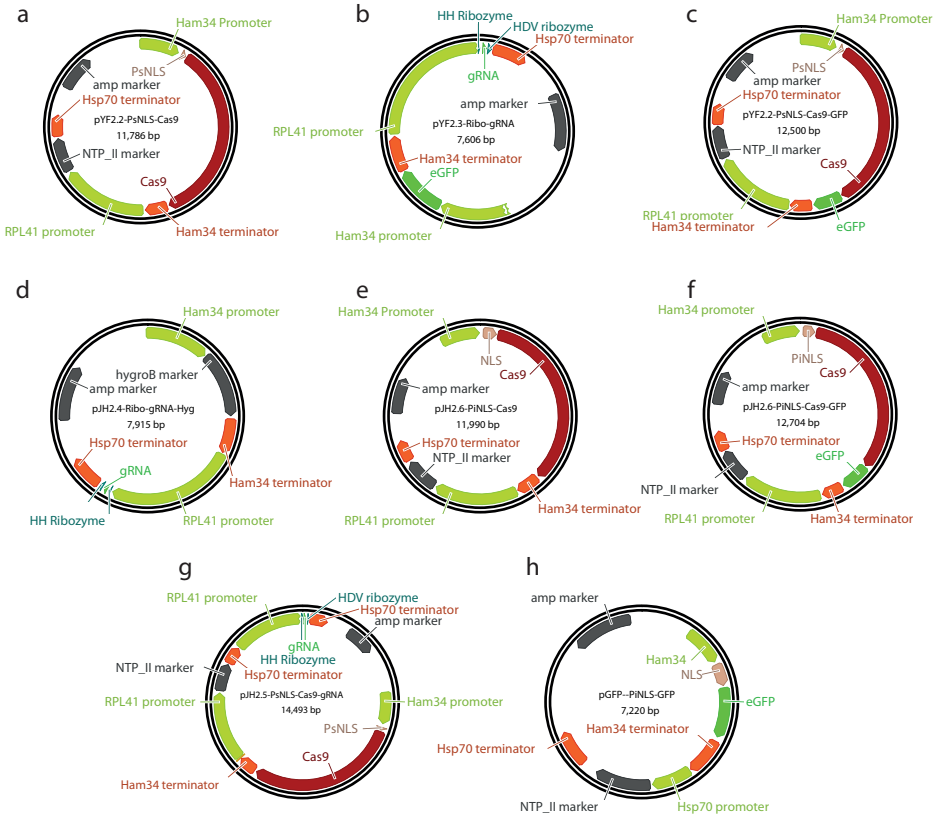

Figure S5.3 | Plasmids used in this study. Plasmids starting with 'pYF' are obtained from Francis Fang (Fang & Tyler 2017), plamids starting with 'pJH' are modified versions as described in this chapter.

Table S5.1 | Primers used in this study.

Name	Sequence (5' - 3')	Purpose
Avr1_F	ATGCACCGCGTATTGCTGC	*P. infestans* T30-2 Avr1
Avr1_F	TTAAAATGGTACCACAACATGTCCACC	*P. infestans* T30-2 Avr1
Avr1_Nested F	GACGTTTGCCCTGTTGTGTA	*P. infestans* T30-2 Avr1 - nested
Avr1_Nested R	ACAACATGTCCACCAAGCATG	*P. infestans* T30-2 Avr1 - nested
pRPL41_seq_F	CAAGCCTCACTTTCTGCTGACTG	Sequence analysis of gRNA constructs
sgRNA_Col_R	AAAAGCACCGACTCGGTGC	Sequence analysis of gRNA constructs
Cas9_RT_F	CCGAAGAGGTCGTGAAGAAG	Expression analysis of Cas9
Cas9_RT_R	GCCTTATCCAGTTCGCTCAG	Expression analysis of Cas9
pHAM34_Pseq_F	TCGCCCGACTCGCCCCAC	Sequence analysis of Cas9
Cas9_Seq_757_F	CTGTTCGGAAACCTGATTGCCC	Sequence analysis of Cas9
Cas9_Seq_1439_F	GGATGACCAGAAAGAGCCAGG	Sequence analysis of Cas9
Cas9_Seq_2163_F	AGAGGACATCCAGAAAGCCCAGG	Sequence analysis of Cas9
Cas9_Seq_2865_F	GAACACTAAGTACGACGAGAATGAC	Sequence analysis of Cas9
Cas9_Seq_3600_F	CAAGGGCTACAAAGAAGTGAAAAAG	Sequence analysis of Cas9
eGFP_F	ATGGGCAAGGGCGAGGAA	Detection of eGFP
eGFP_R	TCACTTGTAGAGTTCATCCATGCCA	Detection of eGFP
Hyg_ApaI_R	GGGCCCCTATTCCTTTGCCCTC	Cloning Hygromycin into pYF2.3
Hyg-AflII_F	CTTAAGATGAAAAAGCCTGAACTCAC	Cloning Hygromycin into pYF2.3
M13F	CGTTGTAAAACGACGGCCAG	General primers
M13R	TGCCAGGAAACAGCTATGACC	General primers
PiNLS_SacII_F	ACACCCGCGGATGCACAAGCGCAAG	Cloning PiNLS in pYF2.2
PiNLS_SpeI_R	ACACACTAGTCTCGCCCATTGCCGCGTC	Cloning PiNLS in pYF2.2
PiNLS_AgeI_F	ACACACCGGTATGCACAAGCGCAAG	Cloning PiNLS in pGFPN
PiNLS_NheI_R	ACACGCTAGCCTCGCCCATTGCCGCGTC	Cloning PiNLS in pGFPN
PiAP5_EcoRI_F	ACACGAATTCATGCGTCTCGGTCTGCTC	PiAp5 full-length
PiAP5_NotI_R	ACACGCGGCCGCATTTGGTCCCATGAGACGCG	PiAp5 full-length
PcS9_F_EcoRI	cacaGAATTCCGTCAATACGGCTGTAAACCAC	*P. capsici S9* promoter
PcS9_F_NheI	cacaGCTAGCTTTGGCGACTTCTTTTGTTCAGG	*P. capsici S9* promoter
Avr1_gRNA_1_pT7_F	GAAATTAATACGACTCACTATAGGTGGCCAAAGCAATGATATTG	In vitro transcription gRNA
Avr1_gRNA_2_pT7_F	GAAATTAATACGACTCACTATAGGTCGTTTATCGAGTCCTTCGT	In vitro transcription gRNA
Avr1_gRNA_3_pT7_F	GAAATTAATACGACTCACTATAGGGAATCCAAGACTCGATTTTT	In vitro transcription gRNA
PiTubA2_gRNA_8_pT7_F	GAAATTAATACGACTCACTATAGGACGCATGTTGCTTTAAGCTT	In vitro transcription gRNA
PiAP5_gRNA_183_pT7_F	GAAATTAATACGACTCACTATAGGGATAAGACGGTGAACAGCAA	In vitro transcription gRNA
gRNA3_Gibson_F	TCGGCATGGCGAATGGGACAGGATTCCTGATGAGTCCGTGA	gRNA2-3 plasmid
gRNA3_Gibson_R	GCTAAGTATTCTAGTCGACAGTCCCATTCGCCATGCCCGAA	gRNA2-3 plasmid

Chapter 6

General discussion

A modified version of this chapter is published as: GPCR-bigrams: enigmatic signaling components in oomycetes, *Plos Pathogens*. doi:10.1371/journal.ppat.1007064

The overall aim of this thesis was to explore and identify unique features of cellular signaling and cytoskeletal dynamic in oomycetes, primarily focused on *Phytophthora infestans*. The work presented comprehends an integrated approach combining *in silico* analyses and wet-lab experiments. In this chapter, the main results are integrated and discussed. Remarkable features of oomycetes and their cellular signaling systems are outlined, and future directions are proposed for how to exploit this knowledge for disease control.

What makes oomycetes exceptional?

Oomycetes are easily mistaken for fungi but differ in many ways. At the organismal level, morphology, growth pattern and mode of dispersal are shared, and the two groups occupy similar ecological niches. Only at the cellular and molecular level, the differences become apparent. For example, the cell walls have a different composition; whereas chitin is the main component in fungi, oomycete cell walls consist of cellulose and β-glucans (Judelson & Blanco 2005). Opposed to the flattened mitochondrial cristae in fungi, oomycete mitochondria have tubular cristae (Powell et al. 1985). Also the actin cytoskeleton has unique features, such as so-called actin plaques. These dot-like structures resemble actin patches in fungi, but unlike patches, plaques have a long lifetime and presumably no role in endocytosis (Meijer et al. 2014). Oomycetes also exhibit distinct features in their protein repertoires, in particular with respect to protein domain organization. The number of distinct protein domain combinations, or bigrams, is significantly higher than in other eukaryotes, and many bigrams are potentially involved in cellular signaling (Seidl et al. 2011). The most abundant oomycete-specific bigram type is a combination of the FYVE-type phosphatidylinositol 3-phosphate-binding zinc finger and a GAF domain. GAF domains are involved in many different cellular processes, and one speculation on the function of the GAF-FYVE bigram type is that it is involved in the targeting of proteins to lipid layers (involving the FYVE domain) in response to second messengers (e.g. cyclic GMP) sensed by the GAF domain (Seidl et al. 2011). This unique bigram type is illustrative for how oomycetes have evolved to combine protein domains involved in different processes. For example, in addition to proteins containing the GAF-FYVE combination as a single bigram, it is also found in combination with other domains, such as the actin-associated motor protein myosin (Richards & Cavalier-Smith 2005; Seidl et al. 2011), possibly linking motor protein movement to cellular signaling. To assess whether more of such unique proteins are present, we inventoried the putative array of microtubule (MT) associated proteins in *P. infestans* (**Chapter 4**). This revealed some distinct features in the domain composition of the motor protein kinesin, with some kinesins in combination with protein domains not observed in other taxa. For example, in some Peronosporalean oomycetes (i.e. *Phytophthora*, *Plasmopara*), a kinesin containing a C-terminal ZZ-type Zinc Finger can be found. Furthermore, several *P. infestans* kinesins contain N-terminal transmembrane domains and one contains a Major Facilitator Superfamily domain. Whether, and if so, how, these proteins link motor protein activity to other cellular processes is unclear.

Obviously, these differences also have consequences for the efficacy of chemical control agents. For example, a major class of fungicides broadly used in health care and agriculture are sterol biosynthesis inhibitors (SBI) but since oomycetes do not synthesize sterols they are insensitive to SBI. The quest for novel compounds for controlling pathogenic oomycetes is a continuous challenge. We postulate that oomycete specific cellular signaling components such as GPCR-bigrams, hold potential as novel drug targets. Likewise, due to their central role in development and pathogenicity, fungal GPCRs have recently been proposed to be druggable targets for novel antifungal agents (Brown et al. 2018).

Cellular signaling and cytoskeleton dynamics

Cellular signaling and cytoskeletal dynamics are interconnected processes. For example, actin nucleators (e.g. WASP, WAVE, and SCAR) are downstream effectors of the small GTPase Rac (Pollitt & Insall 2009). Activation of these nucleators leads to Arp2/3-mediated actin side branching. ELMO proteins are effector proteins of heterotrimeric G-protein subunits and both positively and negatively regulate actin polymerization (Yan et al. 2012; Xu & Jin 2017). In oomycetes, genes encoding these components are not yet described in detail but most are readily detected by BLAST or HMM searches (unpublished data). Hence, it may be assumed that similar processes play a role in the regulation of cytoskeletal dynamics in oomycetes. Consequently, silencing of the gene encoding the G-protein γ (Gγ) subunit gene *Pigpg1* (**Chapter 3**) in *P. infestans* could affect the organization of the actin cytoskeleton in *P. infestans*. This might explain the severe phenotypes observed.

Also the MT cytoskeleton is a downstream target of G-protein signaling. Heterotrimeric G-proteins regulate the stability through activation of microtubule associated proteins (MAPs), but can also directly interact with MTs (Roychowdhury & Rasenick 2008; Etienne-Manneville 2010). By activating the intrinsic GTPase activity of tubulin, activated Gα subunits inhibit MT assembly and increase MT disassembly (Roychowdhury et al. 1999). On the other hand, activated G$\beta\gamma$ subunits stabilize MTs. Depending on the prenylation state of the Gγ subunit, G$\beta\gamma$ dimers stimulate MT assembly (Roychowdhury & Rasenick 2008). Possibly, in *P. infestans*, the aberrant zoospore motility that *Pigpa1*-silenced lines display (Latijnhouwers et al. 2004) is an effect of defects in MT turnover due to reduced Gα levels, resulting in abnormal flagellar movement. The phenotypes that we observed in *Pigpg1*-silenced lines and the overexpression line (**chapter 3**) are not as readily linked to a defect in the MT cytoskeleton. Speculatively, the reduced mycelial growth rate of the *Pigpg1*-overexpression line could be due to an increased stability of MTs, consequently leading to decreased cellular transport.

What are unique features of oomycete cellular signaling?

Cellular signaling in oomycetes is inscrutable and holds many novelties. Several oomycete signaling components are clearly distinct from their homologs in organisms from other

taxa. Many of these contain unique proteins domain combinations, which are not known to exist in other organisms (Meijer & Govers 2006; Judelson & Ah-Fong 2010). For example, *Phytophthora* has several protein kinases and phospholipid kinases with accessory domains that are normally not found in combination with kinase domains. On the other hand, two ubiquitous enzymes, i.e. protein kinase C (PKC) and phospholipase C, seem to be absent, at least in their stereotypical forms (Meijer & Govers 2006; Judelson & Ah-Fong 2010).

One particularly interesting class of unique signaling components comprises the so-called GPCR-bigrams. These proteins have a N-terminal G-protein coupled receptor (GPCR) domain typically composed of seven transmembrane (TM) regions, combined with a C-terminal catalytic accessory domain (Van den Hoogen et al. 2018) (**Chapter 2**). Based on the predicted biochemical activity of the accessory domain we anticipate that these GPCR-bigrams have roles in phospholipid signaling (GPCR-PIPKs, GPCR-INPPs), cyclic nucleotide conversion (GPCR-ACs, GPCR-PDEs), or protein phosphorylation (GPCR-TKLs). One further GPCR-bigram type is AP-GPCR, which has an aspartic protease (AP) domain at the N-terminus that precedes the GPCR domain (Kay et al. 2011; Van den Hoogen et al. 2018). The link between the predicted activity of AP-GPCR, i.e. hydrolytic cleavage, and cellular signaling is less obvious. Most oomycetes have comparable copy numbers of the different GPCR-bigram types, with some types having only a few copies, while others belong to gene families with up to 20 members. All types of GPCR-bigrams are shared by oomycetes, but some types are sparsely present in organisms from other taxa. For example, GPCR-PIPKs are found in a diverse but limited range of eukaryotic microorganisms distributed over nearly all eukaryotic supergroups.

The predicted catalytic activity of the accessory domains of these GPCR-bigrams is unique. There are examples of other GPCRs with accessory domains such as adhesion GPCRs, but their extracellular N-terminal extensions have a role in protein-protein interaction and are not predicted to have catalytic activity (Bjarnadottir et al. 2007). Plants possess regulator of G-protein signaling (RGS) proteins that, similar to GPCR-bigrams, have a N-terminal 7TM receptor domain (Urano & Jones 2014). RGS domains, however, are not catalytically active but rather accelerate the intrinsic GTPase activity of Gα subunits (Urano & Jones 2014).

In oomycetes, GPCR-bigrams occur next to regular conserved enzymes. For example, P. infestans has four GPCR-ACs in addition to eight canonical adenylate cyclases (ACs) (unpublished). This underscores the importance of GPCR-bigrams for oomycetes. In case the catalytic domain in a GPCR-bigram would not have an advantage over the canonical enzyme, there would be no evolutionary pressure for the GPCR-bigram to sustain. Thus, the strong conservation of GPCR-bigrams throughout oomycetes indicates that having GPCR-bigrams is advantageous. Clearly, oomycetes need GPCR-bigrams, but for what purpose?

What is known about GPCR-bigrams?

The conservation of all GPCR-bigram types in oomycetes, and the presence of GPCR-PIPKs in several unicellular eukaryotes, almost indisputably suggests that they are functional proteins. To date, however, there are only a few studies addressing their biological role and these are limited to GPCR-PIPKs. Knockout lines of the single GPCR-PIPK gene *RpkA* in the slime mold *Dictyostelium discoideum* displayed defects in cell density sensing, bacterial defense, and phagocytosis, and had reduced phospholipid levels (Bakthavatsalam et al. 2007; Riyahi et al. 2011). Silencing or overexpression of one of the twelve GPCR-PIPK genes in *P. infestans* resulted in aberrant asexual development and reduced pathogenicity (Hua et al. 2013). *Phytophthora sojae* transformants with a silenced GPCR-PIPK gene showed similar phenotypes, but in addition showed reduced chemotaxis towards soybean root tips and the soybean isoflavone daidzein (Yang et al. 2013). These limited experimental data show that GPCR-PIPKs are important for proper functioning of oomycetes but many questions remain. Are the accessory domains catalytically active? Are GPCR-bigrams capable of sensing a ligand? How is their activity regulated? And what is the mode of action of GPCR-bigrams?

How do GPCR-bigrams work?

The catalytic domains of GPCR-bigrams are usually the core domains in effector proteins regulated by G-protein signaling. Hence, it is conceivable that GPCR-bigrams provide a direct link between GPCR sensing and catalytic activity. Below, we speculate how GPCR-bigrams may transduce signals.

An intriguing possibility is that the catalytic domain is activated directly upon binding of an agonist (i.e., a stimulating ligand) to the GPCR domain (**Figure 6.1a**) or after proteolytic cleavage (**Figure 6.1b**) thereby bypassing intermediate signaling components.Such a direct signal transfer is unprecedented and could be more efficient than via G-proteins. The downside, however, is that only a single downstream effector protein is activated. This in contrast to a canonical GPCR that can activate multiple and different downstream effectors at once. Despite being more efficient the direct activation may limit the signaling system in both amplitude and versatility.

Another possibility is that the GPCR domain activates heterotrimeric G-proteins. The activated G-protein subunits then stimulate the activity of the catalytic domain either directly, or indirectly through effector proteins or the production of second messengers (**Figure 6.1c**). Likewise, the activation could be initiated through a second, canonical GPCR (**Figure 6.1d**). Possibly, this requires dimerization of GPCR domains (not depicted). In case the catalytic domain is non-functional or inactive, the GPCR-bigram might act as a stereotypical GPCR that stimulates the activation of effector proteins and production of second messengers via G-proteins, to elicit a cellular response (**Figure 6.1e**).

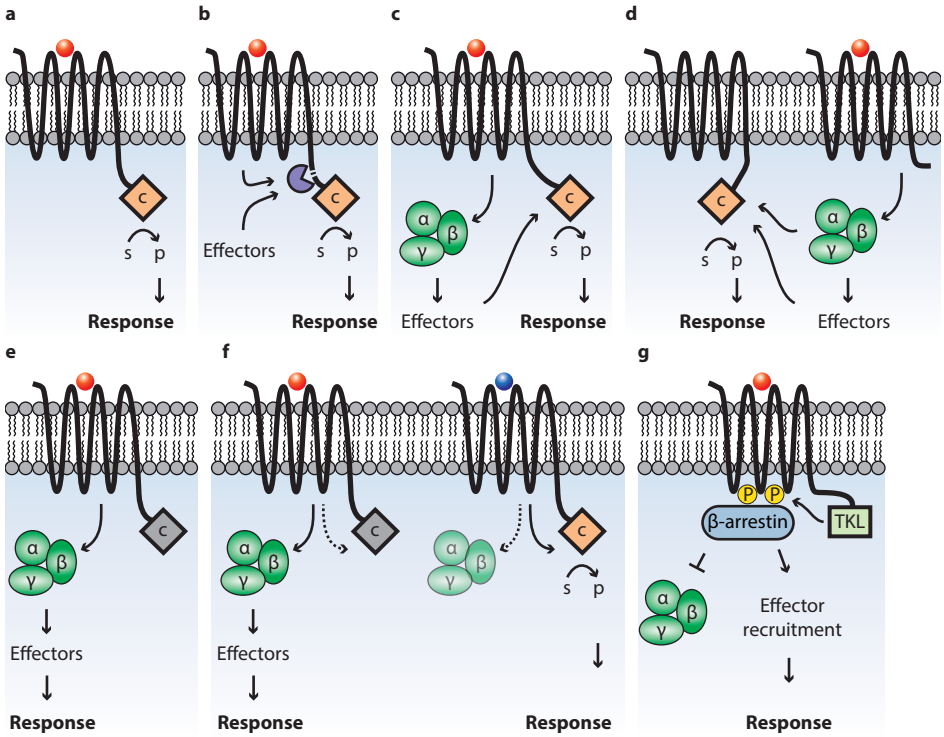

Figure 6.1 | Proposed models of mode of action of GPCR-bigrams. **a**) the catalytic domain (c) is directly activated through agonist binding on the receptor domain, producing a product (p) from a substrate (s); **b**) the catalytic domain and/or the GPCR undergo proteolytic cleavage (purple) to yield a mature GPCR and an active catalytic domain; **c**) agonist binding on the receptor domain activates G-proteins, which either directly or via the production of second messengers activate the catalytic domain; **d**) the catalytic domain is activated by G-proteins or effector proteins, activated by a canonical GPCR; **e**) agonist binding activates G-proteins which induce the production of second messengers to elicit a cellular response, the catalytic domain is inactive (grey); **f**) the receptor displays biased agonism to either stimulate G-protein activation (**left**) or directly activates the catalytic domain (**right**); **g**) phosphorylation of the GPCR (yellow circles) by kinase activity of GPCR-TKLs leads to recruitment of β-arrestin, thereby either blocking signaling via G-proteins (left**)** or scaffolding effector proteins to initiate downstream signaling (**right**).

GPCRs can display biased agonism; a phenomenon signifying that different ligands can induce specific receptor profiles on the same receptor molecule (Wisler et al. 2014). Such profiles, represented by the receptor conformation or phosphorylation pattern, result in different downstream responses by activation of different effectors (Rajagopal et al. 2010). Likewise, GPCR-bigrams could show a bias towards a specific agonist, either activating G-proteins or the catalytic domain (**Figure 6.1f**).

Besides heterotrimeric G-proteins, also β-arrestins can act as molecular switches transmitting GPCR-sensed signals. Initially, β-arrestins were thought to serve a main role in the desensitization of GPCRs, initiating the internalization of an activated GPCR. Later, it was recognized that β-arrestins can facilitate signal transduction to mitogen activated protein kinases (MAPKs), by serving as scaffolds to recruit proteins to an activated GPCR (Smith & Rajagopal 2016). The phosphorylation pattern of the receptor functions as a 'barcode', recruiting different effector proteins to β-arrestins, thereby activating distinct signaling pathways. Phosphorylation of GPCRs is typically performed by GPCR-kinases (GRKs), protein kinase A (PKA), or PKC (Smith & Rajagopal 2016), all kinases which are underrepresented in oomycetes. P. infestans has only a single GRK gene and lacks PKC (Judelson & Ah-Fong 2010). It is conceivable that GPCR-TKLs have the capacity to phosphorylate GPCRs, thereby compensating for the apparent deficiency of GPCR-phosphorylating kinases. This phosphorylation can lead to β-arrestin initiated desensitization of G-protein mediated signaling, or to the recruitment of downstream effectors, such as MAPKs (**Figure 6.1g**). Similarly, GPCR-TKLs could phosphorylate another GPCR(-bigram) to elicit a similar response (not depicted). Yet another possibility is that the single GRK in *P. infestans* phosphorylates GPCR-bigrams to initiate β-arrestin recruitment. *P. infestans* has a total of 15 genes encoding MAPK-like proteins, which are all extracellular signal-regulated kinases (ERKs) (Judelson & Ah-Fong 2010). In comparison, MAPKs are ubiquitous in higher plants and vertebrates but limited in other organisms. For example, the diatom *Thalassiosira pseudonana*, which is relatively closely related to oomycetes, has only five MAPKs (Judelson & Ah-Fong 2010). Although MAPKs can be regulated through many different pathways, the expansive set of MAPK-like proteins supports our hypothesis that β-arrestin signaling is in play in *P. infestans*. Possibly, this involves GPCR-TKLs.

How can ligands of GPCR-bigrams be identified?

Most if not all GPCRs are activated upon recognition of an external signal. Likely, the receptor domains of GPCR-bigrams are also capable of recognizing a ligand, and obvious questions that arise are: what is the nature of these ligands and how can they be identified? So far, the only putative candidate is the isoflavone daidzein, solely based on the fact that silencing of a GPCR-PIPK gene in *P. sojae* leads to loss of chemotaxis towards daidzein (Yang et al. 2013). There is no evidence, though, that daidzein is the ligand that physically interacts with the GPCR-PIPK.

As GPCRs are important drug targets in human medicine, ligand discovery is primarily focused on human GPCRs. A common and popular approach is screening (human) cells expressing the GPCR of interest with chemical libraries, and monitor changes in production of secondary messengers such as cAMP, IP3, or Ca2+ using biosensors, or induction of reporter expression (Zhang & Xie 2012). As yet, no secondary messenger biosensors are available for use in oomycetes. Nevertheless, some of these 'reverse pharmacology' approaches might be amendable for studying GPCR-bigrams.

Though the setup would be artificial, one could envision expressing an oomycete GPCR-bigram in a mammalian cell line, and then screen a chemical library of known compounds or mixtures comprising putative ligands such as exudates from plant tissue or from *Phytophthora*. Alternatively, the GPCR-bigrams could be expressed in yeast taking advantage of the many available signaling mutants and reporter strains. Also, yeast is easy to manipulate and contains only two endogenous GPCR signaling systems that can be eliminated (Ladds et al. 2005). Of the five types of GPCR-bigrams, GPCR-ACs and GPCR-PDEs seem the most straightforward to tackle. By screening a chemical library for induction of cAMP production in yeast expressing a GPCR-AC, one could determine whether the AC domain is active, and, if so, is regulated via the GPCR domain. To rule out that the GPCR domain can activate endogenous signaling leading to second messenger production, a truncated protein lacking the catalytic domain could be used as a control.

To more directly study the possible catalytic activity of GPCR-bigrams, yeast complementation assays could be used, rescuing lethal mutations in effector proteins such as adenylate cyclases or phospholipid kinases. We have used such an approach in an attempt to investigate the role of the LRxGI motif of GPCR-PIPKs (Van den Hoogen et al. 2018) (**Chapter 2**). Different mutated versions of *P. infestans* GPCR-PIPKs were used to complement the growth defect of the yeast mutant strain *mss4ts* (Stefan et al. 2002). This strain contains a temperature sensitive mutation in *mss4*, a gene which encodes a phosphatidylinositol-4-phosphate 5-kinase. The strain is able to grow at the permissive temperature of 28°C, but at an elevated temperature of 37°C growth is arrested. Previous work performed in our lab showed that complementation of *mss4ts* with either wild-type *mss4* or a full-length *P. infestans* GPCR-PIPK D4 gene can restore growth at 37°C, pointing at catalytic activity of the GPCR-PIPK (C. Hua, unpublished data). We constructed deletion mutants of the LRxGI motif in *P. infestans* GPCR-PIPKs D4, D8, and D10, and *D. discoideum* RpkA. Additionally, with the idea to obtain subtle phenotypic changes in the complementation efficiency of GPCR-PIPKs, we chose to construct swap constructs of the LRxGI motif (**Chapter 2**). Even though the setup of the experiment was promising, the results varied and were not reproducible. We, therefore, decided to not continue with these experiments.

The role of β-arrestins in oomycetes has not been studied so far. We identified three arrestin domain containing proteins in *P. infestans* (PITG_10415, PITG_10578, PITG_17413), and given their presence we assume that arrestins have a role in oomycete cellular signaling somehow. One observation indicating that G-protein independent signaling could be

in play in oomycetes was made in *P. sojae*. In a yeast two-hybrid assay no interactions were observed between protein segments including the intracellular loops and the C-terminal tail region of PsGPR11, a GPCR, and the *P. sojae* Gα subunit (Wang et al. 2010), even though both the GPCR and Gα subunit were found to be functional (Hua et al. 2008; Wang et al. 2010). While it is not unlikely that the experimental setup did not provide the right protein topology of the GPCR or that multiple parts of the GPCR are simultaneously involved in Gα binding, it is plausible that PsGPR11 acts independently of PsGPA1. This could, possibly, involve β-arrestins. Further, the presence of only a single Gα, Gβ, and Gγ subunit, seems in contrast to the relatively large set of 88 GPCRs in *P. infestans* (**Chapter 2**). The apparent limitation in flexibility of the number of possible heterotrimeric G-protein complexes might be overcome by signaling through β-arrestins.

For analyzing β-arrestin desensitization and recruitment by GPCRs several assays are available. Some are based on human arrestin fused to a protein that upon activation induces reporter gene expression (e.g. TangoTM) or β-galactosidase activity (e.g. PathHunterTM) (Zhang & Xie 2012; Stoddart et al. 2015). Other assays make use of bioluminescence resonance energy transfer (BRET) (Zhang & Xie 2012), for which the GPCR-bigram has to be tagged with a fluorescent acceptor protein (e.g. GFP) and the β-arrestin with luciferase (e.g. Rluc). When in close proximity, a detectable fluorescent signal is emitted. With the recent development of a CRISPR/Cas9 system in *P. sojae* (Fang & Tyler 2016), it might be achievable to create transgenic lines to study β-arrestin recruitment to GPCR-bigrams using BRET or to monitor secondary messenger production using biosensors or reporter gene expression. By targeted mutagenesis mutants can be generated to study the role of individual domains, for example, by removing the GPCR domain of a GPCR-bigram of interest and analyzing changes in catalytic activity. Moreover, CRISPR/Cas systems could be used to create knockouts of multiple members of one gene family at once, thereby avoiding redundancy.

The availability of a CRISPR/Cas system in *P. infestans*, to perform targeted mutagenesis or create gene knockout lines, would be of great value. Currently, functional gene studies in *P. infestans*, and most other oomycetes, primarily rely on gene silencing and overexpression. However, transgenes are inserted randomly, and often at multiple genomic loci, and consequently, transformed lines frequently display varying levels of silencing efficiency, phenotypic differences, and unwanted traits. Specific gene-knockouts would, in theory, allow for more specific and controlled studies of genes of interest. Moreover, CRISPR/Cas systems could be used to create knockouts of multiple genes to study the role of possibly redundant genes, such as GPCR-PIPKs. Gene knock-ins, for example GFP, give the possibility to study protein localization without possible artefacts related to overexpression of the transgene. However, even though the *P. sojae* CRISPR/Cas9 system proved functional and effective in two other *Phytophthora* species; *Phytophthora palmivora* (Gumtow et al. 2017) and *Phytophthora capsici* (B.M. Tyler, personal communication), it is not readily transferred to *P. infestans*. Similar to our experiences, several colleagues in other laboratories have experienced difficulties in establishing the CRISPR/Cas9 system in *P. infestans* (personal

communication). Determining the exact underlying cause for failure is difficult, as it is likely a combination of multiple factors. Still, we believe that it should be possible to use CRISPR/Cas9 for genome editing in *P. infestans*. We are currently in the process of investigating the use of *Agrobacterium*-mediated transformation, a transformation method which proved effective for CRISPR/Cas9 in *P. palmivora* (Gumtow et al. 2017). Other work in progress focusses on the nuclear localization of Cas9 in *P. infestans*. As described in **Chapter 5**, due to difficulties with obtaining transformed lines with a detectable fluorescent signal, we have not yet been able to confirm the correct localization of Cas9. We are currently testing the nuclear localization efficiency of different nuclear localization sequences in *P. infestans*.

What lies ahead?

Cellular signaling and cytoskeletal dynamics in oomycetes are emerging fields. Challenges lying ahead are determining the role of GPCR-bigrams in cellular signaling and their biochemical mode of action, and answering the question why oomycetes have such unique signaling proteins. What is the advantage of having GPCR domains linked to catalytic accessory domains; does it provide, for example, shortcuts for more efficient signaling? This could be the case if the catalytic domain is under the direct control of the GPCR domain, a situation that is unprecedented. Another major challenge is to identify ligands recognized by GPCR-bigrams and to determine how such ligands can be exploited. With respect to the MT cytoskeleton, GFP-tagged lines for live-cell imaging will be of value in understanding elementary cellular processes in oomycetes, such as nuclear division and intracellular transport. It is likely that oomycetes hold still uncovered features in their MT cytoskeleton, and the role of the unique kinesin and dynein types remains to be uncovered. The addition of a CRISPR/Cas system to the molecular toolbox of *P. infestans* will be an asset for functional gene analyses. There are still hurdles to be taken, but with more dedicated effort it should be possible to effectuate the system in *P. infestans*. Taken together, I envision that insight into unique features of cellular signaling and cytoskeletal dynamics in oomycetes will greatly contribute to the general understanding of oomycetes and will expose new strategies for the design of novel, oomycete-specific control agents to mitigate damage caused by these devastating pathogens.

References

A

Adhikari, B. N., J. P. Hamilton, M. M. Zerillo, N. Tisserat, C. A. Levesque and C. R. Buell (2013). Comparative genomics reveals insight into virulence strategies of plant pathogenic oomycetes, *PLoS One* **8**: e75072. doi: 10.1371/journal.pone.0075072

Aeschlimann, S. H., F. Jonsson, J. Postberg, N. A. Stover, R. L. Petera, H. J. Lipps, . . . E. C. Swart (2014). The draft assembly of the radically organized *Stylonychia lemnae* macronuclear genome, *Genome Biol Evol* **6**: 1707-1723. doi: 10.1093/gbe/evu139

Ah-Fong, A. M., C. A. Bormann-Chung and H. S. Judelson (2008). Optimization of transgene-mediated silencing in *Phytophthora infestans* and its association with small-interfering RNAs, *Fungal Genet Biol* **45**: 1197-1205. doi: 10.1016/j.fgb.2008.05.009

Ah-Fong, A. M. and H. S. Judelson (2011). Vectors for fluorescent protein tagging in *Phytophthora*: tools for functional genomics and cell biology, *Fungal Biol* **115**: 882-890. doi: 10.1016/j.funbio.2011.07.001

Altschul, S. F., T. L. Madden, A. A. Schaffer, J. Zhang, Z. Zhang, W. Miller and D. J. Lipman (1997). Gapped BLAST and PSI-BLAST: a new generation of protein database search programs, *Nucleic Acids Res* **25**: 3389-3402.

Alvaro, C. G. and J. Thorner (2016). Heterotrimeric G Protein-coupled Receptor Signaling in Yeast Mating Pheromone Response, *J Biol Chem* **291**: 7788-7795. doi: 10.1074/jbc.R116.714980

Anantharaman, V., S. Abhiman, R. F. de Souza and L. Aravind (2011). Comparative genomics uncovers novel structural and functional features of the heterotrimeric GTPase signaling system, *Gene* **475**: 63-78. doi: 10.1016/j.gene.2010.12.001

Anderson, R. A., I. V. Boronenkov, S. D. Doughman, J. Kunz and J. C. Loijens (1999). Phosphatidylinositol phosphate kinases, a multifaceted family of signaling enzymes, *J Biol Chem* **274**: 9907-9910. doi: 10.1074/jbc.274.15.9907

Anthony, R. G., T. R. Waldin, J. A. Ray, S. W. Bright and P. J. Hussey (1998). Herbicide resistance caused by spontaneous mutation of the cytoskeletal protein tubulin, *Nature* **393**: 260-263. doi: 10.1038/30484

Aurrecoechea, C., A. Barreto, E. Y. Basenko, J. Brestelli, B. P. Brunk, S. Cade, . . . J. Zheng (2017). EuPathDB: the eukaryotic pathogen genomics database resource, *Nucleic Acids Res* **45**: D581-D591. doi: 10.1093/nar/gkw1105

Aury, J. M., O. Jaillon, L. Duret, B. Noel, C. Jubin, B. M. Porcel, . . . P. Wincker (2006). Global trends of whole-genome duplications revealed by the ciliate *Paramecium tetraurelia*, *Nature* **444**: 171-178. doi: 10.1038/nature05230

Azimzadeh, J. (2014). Exploring the evolutionary history of centrosomes, *Philos Trans R Soc Lond B Biol Sci* **369**. doi: 10.1098/rstb.2013.0453

B

Bakthavatsalam, D., D. Brazill, R. H. Gomer, L. Eichinger, F. Rivero and A. A. Noegel (2007). A G protein-coupled receptor with a lipid kinase domain is involved in cell-density sensing, *Curr Biol* **17**: 892-897. doi: 10.1016/j.cub.2007.04.029

Bakthavatsalam, D., J. M. Choe, N. E. Hanson and R. H. Gomer (2009). A *Dictyostelium* chalone uses G proteins to regulate proliferation, *BMC Biol* **7**: 44. doi: 10.1186/1741-7007-7-44

Bakthavatsalam, D., H. J. G. Meijer, A. A. Noegel and F. Govers (2006). Novel phosphatidylinositol phosphate kinases with a G-protein coupled receptor signature are shared by *Dictyostelium* and *Phytophthora*, *Trends Microbiol* **14**: 378-382. doi: 10.1016/j.tim.2006.07.006

Ballon, D. R., P. L. Flanary, D. P. Gladue, J. B. Konopka, H. G. Dohlman and J. Thorner (2006). DEP-domain-mediated regulation of GPCR signaling responses, *Cell* **126**: 1079-1093. doi: 10.1016/j.cell.2006.07.030

Bartnicki-Garcia, S. (1968). Cell wall chemistry, morphogenesis, and taxonomy of fungi, *Annu Rev Microbiol* **22**: 87-108. doi: 10.1146/annurev.mi.22.100168.000511

Baxter, L., S. Tripathy, N. Ishaque, N. Boot, A. Cabral, E. Kemen, . . . B. M. Tyler (2010). Signatures of adaptation to obligate biotrophy in the *Hyaloperonospora arabidopsidis* genome, *Science* **330**: 1549-1551. doi: 10.1126/science.1195203

Bergsma, C. A. (1845). De aardappel epidemie in Nederland in den jare 1845. Utrecht, J. G. van Terveen en zoon.

Berkeley, M. J. (1846). Observations, Botanical and Physiological, on the Potato Murrain., *The Journal of the Horticultural Society* **1**: 9 - 34.

Bhaya, D., M. Davison and R. Barrangou (2011). CRISPR-Cas systems in bacteria and archaea: versatile small RNAs for adaptive defense and regulation, *Annu Rev Genet* **45**: 273-297. doi: 10.1146/annurev-genet-110410-132430

Bjarnadottir, T. K., R. Fredriksson and H. B. Schioth (2007). The adhesion GPCRs: a unique family of G protein-coupled receptors with important roles in both central and peripheral tissues, *Cell Mol Life Sci* **64**: 2104-2119. doi: 10.1007/s00018-007-7067-1

Bjorklund, A. K., D. Ekman, S. Light, J. Frey-Skott and A. Elofsson (2005). Domain rearrangements in protein evolution, *J Mol Biol* **353**: 911-923. doi: 10.1016/j.jmb.2005.08.067

Bordoli, L., F. Kiefer, K. Arnold, P. Benkert, J. Battey and T. Schwede (2009). Protein structure homology modeling using SWISS-MODEL workspace, *Nat Protoc* **4**: 1-13. doi: 10.1038/nprot.2008.197

Bos, J. L., H. Rehmann and A. Wittinghofer (2007). GEFs and GAPs: critical elements in the control of small G proteins, *Cell* **129**: 865-877. doi: 10.1016/j.cell.2007.05.018

Bourke, P. M. A. (1964). Emergence of Potato Blight 1843-46, *Nature* **203**: 805-808. doi: 10.1038/203805a0

Breviario, D., S. Giani and L. Morello (2013). Multiple tubulins: evolutionary aspects and biological implications, *Plant J* **75**: 202-218. doi:

10.1111/tpj.12243
Brinkman, E. K., T. Chen, M. Amendola and B. van Steensel (2014). Easy quantitative assessment of genome editing by sequence trace decomposition, *Nucleic Acids Res* **42**: e168. doi: 10.1093/nar/gku936
Brown, N. A., S. Schrevens, P. v. Dijck and G. H. Goldman (2018). Fungal G-protein-coupled receptors: mediators of pathogenesis and targets for disease control, *Nature Microbiology* **3**: 402–414. doi: 10.1038/s41564-018-0127-5

C

Capella-Gutierrez, S., J. M. Silla-Martinez and T. Gabaldon (2009). trimAl: a tool for automated alignment trimming in large-scale phylogenetic analyses, *Bioinformatics* **25**: 1972-1973. doi: 10.1093/bioinformatics/btp348
Caten, C. E. and J. L. Jinks (1968). Spontaneous Variability of Single Isolates of *Phytophthora infestans*. Cultural Variation, *Can J Botany* **46**: 329-348. doi: 10.1139/b68-055
Chen, F., S. M. Pruett-Miller, Y. Huang, M. Gjoka, K. Duda, J. Taunton, . . . G. D. Davis (2011). High-frequency genome editing using ssDNA oligonucleotides with zinc-finger nucleases, *Nat Methods* **8**: 753-755. doi: 10.1038/nmeth.1653
Cho, S. W., S. Kim, J. M. Kim and J. S. Kim (2013). Targeted genome engineering in human cells with the Cas9 RNA-guided endonuclease, *Nat Biotechnol* **31**: 230-232. doi: 10.1038/nbt.2507
Cho, S. W., J. Lee, D. Carroll, J. S. Kim and J. Lee (2013). Heritable gene knockout in *Caenorhabditis elegans* by direct injection of Cas9-sgRNA ribonucleoproteins, *Genetics* **195**: 1177-1180. doi: 10.1534/genetics.113.155853
Choi, G. H., B. Chen and D. L. Nuss (1995). Virus-mediated or transgenic suppression of a G-protein alpha subunit and attenuation of fungal virulence, *Proc Natl Acad Sci USA* **92**: 305-309. doi: 10.1073/pnas.92.1.305
Clapham, D. E. and E. J. Neer (1997). G Protein $\beta\gamma$ Subunits, *Annu Rev Pharmacol Toxicol* **37**: 167-203.
Clarke, M., A. J. Lohan, B. Liu, I. Lagkouvardos, S. Roy, N. Zafar, . . . B. J. Loftus (2013). Genome of *Acanthamoeba castellanii* highlights extensive lateral gene transfer and early evolution of tyrosine kinase signaling, *Genome Biol* **14**: R11. doi: 10.1186/gb-2013-14-2-r11
Croft, W., C. Hill, E. McCann, M. Bond, M. Esparza-Franco, J. Bennett, . . . G. Ladds (2013). A physiologically required G protein-coupled receptor (GPCR)-regulator of G protein signaling (RGS) interaction that compartmentalizes RGS activity, *J Biol Chem* **288**: 27327-27342. doi: 10.1074/jbc.M113.497826
Curtis, B. A., G. Tanifuji, F. Burki, A. Gruber, M. Irimia, S. Maruyama, . . . J. M. Archibald (2012). Algal genomes reveal evolutionary mosaicism and the fate of nucleomorphs, *Nature* **492**: 59-65. doi: 10.1038/nature11681

D

de Bary, A. (1876). Researches into the nature of the potato-fungus, *Phytophthora infestans*, *J. R. Agric. Soc. Engl.* **12**: 239 - 269.
de Mendoza, A., A. Sebe-Pedros and I. Ruiz-Trillo (2014). The evolution of the GPCR signaling system in eukaryotes: modularity, conservation, and the transition to metazoan multicellularity, *Genome Biol Evol* **6**: 606-619. doi: 10.1093/gbe/evu038
de Souza, C. P. and S. A. Osmani (2007). Mitosis, not just open or closed, *Eukaryot Cell* **6**: 1521-1527. doi: 10.1128/EC.00178-07
Desai, A. and T. J. Mitchison (1997). Microtubule polymerization dynamics, *Annu Rev Cell Dev Biol* **13**: 83-117. doi: 10.1146/annurev.cellbio.13.1.83
Dick, M. (2001). Straminipilous fungi: systematics of the Peronosporomycetes including accounts of the marine straminipilous protists, the plasmodiophorids and similar organisms, Kluwer Academic Publishers.
Doench, J. G., E. Hartenian, D. B. Graham, Z. Tothova, M. Hegde, I. Smith, . . . D. E. Root (2014). Rational design of highly active sgRNAs for CRISPR-Cas9-mediated gene inactivation, *Nat Biotechnol* **32**: 1262-1267. doi: 10.1038/nbt.3026
Dong, W., M. Latijnhouwers, R. H. Jiang, H. J. Meijer and F. Govers (2004). Downstream targets of the *Phytophthora infestans* Galpha subunit PiGPA1 revealed by cDNA-AFLP, *Mol Plant Pathol* **5**: 483-494. doi: 10.1111/j.1364-3703.2004.00247.x
Dowson, W. J. and D. R. Jones (1951). Bacterial Wet Rot of Potato Tubers Following *Phytophthora infestans*, *Annals of Applied Biology* **38**: 231-236. doi: 10.1111/j.1744-7348.1951.tb07799.x
Du, Y., R. Weide, Z. Zhao, P. Msimuko, F. Govers and K. Bouwmeester (2018). RXLR effector diversity in Phytophthora infestans isolates determines recognition by potato resistance proteins; the case study AVR1 and R1, *Studies in Mycology*. doi: 10.1016/j.simyco.2018.01.003
Dunn, R. (2017). An Island Like Ours. Never Out of Season: How Having the Food We Want When We Want It Threatens Our Food Supply and Our Future, Little, Brown and Company.
Dupre, D. J., M. Robitaille, R. V. Rebois and T. E. Hebert (2009). The role of Gbetagamma subunits in the organization, assembly, and function of GPCR signaling complexes, *Annu Rev Pharmacol Toxicol* **49**: 31-56. doi: 10.1146/annurev-pharmtox-061008-103038

E

Edvardsen, R. B., S. Leininger, L. Kleppe, K. O. Skaftnesmo and A. Wargelius (2014). Targeted mutagenesis in Atlantic salmon (*Salmo salar L.*) using the CRISPR/Cas9 system induces complete knockout individuals in the F0 generation, *PLoS One* **9**: e108622. doi: 10.1371/journal.pone.0108622
Edzuka, T., L. Yamada, K. Kanamaru, H. Sawada and G. Goshima (2014). Identification of the augmin complex in the filamentous fungus *Aspergillus nidulans*, *PLoS One* **9**: e101471. doi: 10.1371/journal.pone.0101471
Eichinger, L., J. A. Pachebat, G. Glockner, M. A. Rajandream, R. Sucgang, M. Berriman, . . . A. Kuspa (2005). The genome of the social amoeba *Dictyostelium discoideum*, *Nature* **435**: 43-57. doi: 10.1038/nature03481
Eisen, J. A., R. S. Coyne, M. Wu, D. Wu, M. Thiagarajan, J. R. Wortman, . . . E. Orias (2006). Macronuclear genome sequence of the ciliate *Tetrahymena thermophila*, a model eukaryote, *PLoS Biol* **4**: e286. doi: 10.1371/journal.pbio.0040286
Erwin, D. C. and O. K. Ribeiro (1996). *Phytophthora* diseases worldwide. St. Paul, Minnesota, The American Phytopathological Society.
Etienne-Manneville, S. (2010). From signaling pathways to microtubule dynamics: the key players, *Curr Opin Cell Biol* **22**: 104-111. doi: 10.1016/j.ceb.2009.11.008

F

Fairclough, S. R., Z. Chen, E. Kramer, Q. Zeng, S. Young, H. M. Robertson, . . . N. King (2013). Premetazoan genome evolution and the

regulation of cell differentiation in the choanoflagellate *Salpingoeca rosetta*, *Genome Biol* **14**: R15. doi: 10.1186/gb-2013-14-2-r15
Fang, Y., H. S. Jang, G. W. Watson, D. P. Wellappili and B. M. Tyler (2017). Distinctive Nuclear Localization Signals in the Oomycete *Phytophthora sojae*, *Front Microbiol* **8**: 10. doi: 10.3389/fmicb.2017.00010
Fang, Y. and B. M. Tyler (2016). Efficient disruption and replacement of an effector gene in the oomycete *Phytophthora sojae* using CRISPR/Cas9, *Mol Plant Pathol* **17**: 127-139. doi: 10.1111/mpp.12318
Feierler, J., M. Wirth, B. Welte, S. Schussler, M. Jochum and A. Faussner (2011). Helix 8 plays a crucial role in bradykinin B(2) receptor trafficking and signaling, *J Biol Chem* **286**: 43282-43293. doi: 10.1074/jbc.M111.256909
Ferguson, S. S. (2001). Evolving concepts in G protein-coupled receptor endocytosis: the role in receptor desensitization and signaling, *Pharmacol Rev* **53**: 1-24.
Finn, R. D., J. Clements, W. Arndt, B. L. Miller, T. J. Wheeler, F. Schreiber, . . . S. R. Eddy (2015). HMMER web server: 2015 update, *Nucleic Acids Res* **43**: W30-38. doi: 10.1093/nar/gkv397
Fredriksson, R. and H. B. Schioth (2005). The repertoire of G-protein-coupled receptors in fully sequenced genomes, *Mol Pharmacol* **67**: 1414-1425. doi: 10.1124/mol.104.009001
Fritz-Laylin, L. K., S. E. Prochnik, M. L. Ginger, J. B. Dacks, M. L. Carpenter, M. C. Field, . . . S. C. Dawson (2010). The genome of *Naegleria gruberi* illuminates early eukaryotic versatility, *Cell* **140**: 631-642. doi: 10.1016/j.cell.2010.01.032
Fry, W. (2008). *Phytophthora infestans*: the plant (and R gene) destroyer, *Mol Plant Pathol* **9**: 385-402. doi: 10.1111/j.1364-3703.2007.00465.x

G

Gamboa-Melendez, H., A. I. Huerta and H. S. Judelson (2013). bZIP transcription factors in the oomycete *Phytophthora infestans* with novel DNA-binding domains are involved in defense against oxidative stress, *Eukaryot Cell* **12**: 1403-1412. doi: 10.1128/EC.00141-13
Gerald, N., B. Mahajan and S. Kumar (2011). Mitosis in the human malaria parasite Plasmodium falciparum, *Eukaryot Cell* **10**: 474-482. doi: 10.1128/EC.00314-10
Gibeaux, R., A. Z. Politi, P. Philippsen and F. Nedelec (2017). Mechanism of nuclear movements in a multinucleated cell, *Mol Biol Cell* **28**: 645-660. doi: 10.1091/mbc.E16-11-0806
Gladfelter, A. S. (2006). Nuclear anarchy: asynchronous mitosis in multinucleated fungal hyphae, *Curr Opin Microbiol* **9**: 547-552. doi: 10.1016/j.mib.2006.09.002
Glockner, G., N. Hulsmann, M. Schleicher, A. A. Noegel, L. Eichinger, C. Gallinger, . . . M. Schliwa (2014). The genome of the foraminiferan *Reticulomyxa filosa*, *Curr Biol* **24**: 11-18. doi: 10.1016/j.cub.2013.11.027
Gobler, C. J., D. L. Berry, S. T. Dyhrman, S. W. Wilhelm, A. Salamov, A. V. Lobanov, . . . I. V. Grigoriev (2011). Niche of harmful alga Aureococcus anophagefferens revealed through ecogenomics, *Proc Natl Acad Sci U S A* **108**: 4352-4357. doi: 10.1073/pnas.1016106108
Goldberg, J. M., G. Manning, A. Liu, P. Fey, K. E. Pilcher, Y. Xu and J. L. Smith (2006). The *Dictyostelium* kinome-analysis of the protein kinases from a simple model organism, *PLoS Genet* **2**: e38. doi: 10.1371/journal.pgen.0020038
Goodson, H. V., J. S. Dzurisin and P. Wadsworth (2010). Methods for expressing and analyzing GFP-tubulin and GFP-microtubule-associated proteins, *Cold Spring Harb Protoc* **2010**: pdb top85. doi: 10.1101/pdb.top85
Goshima, G., M. Mayer, N. Zhang, N. Stuurman and R. D. Vale (2008). Augmin: a protein complex required for centrosome-independent microtubule generation within the spindle, *J Cell Biol* **181**: 421-429. doi: 10.1083/jcb.200711053
Govers, F. and M. Gijzen (2006). *Phytophthora* genomics: the plant destroyers' genome decoded, *Mol Plant Microbe Interact* **19**: 1295-1301. doi: 10.1094/MPMI-19-1295
Grahl, N., E. G. Demers, A. W. Crocker and D. A. Hogan (2017). Use of RNA-Protein Complexes for Genome Editing in Non-albicans *Candida* Species, *mSphere* **2**. doi: 10.1128/mSphere.00218-17
Grunwald, N. J., E. M. Goss and C. M. Press (2008). *Phytophthora ramorum*: a pathogen with a remarkably wide host range causing sudden oak death on oaks and ramorum blight on woody ornamentals, *Mol Plant Pathol* **9**: 729-740. doi: 10.1111/j.1364-3703.2008.00500.x
Gumtow, R., D. Wu, J. Uchida and M. Tian (2017). A *Phytophthora palmivora* extracellular cystatin-like protease inhibitor targets papain to contribute to virulence on papaya, *Mol Plant Microbe Interact*. doi: 10.1094/MPMI-06-17-0131-FI

H

Guo, T., X. W. Wang, K. Shan, W. Sun and L. Y. Guo (2017). The Loricrin-Like Protein (LLP) of Phytophthora infestans Is Required for Oospore Formation and Plant Infection, *Front Plant Sci* **8**: 142. doi: 10.3389/fpls.2017.00142
Haas, B. J., S. Kamoun, M. C. Zody, R. H. Jiang, R. E. Handsaker, L. M. Cano, . . . C. Nusbaum (2009). Genome sequence and analysis of the Irish potato famine pathogen *Phytophthora infestans*, *Nature* **461**: 393-398. doi: 10.1038/nature08358
Hardham, A. R. (2005). *Phytophthora cinnamomi*, *Mol Plant Pathol* **6**: 589-604. doi: 10.1111/j.1364-3703.2005.00308.x
Harting, P. (1846). Recherces sur la nature et les causes de la maladie des pommes de terre en 1845, *Nieuwe verhandelingen der Eerste Klasse van het Koninklijk-Nederlandsche Instituut van Wetenschappen, Letterkunde en Schoone Kunsten te Amsterdam* **12**: 203 - 297.
Harutyunyan, S. R., Z. Zhao, T. Hartog, K. Bouwmeester, A. J. Minnaard, B. L. Feringa and F. Govers (2008). Biologically active *Phytophthora* mating hormone prepared by catalytic asymmetric total synthesis, *Proc Natl Acad Sci USA* **105**: 8507-8512. doi: 10.1073/pnas.0709289105
Haverkort, A. J., P. M. Boonekamp, R. Hutten, E. Jacobsen, L. A. P. Lotz, G. J. T. Kessel, . . . E. A. G. van der Vossen (2008). Societal Costs of Late Blight in Potato and Prospects of Durable Resistance Through Cisgenic Modification, *Potato Research* **51**: 47-57. doi: 10.1007/s11540-008-9089-y
Heath, I. B. (1980). Variant mitoses in lower eukaryotes: indicators of the evolution of mitosis, *Int Rev Cytol* **64**: 1-80.
Heath, I. B. and A. D. Greenwood (1970). Centriole Replication and Nuclear Division in Saprolegnia, *Journal of General Microbiology* **62**: 139-148. doi: 10.1099/00221287-62-2-139
Heath, I. B. and D. Greenwood (1968). Electron Microscopic Observations of Dividing Somatic Nuclei in *Saprolegnia*, *J Gen Microbiol* **53**: 287-289.
Heath, I. B. and S. G. W. Kaminskyj (1989). The organization of tip-growth-related organelles and microtubules revealed by quantitative analysis of freeze-substituted oomycete hyphae, *J Cell Sci*.

Heidel, A. J., H. M. Lawal, M. Felder, C. Schilde, N. R. Helps, B. Tunggal, . . . G. Glockner (2011). Phylogeny-wide analysis of social amoeba genomes highlights ancient origins for complex intercellular communication, *Genome Res* **21**: 1882-1891. doi: 10.1101/gr.121137.111

Higgins, J. and P. Casey (1996). The role of prenylation in G-protein assembly and function, *Cell Signal* **8**: 433-437. doi: 10.1016/s0898-6568(96)00071-x

Hillenbrand, M., C. Schori, J. Schoppe and A. Pluckthun (2015). Comprehensive analysis of heterotrimeric G-protein complex diversity and their interactions with GPCRs in solution, *Proc Natl Acad Sci USA* **112**: E1181-1190. doi: 10.1073/pnas.1417573112

Hirokawa, T., S. Boon-Chieng and S. Mitaku (1998). SOSUI: classification and secondary structure prediction system for membrane proteins, *Bioinformatics* **14**: 378-379.

Hirschman, J. E., G. S. De Zutter, W. F. Simonds and D. D. Jenness (1997). The G$\beta\gamma$ Complex of the Yeast Pheromone Response Pathway, *J Biol Chem* **272**: 240-248. doi: 10.1074/jbc.272.1.240

Hirst, D. J., T. H. Lee, L. K. Pattenden, W. G. Thomas and M. I. Aguilar (2015). Helix 8 of the angiotensin- II type 1A receptor interacts with phosphatidylinositol phosphates and modulates membrane insertion, *Sci Rep* **5**: 9972. doi: 10.1038/srep09972

Hoffman, C. S. (2005). Except in every detail: comparing and contrasting G-protein signaling in *Saccharomyces cerevisiae* and *Schizosaccharomyces pombe*, *Eukaryot Cell* **4**: 495-503. doi: 10.1128/EC.4.3.495-503.2005

Hovde, B. T., C. R. Deodato, H. M. Hunsperger, S. A. Ryken, W. Yost, R. K. Jha, . . . R. A. Cattolico (2015). Genome Sequence and Transcriptome Analyses of *Chrysochromulina tobin*: Metabolic Tools for Enhanced Algal Fitness in the Prominent Order Prymnesiales (Haptophyceae), *PLoS Genet* **11**: e1005469. doi: 10.1371/journal.pgen.1005469

Hsu, P. D., D. A. Scott, J. A. Weinstein, F. A. Ran, S. Konermann, V. Agarwala, . . . F. Zhang (2013). DNA targeting specificity of RNA-guided Cas9 nucleases, *Nat Biotechnol* **31**: 827-832. doi: 10.1038/nbt.2647

Hua, C., H. J. G. Meijer, J. de Keijzer, W. Zhao, Y. Wang and F. Govers (2013). GK4, a G-protein-coupled receptor with a phosphatidylinositol phosphate kinase domain in *Phytophthora infestans*, is involved in sporangia development and virulence, *Mol Microbiol* **88**: 352-370. doi: 10.1111/mmi.12190

Hua, C., Y. Wang, X. Zheng, D. Dou, Z. Zhang, F. Govers and Y. Wang (2008). A *Phytophthora sojae* G-protein alpha subunit is involved in chemotaxis to soybean isoflavones, *Eukaryot Cell* **7**: 2133-2140. doi: 10.1128/EC.00286-08

Hugdahl, J. D. and L. C. Morejohn (1993). Rapid and Reversible High-Affinity Binding of the Dinitroaniline Herbicide Oryzalin to Tubulin from Zea mays L, *Plant Physiology* **102**: 725-740. doi: 10.1104/pp.102.3.725

Huynh, J., W. G. Thomas, M. I. Aguilar and L. K. Pattenden (2009). Role of helix 8 in G protein-coupled receptors based on structure-function studies on the type 1 angiotensin receptor, *Mol Cell Endocrinol* **302**: 118-127. doi: 10.1016/j.mce.2009.01.002

I

Insel, P. A., A. Snead, F. Murray, L. Zhang, H. Yokouchi, T. Katakia, . . . A. Wilderman (2012). GPCR expression in tissues and cells: Are the optimal receptors being used as drug targets?, *British Journal of Pharmacology* **165**: 1613-1616. doi: 10.1111/j.1476-5381.2011.01434.x

Islam, T., T. Ito and S. Tahara (2003). Host-specific plant signal and G-protein activator, mastoparan, trigger differentiation of zoospores of the phytopathogenic oomycete Aphanomyces cochlioides, *Plant and Soil* **255**: 131-142. doi: 10.1023/a:1026114731718

Itagaki, T. and S. Ogawa (1994). Mitosis in the Coenocytic Green-Alga *Boergesenia forbesii* (Harvey) Feldmann (Siphonocladales, Ulvophyceae), *Journal of Plant Research* **107**: 9-15. doi: 10.1007/Bf02344524

J

Jiang, R. H., I. de Bruijn, B. J. Haas, R. Belmonte, L. Lobach, J. Christie, . . . P. van West (2013). Distinctive expansion of potential virulence genes in the genome of the oomycete fish pathogen *Saprolegnia parasitica*, *PLoS Genet* **9**: e1003272. doi: 10.1371/journal.pgen.1003272

Jiang, W., A. J. Brueggeman, K. M. Horken, T. M. Plucinak and D. P. Weeks (2014). Successful transient expression of Cas9 and single guide RNA genes in *Chlamydomonas reinhardtii*, *Eukaryot Cell* **13**: 1465-1469. doi: 10.1128/EC.00213-14

Jinek, M., K. Chylinski, I. Fonfara, M. Hauer, J. A. Doudna and E. Charpentier (2012). A programmable dual-RNA-guided DNA endonuclease in adaptive bacterial immunity, *Science* **337**: 816-821. doi: 10.1126/science.1225829

Jones, P., D. Binns, H. Y. Chang, M. Fraser, W. Li, C. McAnulla, . . . S. Hunter (2014). InterProScan 5: genome-scale protein function classification, *Bioinformatics* **30**: 1236-1240. doi: 10.1093/bioinformatics/btu031

Judelson, H. S. (1997). The genetics and biology of *Phytophthora infestans*: modern approaches to a historical challenge, *Fungal Genet Biol* **22**: 65-76. doi: 10.1006/fgbi.1997.1006

Judelson, H. S. and A. M. Ah-Fong (2010). The kinome of *Phytophthora infestans* reveals oomycete-specific innovations and links to other taxonomic groups, *BMC Genomics* **11**: 700. doi: 10.1186/1471-2164-11-700

Judelson, H. S. and F. A. Blanco (2005). The spores of *Phytophthora*: weapons of the plant destroyer, *Nat Rev Microbiol* **3**: 47-58. doi: 10.1038/nrmicro1064

Judelson, H. S., J. Shrivastava and J. Manson (2012). Decay of genes encoding the oomycete flagellar proteome in the downy mildew Hyaloperonospora arabidopsidis, *PLoS One* **7**: e47624. doi: 10.1371/journal.pone.0047624

Judelson, H. S., B. M. Tyler and R. W. Michelmore (1991). Transformation of the oomycete pathogen, Phytophthora infestans, *Mol Plant Microbe Interact* **4**: 602-607.

K

Kall, L., A. Krogh and E. L. Sonnhammer (2004). A combined transmembrane topology and signal peptide prediction method, *J Mol Biol* **338**: 1027-1036. doi: 10.1016/j.jmb.2004.03.016

Kamasaki, T., E. O'Toole, S. Kita, M. Osumi, J. Usukura, J. R. McIntosh and G. Goshima (2013). Augmin-dependent microtubule nucleation at microtubule walls in the spindle, *J Cell Biol* **202**: 25-33. doi: 10.1083/jcb.201304031

Kamoun, S., O. Furzer, J. D. Jones, H. S. Judelson, G. S. Ali, R. J. Dalio, . . . F. Govers (2015). The Top 10 oomycete pathogens in molecular plant pathology, *Mol Plant Pathol* **16**: 413-434. doi: 10.1111/mpp.12190

Kasahara, S., P. Wang and D. L. Nuss (2000). Identification of bdm-1, a gene involved in G protein beta-subunit function and alpha-subunit accumulation, *Proc Natl Acad Sci USA* **97**: 412-417. doi: 10.1073/pnas.97.1.412

Katoh, K. and D. M. Standley (2013). MAFFT multiple sequence alignment software version 7: improvements in performance and usability, *Mol Biol Evol* **30**: 772-780. doi: 10.1093/molbev/mst010
Katsaros, C., D. Karyophyllis and B. Galatis (2006). Cytoskeleton and morphogenesis in brown algae, *Ann Bot* **97**: 679-693. doi: 10.1093/aob/mcl023
Kay, J., H. J. G. Meijer, A. ten Have and J. A. van Kan (2011). The aspartic proteinase family of three *Phytophthora* species, *BMC Genomics* **12**: 254. doi: 10.1186/1471-2164-12-254
Kearse, M., R. Moir, A. Wilson, S. Stones-Havas, M. Cheung, S. Sturrock, . . . A. Drummond (2012). Geneious Basic: an integrated and extendable desktop software platform for the organization and analysis of sequence data, *Bioinformatics* **28**: 1647-1649. doi: 10.1093/bioinformatics/bts199
Keeling, P. J., G. Burger, D. G. Durnford, B. F. Lang, R. W. Lee, R. E. Pearlman, . . . M. W. Gray (2005). The tree of eukaryotes, *Trends Ecol Evol* **20**: 670-676. doi: 10.1016/j.tree.2005.09.005
Keeling, P. J. and J. D. Palmer (2008). Horizontal gene transfer in eukaryotic evolution, *Nat Rev Genet* **9**: 605-618. doi: 10.1038/nrg2386
Kelley, L. A., S. Mezulis, C. M. Yates, M. N. Wass and M. J. Sternberg (2015). The Phyre2 web portal for protein modeling, prediction and analysis, *Nat Protoc* **10**: 845-858. doi: 10.1038/nprot.2015.053
Kemen, E., A. Gardiner, T. Schultz-Larsen, A. C. Kemen, A. L. Balmuth, A. Robert-Seilaniantz, . . . J. D. Jones (2011). Gene gain and loss during evolution of obligate parasitism in the white rust pathogen of *Arabidopsis thaliana*, *PLoS Biol* **9**: e1001094. doi: 10.1371/journal.pbio.1001094
Khew, K. and G. Zentmyer (1973). Chemotactic response of zoospores of five species of *Phytophthora*, *Phytopathology* **63**: 1-17.
Kim, S., D. Kim, S. W. Cho, J. Kim and J. S. Kim (2014). Highly efficient RNA-guided genome editing in human cells via delivery of purified Cas9 ribonucleoproteins, *Genome Res* **24**: 1012-1019. doi: 10.1101/gr.171322.113
King, N., M. J. Westbrook, S. L. Young, A. Kuo, M. Abedin, J. Chapman, . . . D. Rokhsar (2008). The genome of the choanoflagellate *Monosiga brevicollis* and the origin of metazoans, *Nature* **451**: 783-788. doi: 10.1038/nature06617
Kleinstiver, B. P., S. Q. Tsai, M. S. Prew, N. T. Nguyen, M. M. Welch, J. M. Lopez, . . . J. K. Joung (2016). Genome-wide specificities of CRISPR-Cas Cpf1 nucleases in human cells, *Nat Biotechnol* **34**: 869-874. doi: 10.1038/nbt.3620
Kollmar, M. (2016). Fine-Tuning Motile Cilia and Flagella: Evolution of the Dynein Motor Proteins from Plants to Humans at High Resolution, *Mol Biol Evol* **33**: 3249-3267. doi: 10.1093/molbev/msw213
Koonin, E. V. (2010). The origin and early evolution of eukaryotes in the light of phylogenomics, *Genome Biol* **11**: 209. doi: 10.1186/gb-2010-11-5-209
Koonin, E. V. (2010). Preview. The incredible expanding ancestor of eukaryotes, *Cell* **140**: 606-608. doi: 10.1016/j.cell.2010.02.022
Kots, K., H. J. G. Meijer, K. Bouwmeester, F. Govers and T. Ketelaar (2016). Filamentous actin accumulates during plant cell penetration and cell wall plug formation in Phytophthora infestans, *Cell Mol Life Sci* **74**: 909-920. doi: 10.1007/s00018-016-2383-y
Koumandou, V. L., B. Wickstead, M. L. Ginger, M. van der Giezen, J. B. Dacks and M. C. Field (2013). Molecular paleontology and complexity in the last eukaryotic common ancestor, *Crit Rev Biochem Mol Biol* **48**: 373-396. doi: 10.3109/10409238.2013.821444
Kraakman, L., K. Lemaire, P. S. Ma, A. W. R. H. Teunissen, M. C. V. Donaton, P. Van Dijck, . . . J. M. Thevelein (1999). A *Saccharomyces cerevisiae* G-protein coupled receptor, Gpr1, is specifically required for glucose activation of the cAMP pathway during the transition to growth on glucose, *Mol Microbiol* **32**: 1002-1012. doi: 10.1046/j.1365-2958.1999.01413.x
Krogh, A., B. Larsson, G. von Heijne and E. L. Sonnhammer (2001). Predicting transmembrane protein topology with a hidden Markov model: application to complete genomes, *J Mol Biol* **305**: 567-580. doi: 10.1006/jmbi.2000.4315
Kroon, L. P., H. Brouwer, A. W. de Cock and F. Govers (2012). The genus Phytophthora anno 2012, *Phytopathology* **102**: 348-364. doi: 10.1094/PHYTO-01-11-0025
Krtkova, J., M. Benakova and K. Schwarzerova (2016). Multifunctional Microtubule-Associated Proteins in Plants, *Front Plant Sci* **7**: 474. doi: 10.3389/fpls.2016.00474
Krystofova, S. and K. A. Borkovich (2005). The heterotrimeric G-protein subunits GNG-1 and GNB-1 form a Gbetagamma dimer required for normal female fertility, asexual development, and galpha protein levels in *Neurospora crassa*, *Eukaryot Cell* **4**: 365-378. doi: 10.1128/EC.4.2.365-378.2005
Kubiseski, T. J., Y. M. Chook, W. E. Parris, M. Rozakis-Adcock and T. Pawson (1997). High affinity binding of the pleckstrin homology domain of mSos1 to phosphatidylinositol (4,5)-bisphosphate, *J Biol Chem* **272**: 1799-1804.
Kunz, J., M. P. Wilson, M. Kisseleva, J. H. Hurley, P. W. Majerus and R. A. Anderson (2000). The activation loop of phosphatidylinositol phosphate kinases determines signaling specificity, *Mol Cell* **5**: 1-11. doi: 10.1016/S1097-2765(00)80398-6
Kupper, F. C., I. Maier, D. G. Muller, S. L. D. Goer and L. Guillou (2006). Phylogenetic affinities of two eukaryotic pathogens of marine macroalgae, *Eurychasma dicksonii* (Wright) Magnus and *Chytridium polysiphoniae* Cohn, *Cryptogamie Algologie* **27**: 165-184.

L

Ladds, G., A. Goddard and J. Davey (2005). Functional analysis of heterologous GPCR signalling pathways in yeast, *Trends Biotechnol* **23**: 367-373. doi: 10.1016/j.tibtech.2005.05.007
Lamour, K. H., J. Mudge, D. Gobena, O. P. Hurtado-Gonzales, J. Schmutz, A. Kuo, . . . S. F. Kingsmore (2012). Genome sequencing and mapping reveal loss of heterozygosity as a mechanism for rapid adaptation in the vegetable pathogen *Phytophthora capsici*, *Mol Plant Microbe Interact* **25**: 1350-1360. doi: 10.1094/MPMI-02-12-0028-R
Lander, E. S. (2016). The Heroes of CRISPR, *Cell* **164**: 18-28. doi: 10.1016/j.cell.2015.12.041
Lange, A., R. E. Mills, C. J. Lange, M. Stewart, S. E. Devine and A. H. Corbett (2007). Classical nuclear localization signals: definition, function, and interaction with importin alpha, *J Biol Chem* **282**: 5101-5105. doi: 10.1074/jbc.R600026200
Latijnhouwers, M. and F. Govers (2003). A *Phytophthora infestans* G-protein beta subunit is involved in sporangium formation, *Eukaryot Cell* **2**: 971-977. doi: 10.1128/EC.2.5.971–977.2003
Latijnhouwers, M., W. Ligterink, V. G. A. A. Vleeshouwers, P. van West and F. Govers (2004). A Gα subunit controls zoospore motility and virulence in the potato late blight pathogen *Phytophthora infestans*, *Mol Microbiol* **51**: 925-936. doi: 10.1046/j.1365-2958.2003.03893.x
Latijnhouwers, M., T. Munnik and F. Govers (2002). Phospholipase D in *Phytophthora infestans* and its role in zoospore encystment, *Mol Plant Microbe Interact* **15**: 939-946. doi: 10.1094/MPMI.2002.15.9.939

Lawo, S., M. Bashkurov, M. Mullin, M. G. Ferreria, R. Kittler, B. Habermann, . . . L. Pelletier (2009). HAUS, the 8-subunit human Augmin complex, regulates centrosome and spindle integrity, *Curr Biol* **19**: 816-826. doi: 10.1016/j.cub.2009.04.033

Laxalt, A. M., M. Latijnhouwers, M. van Hulten and F. Govers (2002). Differential expression of G protein alpha and beta subunit genes during development of *Phytophthora infestans*, *Fungal Genet Biol* **36**: 137-146. doi: 10.1016/S1087-1845(02)00012-9

Le Blanc, C., F. Zhang, J. Mendez, Y. Lozano, K. Chatpar, V. Irish and Y. Jacob (2017). Increased efficiency of targeted mutagenesis by CRISPR/Cas9 in plants using heat stress, *Plant J*. doi: 10.1111/tpj.13782

Leondaritis, G., J. Siokos, I. Skaripa and D. Galanopoulou (2013). Genome-wide analysis of the phosphoinositide kinome from two ciliates reveals novel evolutionary links for phosphoinositide kinases in eukaryotic cells, *PLoS One* **8**: e78848. doi: 10.1371/journal.pone.0078848

Letunic, I. and P. Bork (2016). Interactive tree of life (iTOL) v3: an online tool for the display and annotation of phylogenetic and other trees, *Nucleic Acids Res* **44**: W242-245. doi: 10.1093/nar/gkw290

Letunic, I., T. Doerks and P. Bork (2015). SMART: recent updates, new developments and status in 2015, *Nucleic Acids Res* **43**: D257-260. doi: 10.1093/nar/gku949

Lévesque, C. A. (2011). Fifty years of oomycetes—from consolidation to evolutionary and genomic exploration, *Fungal Divers* **50**: 35-46. doi: 10.1007/s13225-011-0128-7

Li, L., S. J. Wright, S. Krystofova, G. Park and K. A. Borkovich (2007). Heterotrimeric G protein signaling in filamentous fungi, *Annu Rev Microbiol* **61**: 423-452. doi: 10.1146/annurev.micro.61.080706.093432

Liang, S., Z. Wang, P. Liu and D. Li (2006). A Gγ subunit promoter T-DNA insertion mutant—A1-412 of *Magnaporthe grisea* is defective in appressorium formation, penetration and pathogenicity, *Chin Sci Bull* **51**: 2214-2218. doi: 10.1007/s11434-006-2117-x

Libert, A.-M. (1845). Journal de Liège.

Links, M. G., E. Holub, R. H. Jiang, A. G. Sharpe, D. Hegedus, E. Beynon, . . . M. H. Borhan (2011). De novo sequence assembly of *Albugo candida* reveals a small genome relative to other biotrophic oomycetes, *BMC Genomics* **12**: 503. doi: 10.1186/1471-2164-12-503

Liu, H., S. Aris-Brosou, I. Probert and C. de Vargas (2010). A time line of the environmental genetics of the haptophytes, *Mol Biol Evol* **27**: 161-176. doi: 10.1093/molbev/msp222

Liu, S. and R. A. Dean (1997). G protein alpha subunit genes control growth, development, and pathogenicity of *Magnaporthe grisea*, *Mol Plant Microbe Interact* **10**: 1075-1086. doi: 10.1094/MPMI.1997.10.9.1075

Livak, K. J. and T. D. Schmittgen (2001). Analysis of relative gene expression data using real-time quantitative PCR and the 2(-Delta Delta C(T)) Method, *Methods* **25**: 402-408. doi: 10.1006/meth.2001.1262

Livingstone, C. D. and G. J. Barton (1993). Protein sequence alignments: a strategy for the hierarchical analysis of residue conservation, *Comput Appl Biosci* **9**: 745-756.

Lu, S., L. Chen, K. Tao, N. Sun, Y. Wu, X. Lu, . . . D. Dou (2013). Intracellular and extracellular phosphatidylinositol 3-phosphate produced by Phytophthora species is important for infection, *Mol Plant* **6**: 1592-1604. doi: 10.1093/mp/sst047

M

Ma, Z., L. Zhu, T. Song, Y. Wang, Q. Zhang, Y. Xia, . . . Y. Wang (2017). A paralogous decoy protects *Phytophthora sojae* apoplastic effector PsXEG1 from a host inhibitor, *Science* **355**: 710-714. doi: 10.1126/science.aai7919

Maday, S., A. E. Twelvetrees, A. J. Moughamian and E. L. Holzbaur (2014). Axonal transport: cargo-specific mechanisms of motility and regulation, *Neuron* **84**: 292-309. doi: 10.1016/j.neuron.2014.10.019

Manning, G., D. S. Reiner, T. Lauwaet, M. Dacre, A. Smith, Y. Zhai, . . . F. D. Gillin (2011). The minimal kinome of Giardia lamblia illuminates early kinase evolution and unique parasite biology, *Genome Biol* **12**: R66. doi: 10.1186/gb-2011-12-7-r66

McCarthy, C. G. P. and D. A. Fitzpatrick (2017). Phylogenomic Reconstruction of the Oomycete Phylogeny Derived from 37 Genomes, *mSphere* **2**. doi: 10.1128/mSphere.00095-17

McHau, G. R. A. and M. D. Coffey (1994). Isozyme diversity in *Phytophthora palmivora*: evidence for a southeast Asian centre of origin, *Mycological Research* **98**: 1035-1043. doi: 10.1016/s0953-7562(09)80430-9

Meijer, H. J. G. and F. Govers (2006). Genomewide analysis of phospholipid signaling genes in *Phytophthora* spp.: novelties and a missing link, *Mol Plant Microbe Interact* **19**: 1337-1347. doi: 10.1094/MPMI-19-1337

Meijer, H. J. G., H. H. Hassen and F. Govers (2011). Phytophthora infestans has a plethora of phospholipase D enzymes including a subclass that has extracellular activity, *PLoS One* **6**: e17767. doi: 10.1371/journal.pone.0017767

Meijer, H. J. G., C. Hua, K. Kots, T. Ketelaar and F. Govers (2014). Actin dynamics in Phytophthora infestans; rapidly reorganizing cables and immobile, long-lived plaques, *Cell Microbiol* **16**: 948-961. doi: 10.1111/cmi.12254

Miller, M. A., W. Pfeiffer and T. Schwartz (2010). Creating the CIPRES Science Gateway for inference of large phylogenetic trees, 1-8. doi: 10.1109/gce.2010.5676129

Montagne, J. F. C. (1845). Note sur la maladie qui ravage les pommes de terre et caracteres du Botrytis infestans, *Memoirs of the Institute of France* **609**: 98–101, 312–313. doi:

Morren, C. (1844). Notice sur le Botrytis devastateur ou le champignon des pommes de terre, *Ann. Soc. R. Agric. Botanique Gand* **1**: 287-292.

Mulligan, T., H. Blaser, E. Raz and S. A. Farber (2010). Prenylation-deficient G protein gamma subunits disrupt GPCR signaling in the zebrafish, *Cell Signal* **22**: 221-233. doi: 10.1016/j.cellsig.2009.09.017

N

Neves, S. R., P. T. Ram and R. Iyengar (2002). G protein pathways, *Science* **296**: 1636-1639. doi: 10.1126/science.1071550

Nishimura, M., G. Park and J.-R. Xu (2003). The G-beta subunit MGB1 is involved in regulating multiple steps of infection-related morphogenesis in *Magnaporthe grisea*, *Mol Microbiol* **50**: 231-243. doi: 10.1046/j.1365-2958.2003.03676.x

O

Odronitz, F. and M. Kollmar (2006). Pfarao: a web application for protein family analysis customized for cytoskeletal and motor proteins (CyMoBase), *BMC Genomics* **7**: 300. doi: 10.1186/1471-2164-7-300

Oldham, W. M. and H. E. Hamm (2006). Structural basis of function in heterotrimeric G proteins, *Q Rev Biophys* **39**: 117-166. doi: 10.1017/S0033583506004306
Overton, M. C., S. L. Chinault and K. J. Blumer (2005). Oligomerization of G-protein-coupled receptors: lessons from the yeast *Saccharomyces cerevisiae*, *Eukaryot Cell* **4**: 1963-1970. doi: 10.1128/EC.4.12.1963-1970.2005

P

Pandey, S. and S. M. Assmann (2004). The *Arabidopsis* putative G protein-coupled receptor GCR1 interacts with the G protein alpha subunit GPA1 and regulates abscisic acid signaling, *Plant Cell* **16**: 1616-1632. doi: 10.1105/tpc.020321
Paps, J., L. A. Medina-Chacon, W. Marshall, H. Suga and I. Ruiz-Trillo (2013). Molecular phylogeny of unikonts: new insights into the position of apusomonads and ancyromonads and the internal relationships of opisthokonts, *Protist* **164**: 2-12. doi: 10.1016/j.protis.2012.09.002
Park, S. J., T. Itoh and T. Takenawa (2001). Phosphatidylinositol 4-phosphate 5-kinase type I is regulated through phosphorylation response by extracellular stimuli, *J Biol Chem* **276**: 4781-4787. doi: 10.1074/jbc.M010177200
Peng, D., S. P. Kurup, P. Y. Yao, T. A. Minning and R. L. Tarleton (2014). CRISPR-Cas9-mediated single-gene and gene family disruption in *Trypanosoma cruzi*, *mBio* **6**: e02097-02014. doi: 10.1128/mBio.02097-14
Pohl, C., J. A. Kiel, A. J. Driessen, R. A. Bovenberg and Y. Nygard (2016). CRISPR/Cas9 Based Genome Editing of *Penicillium chrysogenum*, *ACS Synth Biol* **5**: 754-764. doi: 10.1021/acssynbio.6b00082
Poidevin, L., K. Andreeva, C. Khachatoorian and H. S. Judelson (2015). Comparisons of Ribosomal Protein Gene Promoters Indicate Superiority of Heterologous Regulatory Sequences for Expressing Transgenes in *Phytophthora infestans*, *PLoS One* **10**: e0145612. doi: 10.1371/journal.pone.0145612
Pollitt, A. Y. and R. H. Insall (2009). WASP and SCAR/WAVE proteins: the drivers of actin assembly, *J Cell Sci* **122**: 2575-2578. doi: 10.1242/jcs.023879
Powell, M. J., L. P. Lehnen and R. N. Bortnick (1985). Microbody-like organelles as taxonomic markers among oomycetes, *Biosystems* **18**: 321-334. doi: 10.1016/0303-2647(85)90032-2
Prabhu, Y., S. Mondal, L. Eichinger and A. A. Noegel (2007). A GPCR involved in post aggregation events in *Dictyostelium discoideum*, *Dev Biol* **312**: 29-43. doi: 10.1016/j.ydbio.2007.08.055

R

Radakovits, R., R. E. Jinkerson, S. I. Fuerstenberg, H. Tae, R. E. Settlage, J. L. Boore and M. C. Posewitz (2012). Draft genome sequence and genetic transformation of the oleaginous alga *Nannochloropis gaditana*, *Nat Commun* **3**: 686. doi: 10.1038/ncomms1688
Raffaele, S. and S. Kamoun (2012). Genome evolution in filamentous plant pathogens: why bigger can be better, *Nat Rev Microbiol* **10**: 417-430. doi: 10.1038/nrmicro2790
Rajagopal, S., K. Rajagopal and R. J. Lefkowitz (2010). Teaching old receptors new tricks: biasing seven-transmembrane receptors, *Nat Rev Drug Discov* **9**: 373-386. doi: 10.1038/nrd3024
Ramakrishna, S., A. B. Kwaku Dad, J. Beloor, R. Gopalappa, S. K. Lee and H. Kim (2014). Gene disruption by cell-penetrating peptide-mediated delivery of Cas9 protein and guide RNA, *Genome Res* **24**: 1020-1027. doi: 10.1101/gr.171264.113
Ran, F. A., L. Cong, W. X. Yan, D. A. Scott, J. S. Gootenberg, A. J. Kriz, . . . F. Zhang (2015). In vivo genome editing using Staphylococcus aureus Cas9, *Nature* **520**: 186-191. doi: 10.1038/nature14299
Ran, F. A., P. D. Hsu, J. Wright, V. Agarwala, D. A. Scott and F. Zhang (2013). Genome engineering using the CRISPR-Cas9 system, *Nat Protoc* **8**: 2281-2308. doi: 10.1038/nprot.2013.143
Rask-Andersen, M., M. S. Almen and H. B. Schioth (2011). Trends in the exploitation of novel drug targets, *Nat Rev Drug Discov* **10**: 579-590. doi: 10.1038/nrd3478
Read, B. A., J. Kegel, M. J. Klute, A. Kuo, S. C. Lefebvre, F. Maumus, . . . I. V. Grigoriev (2013). Pan genome of the phytoplankton *Emiliania* underpins its global distribution, *Nature* **499**: 209-213. doi: 10.1038/nature12221
Ren, X. D. and M. A. Schwartz (1998). Regulation of inositol lipid kinases by Rho and Rac, *Curr Opin Genet Dev* **8**: 63-67.
Reuter, J. S. and D. H. Mathews (2010). RNAstructure: software for RNA secondary structure prediction and analysis, *BMC Bioinformatics* **11**: 129. doi: 10.1186/1471-2105-11-129
Ribeiro, O. (2013). A Historical Perspective of *Phytophthora*. Phytophthora: a global perspective. K. Lamour.
Richards, T. A. and T. Cavalier-Smith (2005). Myosin domain evolution and the primary divergence of eukaryotes, *Nature* **436**: 1113-1118. doi: 10.1038/nature03949
Richards, T. A., J. B. Dacks, J. M. Jenkinson, C. R. Thornton and N. J. Talbot (2006). Evolution of filamentous plant pathogens: gene exchange across eukaryotic kingdoms, *Curr Biol* **16**: 1857-1864. doi: 10.1016/j.cub.2006.07.052
Richards, T. A., D. M. Soanes, M. D. Jones, O. Vasieva, G. Leonard, K. Paszkiewicz, . . . N. J. Talbot (2011). Horizontal gene transfer facilitated the evolution of plant parasitic mechanisms in the oomycetes, *Proc Natl Acad Sci USA* **108**: 15258-15263. doi: 10.1073/pnas.1105100108
Richardson, D. N., M. P. Simmons and A. S. Reddy (2006). Comprehensive comparative analysis of kinesins in photosynthetic eukaryotes, *BMC Genomics* **7**: 18. doi: 10.1186/1471-2164-7-18
Ristaino, J. B. (2002). Tracking historic migrations of the Irish potato famine pathogen, *Phytophthora infestans*, *Microbes Infect* **4**: 1369-1377.
Riyahi, T. Y., F. Frese, M. Steinert, N. N. Omosigho, G. Glockner, L. Eichinger, . . . A. A. Noegel (2011). RpkA, a highly conserved GPCR with a lipid kinase domain, has a role in phagocytosis and anti-bacterial defense, *PLoS One* **6**: e27311. doi: 10.1371/journal.pone.0027311
Rizzo, D. M. and M. Garbelotto (2003). Sudden oak death: endangering California and Oregon forest ecosystems, *Frontiers in Ecology and the Environment* **1**: 197-204. doi: 10.1890/1540-9295(2003)001[0197:Sodeca]2.0.Co;2
Rosenbaum, D. M., S. G. Rasmussen and B. K. Kobilka (2009). The structure and function of G-protein-coupled receptors, *Nature* **459**: 356-363. doi: 10.1038/nature08144
Roychowdhury, S., D. Panda, L. Wilson and M. M. Rasenick (1999). G Protein α Subunits Activate Tubulin GTPase and Modulate Microtubule Polymerization Dynamics, *Journal of Biological Chemistry* **274**: 13485-13490. doi: 10.1074/jbc.274.19.13485
Roychowdhury, S. and M. M. Rasenick (2008). Submembraneous microtubule cytoskeleton: regulation of microtubule assembly by het-

erotrimeric Gproteins, *FEBS J* **275**: 4654-4663. doi: 10.1111/j.1742-4658.2008.06614.x

S

Sah, V. P., T. M. Seasholtz, S. A. Sagi and J. H. Brown (2000). The role of Rho in G protein-coupled receptor signal transduction, *Annu Rev Pharmacol Toxicol* **40**: 459-489. doi: 10.1146/annurev.pharmtox.40.1.459

Sander, J. D. and J. K. Joung (2014). CRISPR-Cas systems for editing, regulating and targeting genomes, *Nat Biotech* **32**: 347-355. doi: 10.1038/nbt.2842

Santos, R., O. Ursu, A. Gaulton, A. P. Bento, R. S. Donadi, C. G. Bologa, . . . J. P. Overington (2017). A comprehensive map of molecular drug targets, *Nat Rev Drug Discov* **16**: 19-34. doi: 10.1038/nrd.2016.230

Savory, F., G. Leonard and T. A. Richards (2015). The role of horizontal gene transfer in the evolution of the oomycetes, *PLoS Pathog* **11**: e1004805. doi: 10.1371/journal.ppat.1004805

Schneider, C. A., W. S. Rasband and K. W. Eliceiri (2012). NIH Image to ImageJ: 25 years of image analysis, *Nature Methods* **9**: 671-675. doi: 10.1038/nmeth.2089

Schrodinger, L. (2015). The PyMOL Molecular Graphics System, Version 1.8.

Schultz, J., F. Milpetz, P. Bork and C. P. Ponting (1998). SMART, a simple modular architecture research tool: identification of signaling domains, *Proc Natl Acad Sci U S A* **95**: 5857-5864.

Schwindinger, W. F., K. E. Giger, K. S. Betz, A. M. Stauffer, E. M. Sunderlin, L. J. Sim-Selley, . . . J. D. Robishaw (2004). Mice with deficiency of G protein gamma3 are lean and have seizures, *Mol Cell Biol* **24**: 7758-7768. doi: 10.1128/MCB.24.17.7758-7768.2004

Seidl, M. F., G. Van den Ackerveken, F. Govers and B. Snel (2011). A domain-centric analysis of oomycete plant pathogen genomes reveals unique protein organization, *Plant Physiol* **155**: 628-644. doi: 10.1104/pp.110.167841

Sharma, R., X. Xia, L. M. Cano, E. Evangelisti, E. Kemen, H. Judelson, . . . M. Thines (2015). Genome analyses of the sunflower pathogen *Plasmopara halstedii* provide insights into effector evolution in downy mildews and *Phytophthora*, *BMC Genomics* **16**: 741. doi: 10.1186/s12864-015-1904-7

Shearer, C. A., E. Descals, B. Kohlmeyer, J. Kohlmeyer, L. Marvanová, D. Padgett, . . . H. Voglymayr (2006). Fungal biodiversity in aquatic habitats, *Biodiversity and Conservation* **16**: 49-67. doi: 10.1007/s10531-006-9120-z

Smith, J. J., J. S. Yakisich, G. M. Kapler, E. S. Cole and D. P. Romero (2004). A beta-tubulin mutation selectively uncouples nuclear division and cytokinesis in Tetrahymena thermophila, *Eukaryot Cell* **3**: 1217-1226. doi: 10.1128/EC.3.5.1217-1226.2004

Smith, J. S. and S. Rajagopal (2016). The beta-Arrestins: Multifunctional Regulators of G Protein-coupled Receptors, *J Biol Chem* **291**: 8969-8977. doi: 10.1074/jbc.R115.713313

Smith, M. G., S. R. Swamy and L. A. Pon (2001). The life cycle of actin patches in mating yeast, *J Cell Sci* **114**: 1505-1513.

Soares Medeiros, L. C., L. South, D. Peng, J. M. Bustamante, W. Wang, M. Bunkofske, . . . R. L. Tarleton (2017). Rapid, Selection-Free, High-Efficiency Genome Editing in Protozoan Parasites Using CRISPR-Cas9 Ribonucleoproteins, *mBio* **8**. doi: 10.1128/mBio.01788-17

Srivastava, M., O. Simakov, J. Chapman, B. Fahey, M. E. Gauthier, T. Mitros, . . . D. S. Rokhsar (2010). The *Amphimedon queenslandica* genome and the evolution of animal complexity, *Nature* **466**: 720-726. doi: 10.1038/nature09201

Stajich, J. E., T. Harris, B. P. Brunk, J. Brestelli, S. Fischer, O. S. Harb, . . . D. S. Roos (2012). FungiDB: an integrated functional genomics database for fungi, *Nucleic Acids Res* **40**: D675-681. doi: 10.1093/nar/gkr918

Stamatakis, A. (2014). RAxML version 8: a tool for phylogenetic analysis and post-analysis of large phylogenies, *Bioinformatics* **30**: 1312-1313. doi: 10.1093/bioinformatics/btu033

Stefan, C. J., A. Audhya and S. D. Emr (2002). The yeast synaptojanin-like proteins control the cellular distribution of phosphatidylinositol (4,5)-bisphosphate, *Mol Biol Cell* **13**: 542-557. doi: 10.1091/mbc.01-10-0476

Stoddart, L. A., E. K. M. Johnstone, A. J. Wheal, J. Goulding, M. B. Robers, T. Machleidt, . . . K. D. G. Pfleger (2015). Application of BRET to monitor ligand binding to GPCRs, *Nat Methods* **12**: 661-663. doi: 10.1038/nmeth.3398

Strachan, S. D. and F. D. Hess (1983). The biochemical mechanism of action of the dinitroaniline herbicide oryzalin, *Pesticide Biochemistry and Physiology* **20**: 141-150. doi: 10.1016/0048-3575(83)90018-4

Strullu-Derrien, C., P. Kenrick, J. P. Rioult and D. G. Strullu (2011). Evidence of parasitic Oomycetes (Peronosporomycetes) infecting the stem cortex of the Carboniferous seed fern Lyginopteris oldhamia, *Proc Biol Sci* **278**: 675-680. doi: 10.1098/rspb.2010.1603

Studholme, D. J., R. L. McDougal, C. Sambles, E. Hansen, G. Hardy, M. Grant, . . . N. M. Williams (2016). Genome sequences of six *Phytophthora* species associated with forests in New Zealand, *Genom Data* **7**: 54-56. doi: 10.1016/j.gdata.2015.11.015

Sucgang, R., A. Kuo, X. Tian, W. Salerno, A. Parikh, C. L. Feasley, . . . I. V. Grigoriev (2011). Comparative genomics of the social amoebae *Dictyostelium discoideum* and *Dictyostelium purpureum*, *Genome Biol* **12**: R20. doi: 10.1186/gb-2011-12-2-r20

Suga, H., Z. Chen, A. de Mendoza, A. Sebe-Pedros, M. W. Brown, E. Kramer, . . . I. Ruiz-Trillo (2013). The *Capsaspora* genome reveals a complex unicellular prehistory of animals, *Nat Commun* **4**: 2325. doi: 10.1038/ncomms3325

Swart, E. C., J. R. Bracht, V. Magrini, P. Minx, X. Chen, Y. Zhou, . . . L. F. Landweber (2013). The *Oxytricha trifallax* macronuclear genome: a complex eukaryotic genome with 16,000 tiny chromosomes, *PLoS Biol* **11**: e1001473. doi: 10.1371/journal.pbio.1001473

T

Takahashi, F., K. Yamaguchi, T. Hishinuma and H. Kataoka (2003). Mitosis and mitotic wave propagation in the coenocytic alga, Vaucheria terrestris sensu Goetz, *J Plant Res* **116**: 381-387. doi: 10.1007/s10265-003-0117-3

Takai, Y., T. Sasaki and T. Matozaki (2001). Small GTP-binding proteins, *Physiol Rev* **81**: 153-208.

Torres, G. A., G. A. Sarria, G. Martinez, F. Varon, A. Drenth and D. I. Guest (2016). Bud Rot Caused by Phytophthora palmivora: A Destructive Emerging Disease of Oil Palm, *Phytopathology* **106**: 320-329. doi: 10.1094/PHYTO-09-15-0243-RVW

Trusov, Y., D. Chakravorty and J. R. Botella (2012). Diversity of heterotrimeric G-protein gamma subunits in plants, *BMC Res Notes* **5**: 608. doi: 10.1186/1756-0500-5-608

Tusnady, G. E. and I. Simon (2001). The HMMTOP transmembrane topology prediction server, *Bioinformatics* **17**: 849-850. doi: 10.1093/bioinformatics/17.9.849

Tyler, B. M., S. Tripathy, X. Zhang, P. Dehal, R. H. Jiang, A. Aerts, . . . J. L. Boore (2006). *Phytophthora* genome sequences uncover evolution-

ary origins and mechanisms of pathogenesis, *Science* **313**: 1261-1266. doi: 10.1126/science.1128796

U

Urano, D., J. G. Chen, J. R. Botella and A. M. Jones (2013). Heterotrimeric G protein signalling in the plant kingdom, *Open Biol* **3**: 120186. doi: 10.1098/rsob.120186

Urano, D. and A. M. Jones (2014). Heterotrimeric G protein-coupled signaling in plants, *Annu Rev Plant Biol* **65**: 365-384. doi: 10.1146/annurev-arplant-050213-040133

Urushihara, H., H. Kuwayama, K. Fukuhara, T. Itoh, H. Kagoshima, I. T. Shin, . . . A. Fujiyama (2015). Comparative genome and transcriptome analyses of the social amoeba *Acytostelium subglobosum* that accomplishes multicellular development without germ-soma differentiation, *BMC Genomics* **16**: 80. doi: 10.1186/s12864-015-1278-x

V

van den Hoogen, D. J., H. J. G. Meijer, M. F. Seidl and F. Govers (2018). The ancient link between G-protein coupled receptors and C-terminal phospholipid kinase domains, *mBio* **9**. doi: 10.1128/mBio.02119-17

van der Lee, T., A. Robold, A. Testa, J. W. van 't Klooster and F. Govers (2001). Mapping of avirulence genes in *Phytophthora infestans* with amplified fragment length polymorphism markers selected by bulked segregant analysis, *Genetics* **157**: 949-956. doi:

van der Lee, T., A. Testa, A. Robold, J. van 't Klooster and F. Govers (2004). High-density genetic linkage maps of *Phytophthora infestans* reveal trisomic progeny and chromosomal rearrangements, *Genetics* **167**: 1643-1661. doi: 10.1534/genetics.104.029652

van West, P., S. Kamoun, J. W. van 't Klooster and F. Govers (1999). Internuclear gene silencing in Phytophthora infestans, *Mol Cell* **3**: 339-348.

van West, P., B. Reid, T. A. Campbell, R. W. Sandrock, W. E. Fry, S. Kamoun and N. A. R. Gow (1999). Green fluorescent protein (GFP) as a reporter gene for the plant pathogenic oomycete *Phytophthora palmivora*, *FEMS Microbiology Letters* **178**: 71-80. doi: 10.1111/j.1574-6968.1999.tb13761.x

Verdonk, J. (2014). RNA isolation with homemade TRIzol reagent. from https://julianverdonk.wordpress.com/2014/01/14/rna-isolation-with-homemade-trizol-reagent/

Versele, M., K. Lemaire and J. M. Thevelein (2001). Sex and sugar in yeast: two distinct GPCR systems, *EMBO Rep* **2**: 574-579. doi: 10.1093/embo-reports/kve132

Vijn, I. and F. Govers (2003). Agrobacterium tumefaciens mediated transformation of the oomycete plant pathogen Phytophthora infestans, *Mol Plant Pathol* **4**: 459-467. doi: 10.1046/j.1364-3703.2003.00191.x

Vogler, O., J. M. Barcelo, C. Ribas and P. V. Escriba (2008). Membrane interactions of G proteins and other related proteins, *Biochim Biophys Acta* **1778**: 1640-1652. doi: 10.1016/j.bbamem.2008.03.008

W

Wagih, O. (2017). ggseqlogo: a versatile R package for drawing sequence logos, *Bioinformatics*. doi: 10.1093/bioinformatics/btx469

Wang, X., S. P. Devaiah, W. Zhang and R. Welti (2006). Signaling functions of phosphatidic acid, *Prog Lipid Res* **45**: 250-278. doi: 10.1016/j.plipres.2006.01.005

Wang, Y., A. Li, X. Wang, X. Zhang, W. Zhao, D. Dou, . . . Y. Wang (2010). GPR11, a putative seven-transmembrane G protein-coupled receptor, controls zoospore development and virulence of *Phytophthora sojae*, *Eukaryot Cell* **9**: 242-250. doi: 10.1128/EC.00265-09

Weste, G. and G. C. Marks (1987). The Biology of Phytophthora-Cinnamomi in Australasian Forests, *Annual Review of Phytopathology* **25**: 207-229. doi: 10.1146/annurev.py.25.090187.001231

Wickstead, B. and K. Gull (2011). The evolution of the cytoskeleton, *J Cell Biol* **194**: 513-525. doi: 10.1083/jcb.201102065

Wickstead, B., K. Gull and T. A. Richards (2010). Patterns of kinesin evolution reveal a complex ancestral eukaryote with a multifunctional cytoskeleton, *BMC Evol Biol* **10**: 110. doi: 10.1186/1471-2148-10-110

Wisler, J. W., K. Xiao, A. R. Thomsen and R. J. Lefkowitz (2014). Recent developments in biased agonism, *Curr Opin Cell Biol* **27**: 18-24. doi: 10.1016/j.ceb.2013.10.008

Wistrand, M., L. Kall and E. L. Sonnhammer (2006). A general model of G protein-coupled receptor sequences and its application to detect remote homologs, *Protein Sci* **15**: 509-521. doi: 10.1110/ps.051745906

Woo, J. W., J. Kim, S. I. Kwon, C. Corvalan, S. W. Cho, H. Kim, . . . J. S. Kim (2015). DNA-free genome editing in plants with preassembled CRISPR-Cas9 ribonucleoproteins, *Nat Biotechnol* **33**: 1162-1164. doi: 10.1038/nbt.3389

X

Xiang, X. and R. Fischer (2004). Nuclear migration and positioning in filamentous fungi, *Fungal Genet Biol* **41**: 411-419. doi: 10.1016/j.fgb.2003.11.010

Xiang, X. and M. Plamann (2003). Cytoskeleton and motor proteins in filamentous fungi, *Curr Opin Microbiol* **6**: 628-633. doi: 10.1016/j.mib.2003.10.009

Xiong, J., G. Wang, J. Cheng, M. Tian, X. Pan, A. Warren, . . . W. Miao (2015). Genome of the facultative scuticociliatosis pathogen *Pseudocohnilembus persalinus* provides insight into its virulence through horizontal gene transfer, *Sci Rep* **5**: 15470. doi: 10.1038/srep15470

Xu, X. and T. Jin (2017). ELMO proteins transduce G protein-coupled receptor signal to control reorganization of actin cytoskeleton in chemotaxis of eukaryotic cells, *Small GTPases*1-9. doi: 10.1080/21541248.2017.1318816

Xue, C., Y. P. Hsueh and J. Heitman (2008). Magnificent seven: roles of G protein-coupled receptors in extracellular sensing in fungi, *FEMS Microbiol Rev* **32**: 1010-1032. doi: 10.1111/j.1574-6976.2008.00131.x

Y

Yan, J., V. Mihaylov, X. Xu, J. A. Brzostowski, H. Li, L. Liu, . . . T. Jin (2012). A Gbetagamma effector, ElmoE, transduces GPCR signaling to the actin network during chemotaxis, *Dev Cell* **22**: 92-103. doi: 10.1016/j.devcel.2011.11.007

Yang, X., W. Zhao, C. Hua, X. Zheng, M. Jing, D. Li, . . . Y. Wang (2013). Chemotaxis and oospore formation in *Phytophthora sojae* are controlled by G-protein-coupled receptors with a phosphatidylinositol phosphate kinase domain, *Mol Microbiol* **88**: 382-394. doi: 10.1111/mmi.12191

Z

Zetsche, B., J. S. Gootenberg, O. O. Abudayyeh, I. M. Slaymaker, K. S. Makarova, P. Essletzbichler, . . . F. Zhang (2015). Cpf1 is a single RNA-guided endonuclease of a class 2 CRISPR-Cas system, *Cell* **163**: 759-771. doi: 10.1016/j.cell.2015.09.038

Zhang, N., Y. Long and P. N. Devreotes (2001). Gγ in *Dictyostelium*: Its Role in Localization of G$\beta\gamma$ to the Membrane Is Required for Chemotaxis in Shallow Gradients, *Mol Biol Cell* **12**: 3204–3213. doi: 10.1091/mbc.12.10.3204

Zhang, R. and X. Xie (2012). Tools for GPCR drug discovery, *Acta Pharmacol Sin* **33**: 372-384. doi: 10.1038/aps.2011.173

Zhang, X., C. Zhai, C. Hua, M. Qiu, Y. Hao, P. Nie, . . . Y. Wang (2016). *PsHint1*, associated with the G-protein alpha subunit PsGPA1, is required for the chemotaxis and pathogenicity of *Phytophthora sojae*, *Mol Plant Pathol* **17**: 272-285. doi: 10.1111/mpp.12279

Zhao, Z., H. Liu, Y. Luo, S. Zhou, L. An, C. Wang, . . . J. R. Xu (2014). Molecular evolution and functional divergence of tubulin superfamily in the fungal tree of life, *Sci Rep* **4**: 6746. doi: 10.1038/srep06746

Zuris, J. A., D. B. Thompson, Y. Shu, J. P. Guilinger, J. L. Bessen, J. H. Hu, . . . D. R. Liu (2015). Cationic lipid-mediated delivery of proteins enables efficient protein-based genome editing in vitro and in vivo, *Nat Biotechnol* **33**: 73-80. doi: 10.1038/nbt.3081

Zysset-Burri, D. C., N. Muller, C. Beuret, M. Heller, N. Schurch, B. Gottstein and M. Wittwer (2014). Genome-wide identification of pathogenicity factors of the free-living amoeba *Naegleria fowleri*, *BMC Genomics* **15**: 496. doi: 10.1186/1471-2164-15-496

Summary

Many oomycetes are economically important pathogens, causing enormous yield losses in crop plants. Others threaten natural vegetation, while some species can cause harmful diseases in animals. Oomycetes, also known as water molds, are morphologically similar to fungi and also occupy similar environmental niches, but during evolution the two groups evolved independently (**Chapter 1**). They show many differences, in particular at the subcellular level, and this often has consequences for the efficacy of chemical control agents and hence, the efficient control of oomycete disesases. The research described in this thesis is aimed at enhancing our basic knowledge of plant pathogenic oomycetes in the genus *Phytophthora* and to gain more insight in their remarkable biology. It focusses on two processes, cellular signaling and cytoskeleton dynamics. Uncovering mechanisms that govern these processes may help in designing novel, oomycete-specific control strategies.

Cellular signaling is crucial for every living organism. It controls important processes, allows for communication, and enables organisms to respond to environmental cues. Two important eukaryotic signal transduction pathways that are usually interconnected through intermediate signaling components, are G-protein signaling and phospholipid signaling. Oomycetes, however, possess a unique class of G-protein coupled receptors (GPCRs) that have a phosphatidylinositol kinase (PIPK) as an accessory domain pointing to a more direct connection between the two major signaling pathways. When first discovered, these so-called GPCR-PIPKs were thought to be restricted to oomycetes. In **Chapter 2**, we show the sporadic occurrence of these so-called GPCR-PIPKs in a diverse but limited group of unicellular microorganisms, divided over nearly all eukaryotic supergroups. Our analyses revealed that nearly all GPCR-PIPKs contain a unique, conserved motif located in between the GPCR domain and the PIPK domain. GPCR-PIPKs are likely ancestral to eukaryotes and significantly expanded in the last common ancestor of oomycetes. We further identified five hitherto unknown classes of GPCRs with accessory domains, GPCR-bigrams. All classes of GPCR-bigrams are shared by oomycetes, and except for three, some classes are sparsely present in organisms from other taxa. Most accessory domains of GPCR-bigrams are universal players in signal transduction. Our findings point to an ancestral signaling system in eukaryotic microorganisms where GPCR-mediated sensing is directly linked to downstream responses.

In classical G-protein signaling, a GPCR senses extracellular signals and changes confor-

mation upon ligand binding, thereby activating the associated heterotrimeric G-protein complex, consisting of a G-protein α (Gα), β (Gβ), and γ (Gγ) subunit. In turn, the activated G-protein complex dissociates from the receptor and its subunits stimulate downstream effector proteins. In **Chapter 3**, we investigated the function of the Gγ subunit of *Phytophthora infestans*. The overall similarity of this Gγ subunit with non-oomycete Gγ subunits is low, but the similarity with its homologs in other oomycetes is high. The Gγ-encoding gene, *Pigpg1*, is expressed in all life stages and peaks in spores. To elucidate the function of the *P. infestans* Gγ subunit, we generated *Pigpg1*-silenced and overexpression transformants and analyzed their phenotypes. However, many transformed lines had severe growth defects and were not viable. The few that could be maintained produced less sporangia, that were malformed. These findings demonstrate that the Gγ subunit has an important role in *P. infestans.* It is crucial for proper sporangia development, and likely forms a dimer with the *P. infestans* Gβ subunit, thereby mediating signaling.

The microtubule (MT) cytoskeleton is a system of intracellular filaments, that is able to quickly adapt different configurations. This process is regulated by microtubular dynamics and MT-associated proteins (MAPs). The MT cytoskeleton has a myriad of roles, for example in processes that provide structural rigidity to cells or allow for polarized cell growth and cell movement. **Chapter 4** focuses on the MT cytoskeleton in *Phytophthora*. Live cell imaging of transgenic *Phytophthora palmivora* lines carrying an ectopically integrated GFP-α-tubulin fusion gene provided insight in the spatio-temporal organization of the MT cytoskeleton in *Phytophthora*. In addition, we provide an inventory of putative MT-associated proteins in *P. infestans*. Unique types of the motor proteins dynein and kinesin were found, including some members with accessory domains not found elsewhere in combination with a motor protein domain. This study provides a basis for future research on MTs and MAPs in *Phytophthora* and a first glimpse of the dynamics of the MT cytoskeleton in an oomycete.

The low rate of homologous recombination in oomycetes makes that transgenes are integrated randomly and until recently genome editing was unattainable. The implementation of a CRISPR/Cas9 system in *Phytophthora sojae* is a significant asset for the molecular toolbox of oomycetes. So far, genome editing using CRISPR/Cas9 has been successfully applied in only a few *Pyhytophthora* species. In **Chapter 5** we explore the effectuation of CRISPR/Cas9 for targeted genome editing in *P. infestans*. With the original constructs that were developed for *P. sojae*, we did not obtain any transformants in which the target gene was mutagenized. In an effort to pinpoint the reason for failure, we tailored the constructs for *P. infestans* and implemented several modifications in the CRISPR/Cas9 system but without success. We also explored the delivery of pre-assembled ribonucleoprotein complexes. We describe an extensive effort in optimization of the system and outline possible causes for failure.

In **Chapter 6**, the main results of this thesis are integrated and discussed. Remarkable features of oomycetes and their cellular signaling systems are outlined. Possible modes of

action of GPCR-bigrams are proposed as well as future directions for research on cellular signaling in *Phytophthora*. More knowledge on the elementary processes addressed in this thesis will expose new strategies for the design of novel, oomycete-specific control agents to mitigate damage caused by these devastating pathogens.

Acknowledgements

This may be the first part of my thesis that you are reading (or second, after the propositions), but it was the very last to write. And yet I feel it may be one of the most important chapters, because without the support of you, friends, colleagues, and family, I wouldn't have been able to keep on going. Thanks for that! Completing this work has been a feat of perseverance and determination, but I couldn't have done it by myself.

First off, **Francine**, thanks for all the support and guidance over the past years. It surely has not been an easy time, but I have learned a lot. I have definitely become a better scientist under your supervision. I'm also very grateful to all other colleagues and former colleagues from Phytopathology and in particular those from the *Phytophthora* group, for providing a great working environment. A special thanks to **Michael** and **Harold**, with whom I had the pleasure to collaborate and publish with. **Jan**, your inexhaustible knowledge of molecular techniques has pointed me in the right direction more than once. I'm also deeply thankful to my undergraduate students, **Max**, **Costas**, **Paul**, **Juliette**, and **Joram**, who provided me with important insights on science and people management.

Natalie, your help with the phenotyping assays has been invaluable. *Phytophthora* is not the easiest genus to work with but you have made it happen. The behaviour of the silenced lines was temperamental to say the least, but your diligence has resulted in an important contribution to this thesis. **Luis**, thanks for being a friend in and outside the lab, always being interested in my pursuits, and for our dinners out in town. **Klaas**, I've always enjoyed our little chats on many different topics – ranging from traveling adventures to semi-political discussions. Many thanks to the PhDs at Phytopathology, with whom I had the pleasure to share the lab with. Your help has been wonderful. **Sander**, thanks for always being helpful with the bioinformatic-related problems I've encountered. **Hanna**, **Chara**, **Elysa**, and **Kiki**, I really appreciate the chats we had on both science and real life.

I'm very grateful to all the colleagues who have fed me. **Shuqing** (your dumplings are the best!), **Malaika**, **Hui**, **Grardy**, **Mireille**, **Ester**: thanks for all the cookies, cake, Chinese food, eggs, fruit, and lunch leftovers. Without you I would have starved.

Pierre, **Gauthier**, **Luytzen**, **Diesel**, **Willem**, and other former housemates for making the stay in Wageningen so much more pleasant by providing a great atmosphere to get home

to. It have been three great years!

A very special thanks to all my sports friends for joining me on my almost obsessive quest for physical exercise. **Danny**, **Peter**, **Joris**, **Melle**, **Jornt**, **Jorrit**, **Sigrid**, **Jorien**, **Christoph**, **Joost**, **Folmer**, **Ben**, **Erik**, **Thomas**, **Annika**, **Roy**, **Lottie**, **Danique Diede**, **Vasco**, **Steven**, **Menno**, **Nicole**, **Kim**, and many others: thank you for all the hours outside, while cycling, mountain biking, running, skiing, hiking, ice skating, climbing, and all other obscure sports we did together.

Diede en **Tom**, dankje. **Jeroen**, jij ook bedankt.

Rosa, **papa** en **mama**, bedankt voor alle steun, en misschien nog wel meer voor alle vrijheid die jullie me altijd hebben gegeven om te kunnen doen wat ik zelf het liefste wil. **Opa**, bedankt voor het stimuleren van de educatieve ontwikkeling van alle kleinkinderen – inclusief die van mijzelf. Uw ontembare leergierigheid zal me altijd blijven inspireren. Ik teken ervoor om op uw leeftijd nog een wetenschappelijke cursus astronomie te volgen.

En natuurlijk **Nienke**. Duizend maal dank voor alles wat je voor me doet, bent en geeft. Nu we Skype hebben uitgespeeld en eindelijk op dezelfde plek wonen, kan ik alleen maar uitkijken naar de toekomst.

About the author

After graduating from HAVO (2005) and VWO (2007) in Nijmegen, the Netherlands, I moved to Wageningen for my BSc in Biotechnology. Being interested in medical biotechnology, I spent a semester in Trondheim, Norway. Later my interest shifted more towards plants, so I specialized in cellular and molecular biotechnology in my MSc, and spent six months in New Zealand for an internship. My MSc concluded with two master theses, both addressing root nodule formation. The second thesis focussed on the only non-legumes that can establish nitrogen-fixing nodules with *Rhizobium*, tropical trees from the genus *Parasponia*.

In 2013, I started my PhD in the group of Prof. Dr. Francine Govers at the Laboratory of Phytopathology at Wageningen University, resulting in this thesis. After finishing the experimental work for my PhD I changed gears from molecular biology on the sub-cellular level, to microbiology on a global scale. Since January 2018, I work at ETH Zürich as a post-doctoral researcher and laboratory manager in the group of Prof. Dr. Thomas Crowther. My research focusses on global distribution patterns of soil microbiota, to understand their role in global carbon cycling.

In daily life, I enjoy adventurous and endurance sports.

List of publications

van den Hoogen, J., F. Govers (2018). GPCR-bigrams, enigmatic signaling components in oomycetes, *Plos Pathogens*. doi:10.1371/journal.ppat.1007064

van den Hoogen, J., N. Verbeek - de Kruif, F. Govers (2018). The G-protein γ subunit of *Phytophthora infestans* is involved in sporangial development, *Fungal Genetics and Biology*. doi: 10.1016/j.fgb.2018.04.012

van Velzen, R., R. Holmer, F. Bu, L. Rutten, A. Van Zeijl, W. Liu, L. Santuari, Q. Cao, T. Sharma, D. Shen, Y. Roswanjaya, T. Wardhani, M. Seifi Kalhor, J. Jansen, **J. van den Hoogen**, B. Gungor, M. Hartog, J. Hontelez, J. Verver, W.-C. Yang, E. Schijlen, R. Repin, M. Schilthuizen, E. Schranz, R. Heidstra, K. Miyata, E. Fedorova, W. Kohlen, T. Bisseling, S. Smit, R. Geurts (2018). Parallel loss of symbiosis genes in relatives of nitrogen-fixing non-legume *Parasponia*, *PNAS*. doi:10.1073/pnas.1721395115

van den Hoogen, J., F. Govers (2018). Attempts to implement CRISPR/Cas9 for genome editing in the oomycete *Phytophthora infestans*, *bioRxiv*. doi: 10.1101/274829

van den Hoogen, D. J., H. J.G. Meijer, M. S. Seidl, F. Govers (2018). The ancient link between G-protein coupled receptors and C-terminal phospholipid kinase domains, *mBio* **9**. doi: 10.1128/mBio.02119-17

Sharma, R., X. Xia, L. M. Cano, E. Evangelisti, E. Kemen, H. Judelson, S. Oome, C. Sambles, **D. J. van den Hoogen**, M. Kitner, J. Klein, H. J. Meijer, O. Spring, J. Win, R. Zipper, H. B. Bode, F. Govers, S. Kamoun, S. Schornack, D. J. Studholme, G. Van den Ackerveken, M. Thines (2015). Genome analyses of the sunflower pathogen *Plasmopara halstedii* provide insights into effector evolution in downy mildews and *Phytophthora*, *BMC Genomics* **16**. doi: 10.1186/s12864-015-1904-7

Education Statement of the Graduate School

Experimental Plant Sciences

The Graduate School EXPERIMENTAL PLANT SCIENCES

Issued to: Johan van den Hoogen
Date: 8 Juni 2018
Group: Laboratory of Phytopathology
University: Wageningen University & Research

1) Start-up phase	*date*
► **First presentation of your project**	
Title: 'Phospholipid and GPCR signalling in Phytophthora'	12 Sep 2014
► **Writing or rewriting a project proposal**	
► **Writing a review or book chapter**	
GPCR-bigrams: enigmatic signaling components in oomycetes (PLOS Pathogens Pearl)	Dec 2017
► **MSc courses**	
► **Laboratory use of isotopes**	
Subtotal Start-up Phase	*7.5 credits**

2) Scientific Exposure	*date*
► **EPS PhD student days**	
EPS PhD student Day, Leiden, NL	29 Nov 2013
EPS PhD Student Day 'Get2Gether', Soest, NL	29-30 Jan 2015
EPS PhD Student Day 'Get2Gether', Soest, NL	28-29 Jan 2016
► **EPS theme symposia**	
EPS Theme 2 Symposium 'Interactions between plants and biotic agents', together with Willie Commelin Scholten Day, Utrecht, NL	20 Feb 2015
EPS Theme 2 Symposium 'Interactions between plants and biotic agents', together with Willie Commelin Scholten Day, Leiden, NL	22 Jan 2016
EPS Theme 2 Symposium 'Interactions between plants and biotic agents', together with Willie Commelin Scholten Day, Wageningen, NL	23 Jan 2017
► **National meetings (e.g.Lunteren days) and other National Platforms**	
ALW Platform Molecular Genetics, Lunteren, NL	10-11 Oct 2013
Annual Meeting 'Experimental Plant Sciences', Lunteren, NL	14-15 Apr 2014
Annual Meeting 'Experimental Plant Sciences', Lunteren, NL	13-14 Apr 2015
Annual Meeting 'Experimental Plant Sciences', Lunteren, NL	11-12 Apr 2016
Annual Meeting 'Experimental Plant Sciences', Lunteren, NL	10-11 Apr 2017
Host-Microbe Genetics, Wageningen, NL	27 Oct 2017
► **Seminars (series), workshops and symposia (highly recommended)**	
Eric Schranz - 'Whole genome duplications as drivers of evolutionary innovations and radiations?'	21 Nov 2013
Jos Raaijmakers - 'Back to the roots'	07 Jan 2014
Farewell symposium Pierre de Wit	05 Jun 2014
Jeroen Mesters - 'From protein solution to single crystal X-ray diffraction: Chitin binding by LysM domains	31 Mar 2014
Sophien Kamoun - 'Genome and effector evolution in the Irish potato famine pathogen lineage'	28 May 2014
Yuanchao Wang - 'Dissecting the interaction between Phytophthora sojae and soybean: making sense out of signalling and effectors'	16 Jul 2014
Michael Freitag - 'Chromatin structure controls centromeres and secondary metabolism in filamentous fungi'	21 Oct 2014
Public lecture Gert Kema	17 Jan 2015
Jeff Doyle - 'Polyploidy in wild relatives of soybean and other legumes: systematics, comparative and functional genomics, and nodulation'	12 May 2015
Gero Steinberg - 'Long-distance endosome trafficking drives fungal effector production during plant infection'	05 Jun 2016
Jane Parker - 'Plant intracellular immunity: evolutionary and molecular underpinnings'	21 Jan 2016
Laura Grennvile Briggs - 'Molecular Oomycete-Host Interactions: The Good, the Bad and the ugly'	19 Feb 2016
Caitlyn Allen - 'How Ralstonia solanacearum succeeds in plant xylem vessels'	29 Apr 2016
Kate Goodrich - 'The volatile 'language' of plants: from attraction to deterrence and back again'	23 May 2016
Wenbo Ma - 'Effectors as molecular probes to understand pathogenesis'	20 Jun 2016
Rene Geurts, Wageningen University, NL	06 Sep 2016
Gabino Sanchez Perez, Wageningen University, NL	14 Oct 2016
Jan Lochman - 'Elicitins - what we know and do not know'	24 Jan 2017
Fons Debets, Wageningen University, NL	24 Feb 2017
Richard Kormelink, Wageningen University, NL	09 Jun 2017
Marc van Mil, René Smulders - 'Tinkering with DNA' (WURtalks)	13 Sep 2017
Urs Wyss - 'Highlights of hidden insect-worlds'	02 Oct 2017
► **Seminar plus**	
Michaeil Freitag, Oregon State University, USA	21 Oct 2014
Caitlyn Allen, University of Wisconsin-Madison, USA	29 Apr 2016

►	**International symposia and congresses**	
	Oomycete Molecular Genetics Meeting 2014, Norwich, UK	02-05 Jul 2014
	Oomycete Molecular Genetics Meeting 2015, Asilomar, CA, USA	14-17 Mar 2015
	Fungal Genetics Conference, Asilomar, CA, USA	17-22 Mar 2015
	Oomycete Molecular Genetics Meeting 2016, Malmö, Sweden	14-17 Jun 2016
►	**Presentations**	
	Poster: 'Phytophthora infestans GK4 is a GPCR-PIPK that functions as a PI(4)P 5-kinase', EPS Spring School, Wageningen, NL	02-04 Jun 2014
	Poster: 'Phytophthora infestans GK4 is a GPCR-PIPK that functions as a PI(4)P 5-kinase', Norwich, UK	02-05 Jul 2014
	Poster: 'The inositol polyphosphate phosphatase family in oomycetes shows unique features', Asilomar, CA, USA	14-17 Mar 2015
	Poster: 'Phytophthora infestans GK4 is a GPCR-PIPK that functions as a PI(4)P 5-kinase', Lunteren, NL	13-14 Apr 2015
	Poster: 'The inositol polyphosphate phosphatase family in oomycetes shows unique features', Lunteren, NL	13-14 Apr 2015
	Talk: 'Phytophthora infestans GPCR-PIPK GK4 is a membrane localized PI4P5-kinase and is required for virulence', Asilomar, CA, USA	15 Mar 2015
	Talk: 'Towards targeted genome editing with CRISPR/Cas9 in the potato late blight pathogen Phytophthora infestans', Soest, NL	29 Jan 2016
	Poster: 'Characterization of a putative G-protein γ subunit in Phytophthora infestans', Malmö, Sweden	14-17 Jun 2016
	Talk: 'GPCRs with a phospholipid kinase domain are present in a diverse range of eukaryotic microorganisms', Leiden, NL	23 Jan 2017
►	**IAB interview**	
►	**Excursions**	
	Subtotal Scientific Exposure	*18.4 credits**

3) In-Depth Studies	*date*
► **EPS courses or other PhD courses**	
PhD spring School Host-Microbe Interactomics, Wageningen, NL	02-04 Jun 2014
PhD course: Phylogenetics: principles & methods, Wageningen, NL	17-19 May 2016
PhD course: Data analyses and visualization in R (for biologists), Wageningen, NL	12-13 Dec 2016
► **Journal club**	
Member of the Phytophthora literature discussion group of Phytoppathology	2013-2017
► **Individual research training**	
Subtotal In-Depth Studies	*5.5 credits**

4) Personal development	*date*
► **Skill training courses**	
Information Literacy including EndNote Introduction	09-10 Apr 2014
PhD competence assesment	09 Sep 2014
Project and Time Management	9, 23 April, 21 May 2015
WGS PhD Workshop Carousel	17 Apr 2015
Last Stretch of the PhD Programme	12 May 2017
► **Organisation of PhD students day, course or conference**	
EPS Get2Gether pubquiz	09 Feb 2017
► **Membership of Board, Committee or PhD council**	
Subtotal Personal Development	*3.2 credits**

TOTAL NUMBER OF CREDIT POINTS*	**34.6**

Herewith the Graduate School declares that the PhD candidate has complied with the educational requirements set by the Educational Committee of EPS which comprises of a minimum total of 30 ECTS credits

** A credit represents a normative study load of 28 hours of study.*

This thesis is printed on 100% recycled paper.

This work was supported by the Division for Earth and Life Sciences (ALW) with financial aid from the Netherlands Organization for Scientific Research (NWO) in the framework of the ALW-JSTP programme. The work was performed in the Laboratory of Phytopathology, Wageningen University, The Netherlands.

Cover design: Erik Crins - Binnestebuiten Illustraties
Layout: Johan van den Hoogen
Print: GVO drukkers & vormgevers B.V.